STUDY REPORT

No. 195 (2008)

Smoke filling in large spaces using BRANZFIRE

C.A. Wade and A.P. Robbins

FUNDED BY
THE BUILDING
RESEARCH LEVY
BUILDING RESEARCH

The work reported here was funded by Building Research Levy.

ISSN: 1178-4938

Preface

This report has been prepared to provide guidance on modelling smoke filling in large spaces using the fire zone model BRANZFIRE.

Acknowledgments

This work was funded by the Building Research Levy.

Note

This report is intended for fire engineers, users of fire zone models, and regulators or reviewers of fire safety designs where fire zone models have been used to simulate smoke transport.

Smoke filling in large spaces using BRANZFIRE

BRANZ Study Report SR 195

C. A. Wade and A.P. Robbins

Reference

Wade CA and Robbins AP. 2008. 'Smoke Filling in Large Spaces Using BRANZFIRE'. BRANZ *Study Report 195*. BRANZ Ltd, Judgeford, New Zealand.

Abstract

This study provides guidance to fire engineers, design reviewers and regulators regarding the limitations and appropriateness of using a two-zone fire model to simulate smoke development in large spaces. Smoke filling of seven enclosures ranging in area from 625–5000 m^2 and height 6–12 m was simulated using the zone model BRANZFIRE and the computational fluids dynamics model FDS and the results were compared. For the cases examined, it was found that the BRANZFIRE zone model provides good agreement with FDS for room areas up to about 1200 m^2. Multicell (virtual room) simulations were also investigated using the zone model and were found to provide more realistic representation of the smoke layer position compared to a zone model single room simulation, however average gas temperatures may be overestimated close to the fire plume and underestimated far from the plume. It was recommended that for larger enclosures up to 5000 m^2, additional simulations and sensitivity analysis should be conducted subdividing the enclosure into virtual rooms as well as a single zone simulation.

CONTENTS .... PAGE

Figures Page

Nomenclature

A_f	=	floor area (m^2)
c_p	=	specific heat
$\dot{h}_U, \dot{h}_L$	=	enthalpy gain/loss to the upper or lower layer (kJ)
$\dot{M}_u, \dot{M}_l$	=	rate of change of mass in the upper or lower layer (kg/s)
$\dot{m}_p$	=	plume entrainment rate (kg/s)
$\dot{m}_f$	=	mass loss rate of fuel (kg/s))
$\dot{m}_o$	=	mass flow rate leaving through vent (kg/s)
$\dot{m}_d$	=	door mixing flow (kg/s)
$\dot{m}_i$	=	mass flow rate entering through vent (kg/s)
P	=	offset pressure at the elevation of the floor (Pa)
$\dot{Q}_f$	=	combustion energy from the fire (kW)
T_u, T_l	=	temperature of the upper or lower layer (K)
V_R	=	room volume (m^3)
V_u, V_l	=	volume of upper or lower layer (m^3)
$Y_{s,u}, Y_{s,l}$	=	mass fraction of species in the upper or lower layer (-)
$Y_{s,\infty}$	=	mass fraction of species in ambient conditions (-)
Z	=	layer height above floor (m)
ρ_u, ρ_l	=	density of the upper or lower layer (kg/ m^3)
Ψ_s	=	mass generation rate of species per unit mass of fuel burned (kg/kg)
γ	=	ratio of specific heats

1. INTRODUCTION

1.1 Motivation

This study was motivated by a lack of knowledge and uncertainty about the applicability and limitations of simple two-zone fire models for predicting smoke transport and development of hazardous conditions in large spaces. While sophisticated computational fluid dynamics models are readily available for this purpose, they are expensive to run in terms of computation time, and therefore zone models with much shorter set-up and run times are an attractive option provided they can be applied in ways that can reliably produce conservative assessments of the smoke hazard.

The perceived issue or potential problem with using a simple zone model for fire hazard calculations in a large space depends on how the results are used. Applying a zone model is straightforward, and providing the fire is large enough to ensure that the combustion gases reach the ceiling (and do not become stratified at a lower height), the zone model calculation of the *average* upper layer temperature is then valid. However, the extent to which the properties of the layer are uniform over the cross-section of the compartment can be debated. If the smoke loses buoyancy at the far ends of an enclosure the interface height will not be constant, with the layer being cooler and thicker further away from the fire plume. This has ramifications if tenability assessment is based on the position of the layer interface relative to the location of occupants during escape.

1.2 Objective

The objective of this study was to provide guidance to fire engineers, design reviewers and regulators regarding the limitations and appropriateness of using two-zone fire models for predicting smoke transport in large enclosures. Specific reference is made to the BRANZFIRE model for simulating smoke spread and development of hazardous conditions in large spaces, but conclusions may also be valid for other similar models.

1.3 Scope

This study is based on a comparative analysis between the two-zone fire model BRANZFIRE and the computational fluid dynamics (CFD) model Fire Dynamics Simulator (FDS) where each is used to model smoke transport in seven enclosures ranging in area from 625 m^2 to 5000 m^2 and 6 to 12 m in height. Enclosure volumes were in the range 3,750 to 60,000 m^3. The enclosures were intended to be representative of light industrial or storage-type buildings.

A single design fire comprising a fast t^2 fire growing to a peak of 10 MW was modelled in each case. The simulations assume relatively simple building geometry and non-complicated flat ceiling profiles.

The study is only concerned with application and limitations of two-zone fire models in large area spaces.

2. BACKGROUND

2.1 Zone models

2.1.1 General

Two-zone fire models represent the fire environment within an enclosure as two homogenous layers, comprising an upper smoke layer and a lower ambient layer.

Some common two-zone fire models include BRANZFIRE (Wade 2004, Wade 2007), CFAST (Jones et al 2000) and BRI2002 (Tanaka and Yamada 2004). A general overview of representative zone fire models is provided by Walton (2002).

2.1.2 Mathematical description

Conservation of mass and energy leads to a set of first order differential equations which allow the upper layer volume, upper and lower layer temperatures, and the pressure equation to be solved. The forms of the equations are as given by Peacock et al (1993). The equation for the pressure in the room is:

$$\frac{dP}{dt} = \frac{\gamma - 1}{V_R}(\dot{h}_L + \dot{h}_U)$$

The pressure is nominally the pressure at the elevation of the floor and is relative to the atmospheric pressure at a nominated reference elevation. The offset pressure is used to avoid unnecessary loss of significant digits when solving vent flow equations, where the pressure differences across the vent are very small.

The net enthalpy gain $\dot{h}_U$ to the upper layer control volume is the sum of the vent flow enthalpies $\Sigma \dot{m} c \Delta T$, the enthalpy of the plume flow entrainment $\dot{m}_p c \Delta T$, net radiation absorption/emission from the gas layer (due to radiation exchange between surfaces), as well as the convective portion of the combustion energy from the fire source $\dot{Q}_f$.

The equation for the volume of the upper layer becomes:

$$\frac{dV_u}{dt} = \frac{1}{\gamma P}\left[(\gamma - 1)\dot{h}_U - V_U \frac{dP}{dt}\right]$$

The lower layer volume is the difference between the room volume (a constant) and the upper layer volume. The height of the smoke layer interface above the floor for a room of uniform area and flat ceiling is then given by:

$$Z = \frac{V_R - V_u}{A_f}$$

The equation for the temperature of the upper layer is:

$$\frac{dT_u}{dt} = \frac{1}{c_p \rho_u V_u}\left[\dot{h}_U - c_p \dot{M}_U T_u + V_u \frac{dP}{dt}\right]$$

The equation for the temperature of the lower layer is:

$$\frac{dT_l}{dt} = \frac{1}{c_p \rho_l V_l}\left[\dot{h}_l - c_p \dot{M}_l T_l + V_l \frac{dP}{dt}\right]$$

The equations for the rate of change of mass in the upper and lower layers are given by:

$$\frac{dM_u}{dt} = \dot{m}_p + \dot{m}_f + \dot{m}_d - \dot{m}_o$$

$$\frac{dM_l}{dt} = \dot{m}_i + \dot{m}_d - \dot{m}_p$$

Species (e.g. soot, CO, CO2) are modelled as 'gas' species uniformly distributed throughout a layer. The applicable mass conservation equations for the respective layers are:

$$\frac{dY_{s,u}}{dt} = \frac{1}{M_u}\left[\dot{m}_p Y_{s,l} + \dot{m}_f \Psi_s - (\dot{m}_d + \dot{m}_w + \dot{m}_o) Y_{s,u} - Y_{s,u}\frac{dM_u}{dt}\right]$$

$$\frac{dY_{s,l}}{dt} = \frac{1}{M_l}\left[\dot{m}_i Y_{s,\infty} - \dot{m}_p Y_{s,l} + (\dot{m}_d + \dot{m}_w) Y_{s,u} - Y_{s,l}\frac{dM_l}{dt}\right]$$

Where:

P = offset pressure at the elevation of the floor (Pa)

$Y_{s,u}$, $Y_{s,l}$ = the respective mass fractions of species in the upper and lower layers

M_u and M_l = the respective masses of the upper and lower layer (kg)

$\dot{m}_p$ = rate of air entrained in the fire plume (kg/s)

$\dot{m}_f$ = fuel mass loss rate (kg/s)

$\dot{m}_d$ = vent/door mixing flow rate (kg/s)

$\dot{m}_o$, $\dot{m}_i$ = air flow rates leaving and entering through the vent respectively (kg/s)

Ψ_s = mass generation rate of species per unit mass of fuel burned (kg/kg).

These mass flow terms are generically illustrated in Figure 1.

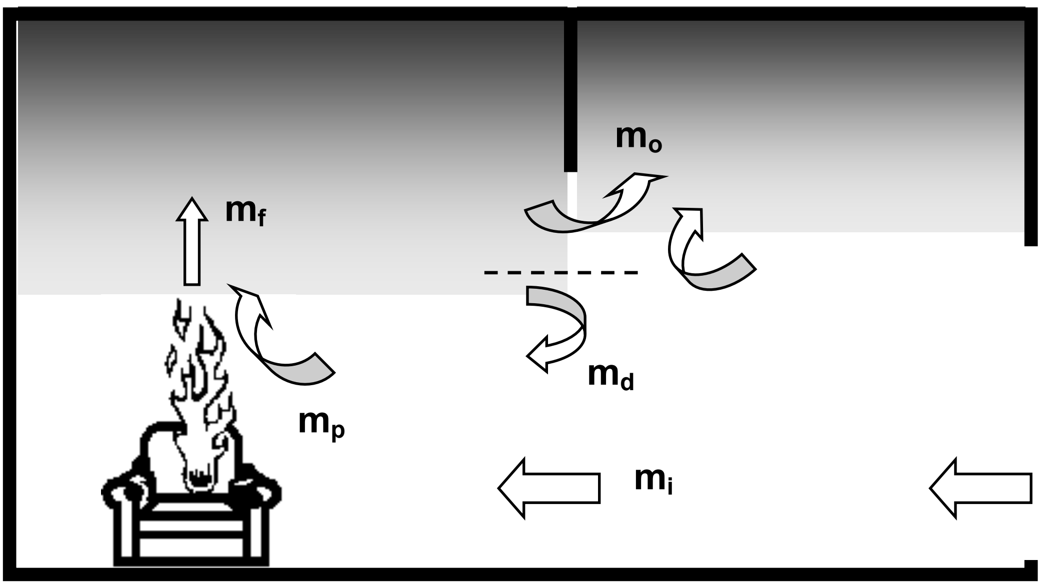

Figure 1. Idealised mass flows in zone-type model

2.1.3 Principal assumptions

Zone models usually require rooms to be represented as rectangle volumes with flat ceilings. The rooms may be connected to the outside with rectangular planar openings (vents) in the walls or ceiling. Rooms may be connected to each other with rectangular shaped door openings or vents included in the connecting walls or floor/ceiling.

The major assumption upon which zone models are premised is that the properties (temperature, density, concentrations) of the gas layer control volumes are uniform at any instant in time. Zone models solve coupled conservation equations of mass and energy but the momentum equations are not explicitly solved. Most zone models use just two control volumes to divide each room into an upper and lower layer. For small rooms this is considered to be a realistic representation of the situation, where smoke rises to the ceiling and fills the room from the ceiling downward, forming a well-stratified hot gas layer.

A fire in a room is treated as a source of fuel released into the fire plume at a prescribed rate. The fuel is converted to a gaseous mass and enthalpy as it burns, in the presence of oxygen, with the combustion products and enthalpy transported into the upper layer control volume via the plume.

Zone models typically do not attempt to predict pyrolysis or the fire growth rate. Rather this is provided by the user as an input. However, some models do include pyrolysis sub-models (including BRANZFIRE) but these are beyond the scope of this study.

The plume provides a mechanism for transporting mass and energy from the fire and ambient entrained air from the lower layer to the upper layer. Empirical correlations are used to determine how much air is entrained into the plume and mixed with the combustion products. The entrainment is a function of the size of the fire and the vertical distance between the fuel and interface layer between the two control volumes.

There are also other means of moving mass and enthalpy between the control volumes, including mixing between the layers at the location of the vents. Again, empirical equations (correlations) are used to determine the magnitude of these transfer flows, and these result in mass being removed from one control volume and being deposited into another. Additional entrainment may also occur for a vent flow into a connected room. All entrainment coefficients are empirically derived.

Vent flows are driven by pressure differences across an opening resulting from variations in gas temperature and density on each side of the vent over its height.

Most zone models allow burning rates to be constrained by low oxygen availability but potential enhancement of the burning rate due to radiation feedback within a room is normally ignored. Where insufficient oxygen is available to ensure complete combustion, unburned fuel may be transported along with the combustion products as a 'species'. Depending on the particular model, it may subsequently be allowed to burn in the upper layer or as it enters another room should there be enough oxygen available there to allow combustion.

2.1.4 Vertical vent flow deposition rules

Zone models use 'rules' to determine how/where mass, enthalpy and products of combustion are exchanged between rooms connected by a vertical vent (e.g. door, windows). For instance, the CFAST model (Peacock et al 1993) uses the simple rule of depositing a vent flow 'slab' that originates from an upper layer into the upper layer of the adjacent room. Similarly, it deposits a vent flow 'slab' that originates from the lower layer into the lower layer of the adjacent room.

The BRANZFIRE model (up to Version 2008.1) applies different deposition rules using those for the CCFM code. This means that:

- For the case where the upper layer in the adjacent room has not yet formed, if the temperature of the slab is more than a specified value (3 K for BRANZFIRE) above the lower layer temperature in the adjacent room, the entire flow is deposited into the upper layer (initiating the formation of the layer), otherwise it is deposited into the lower layer.
- For the case where the lower layer in the receiving room has zero thickness (interface at the floor), if the temperature of the slab is within a specified (3 K for BRANZFIRE) value of the upper layer temperature in the receiving room, the entire slab will be deposited into the upper layer, preventing the lower layer from growing.
- In all other cases, if the temperature of the slab is greater than the upper layer of the receiving room the entire slab is deposited in the upper layer. If the temperature of the slab is less than the lower layer of the receiving room the entire slab is deposited in the lower layer. If the slab temperature falls between the upper and lower layers in the receiving room, the slab flow is divided between the two layers in direct proportion to the temperature differences.

These deposition rules impact on the development of the layer in the receiving room, and on the position of the layer interface height in both rooms. The CCFM rules result in layer development in an adjacent room commencing at an earlier time compared to using the CFAST deposition rules, and often before the layer has dropped below the top of the vent connecting the two rooms. In the latter case (CFAST rules), the adjacent room upper layer will only start once the upper layer in the source room has dropped below the soffit of an open vent connecting the two rooms. CCFM versus CFAST rules only matter for multiple compartment simulations and not in single room models.

2.1.5 Virtual room methodology

A multi-cell approach that divides a large compartment into a number of smaller compartments connected by large (full width/height vents) has been suggested by several authors in the literature as a means of allowing zone models to produce more realistic results in larger compartments. A disadvantage to this approach is that additional uncertainties and propagation of errors in the vent entrainment calculations are accumulated each time gases pass through a vent opening. Jones (2001) stated that for multi-compartment modelling that most zone models produce good agreement for a three room configuration but more data are needed for a larger number of connected rooms.

Rockett (1993) discussed the potential application of pseudo-rooms for large area, low ceiling rooms (or long corridors). He noted that it was an attractive but untested approach, but satisfactory where internal construction such as beams or other structures within the room provide natural subdivisions of the space. He says that where the room walls are smooth and the room is free of internal obstructions, only an arbitrary subdivision with large friction factor equivalent vents is justified. Vents with transom depths selected using ceiling jet flow and a Richardson Number of 1 may give approximately correct ceiling jet spreading times i.e. estimate the thickness of the ceiling jet at the location of the vent and specify a vent with a transom of that depth.

Duong (1990) modelled fires (4 and 36 MW) in an aircraft hangar (94 × 54 × 15 m) using various zone models. The building was modelled using multiple adjacent compartments. The results for the 4 MW fire scenario were in reasonable agreement compared to previous experimental data for all modelling considered. For the 36 MW fire, the model results using FAST over-predicted the experimental results. Also it was noted that selection of the plume equation influenced the model results for the large enclosure. This was attributed to the influence on the heat and mass transfer into the hot layer.

Chow (1996) applied the multi-cell concept to simulate fire in a big compartment (60 x 60 x 3 m high) by subdividing it into sub-compartments. There was a 20 m wide by 3 m high vent to the outside. He investigated 1, 3, 9 and 15 sub-compartments and used the CFAST model. Each sub-compartment was connected to its neighbour with a full height/width opening. Chow concluded that a zone model is suitable for simulating fire in a big space but further experimental verification is necessary. For the 15 cell example, the maximum temperature deviation from the 1 cell case was about 20%.

Hu et al (2005) used a multi-cell concept using CFAST to simulate the smoke filling process due to a fast growing 2 MW fire in a domestic boarding-arrival passage of an airport terminal, 392.5 m long x 7.5 m wide x 3.5 m high with an aspect ratio of about 50. The terminal enclosure was modelled in CFAST using 9, 19, and 29 compartments in series connected with full height/width vents. The results were also compared with FDS simulations. They present comparisons to show that more reasonable results for the layer temperature and the smoke layer interface height are achieved using this multi-cell method compared to using the traditional one room two layer zone model. They also say that better results were achieved when the passage was divided into smaller compartments (i.e. more cells). The impingement time of the smoke flow to reach the end of the passage was noted to be somewhat earlier than that predicted by FDS.

2.1.6 Fire size versus room size

Clearly there must be a relationship between the fire size and the room size within which fire zone models can sensibly be applied. The fire must be large enough for there to be sufficient enthalpy in the plume to drive the fire gases to the ceiling, where they are assumed to instantaneously spread, forming a uniform hot layer that increases in volume and depth over time. Collier and Soja (1999) previously suggested a minimum fire size of ~0.1 kW per m^3 of compartment volume as a guide for ensuring establishment of a hot layer.

If the fire is too small, ambient temperature variations over the height of the space may result in a stratified layer at some distance below the ceiling. However, in practical applications involving transient growing fires (e.g. t-squared) there will always be an initial period where the fire size is small compared to the ceiling height. During this period, the predicted smoke layer height from a zone model cannot be relied on. However, it is also likely that at this early stage the fire conditions will not be life threatening.

The presence of a stable smoke-air layer structure is governed by the Richardson Number (Ri) (van de Leur et al 1989). A stratified flow occurs when Ri > 0.8 and stratification is lost when Ri < 0.8 based on salt water experiments. However, the calculations by van de Leur et al (1989) did not support the use of a critical Richardson Number as a criterion for the occurrence of stratification of a hot smoke layer in a corridor.

$$Ri = \frac{g\Delta\rho Z_s}{\rho_s \Delta U^2}$$

where ρ_s is the density of the local smoke, $\Delta\rho$ is the difference between the local smoke and the air, ΔU is the difference between the local velocity of the upper smoke layer and the lower layer air, g is the gravitational constant and Z_s is the depth of the smoke layer.

At the other extreme, according to US Nuclear Regulatory Commission (USNRC 2007), the ratio of heat release to compartment volume should not exceed about 1 MW/m^3 due to limitations on the numerical routine. The two layer assumption is likely to break down well before this limit is reached.

In tall compartments, the plume entrainment will most likely be over-predicted (particularly based on the McCaffrey plume correlation), thus the layer will be deeper and cooler. This could have a significant impact if the design is to provide smoke extract to raise the layer height. Rockett (1995) gives an example for a 36.6 m high room. BRANZFIRE uses the McCaffrey plume correlation by default to calculate the plume entrainment.

2.1.7 Validation against experimental data

There are very few examples of zone model predictions compared to experimental measurements in large area (>500 m^2) spaces.

Chow et al (2005) compared a set of 19 experiments with fire sizes in the range 1.8 to 5 MW in an enclosure measuring 22.4 x 12.0 x 27 m high (269 m^2) with a simple zone model. Agreement for the average smoke temperature with experiments was considered satisfactory with no more than about 10% deviation. Various mechanical extraction rates were used and the average smoke temperature rise above ambient was relatively low (in the range 21–54 K).

The CFAST model has been subjected to extensive validation by NIST and others. In a recent verification and validation study (USNRC 2007) for nuclear power plant applications conducted by the USNRC and the Electric Power Research Institute, the CFAST model was included and its accuracy assessed for six series of experimental studies. The largest compartment considered was the VTT fire test hall measuring 27 x 14 x 27 m high (378 m^2).

Hinkley (1988) compared measurements by Yamana and Tanaka (1985) in a building 24 x 30 x 26 m high (720 m^2), noting that they found good agreement between the experimental results and their theoretical predictions. Hinkley also compared their measurements with a simple calculation method based on large fire plume theory and found good correlation with the experimental results of Yamana and Tanaka.

2.2 Field models

Fire field models are computational fluid dynamics programs for predicting smoke spread with a much higher spatial resolution compared to a zone model. The enclosure of interest is divided into a large number of cells and the governing equations of fluid dynamics for the conservation of mass, momentum and energy are solved for each. FDS, developed at the National Institute of Standards, is the most commonly used field model for fire applications (McGrattan 2005). It is used in the present study as a benchmark against which the performance of a zone model is assessed.

A relatively small range of studies have included the comparison of zone model and field models and experimental results (Floyd, 2002; Rein, et al., 2006; Merci & Vandevelde, 2007). There are even fewer studies for the validation of field models with experimental results for large volume compartments.

2.2.1.1 Large-compartment field model fire modelling approaches

One of the difficulties encountered when using a field model to simulate a single large compartment is how to apply the mesh. For example, there are no natural divisions where a mesh could be divided and when using a non-uniform mesh must the influence on the resulting estimates must be considered. If a single uniform mesh is used, the advantages are that there are no anomalies at mesh boundaries in the single compartment that must be considered and the uniform mesh makes interpretation of results comparatively more straight forward than when using a non-uniform mesh. However the obvious disadvantage is that computational capacity can be quickly used up.

2.2.1.2 Comparison and validation of field model results

Model results were compared with experimental results for fire tests performed in the containment building for the Heiss-Dampf Reaktor (HDR) facility (Floyd, 2002). This was a decommissioned, experimental nuclear power reactor in Germany. The building was a cylinder 20 m in diameter by 50 m in height topped by a 10 m radius hemispherical dome for a total facility height of 60 m. Internally the building was divided into eight levels with each level further subdivided into smaller compartments. The total free air volume of the facility was 11,000 m³ with 4,800 m³ above the operating deck, which was the topmost floor of the facility.

Several series of fire tests were conducted in this facility and some of the results were compared to model results. Of most interest to the current study were the experiments and subsequent modelling attempts that incorporated the large volume at the top of the facility.

The T52 series of fire tests consisted of four hydrocarbon oil pool tests. The burn room (with a floor area of 8 m² and volume of 24 m³) was adjacent to the curtained room containing the equipment hatch (with a combined floor area of 12 m², and volume of 54 m³) that was open to the dome of the building. The fuel used for the pool tests was Shellsol T (density 761 kg/m³, boiling temperature 191 – 213°C, flashpoint 60°C, and heat of combustion 42,500 kJ/kg). The T52.14 test was chosen for comparison purposes, based on the input burning function having been intentionally generated for a prior international computer modelling effort and since fire models are highly sensitive to the input burning function. FDS (version 2.0) results were in reasonable agreement with the experimental results for the grid of thermocouples located at the base of the hemispherical dome at the top of the facility. However the model underpredicted the width of the plume and predicted a slightly different location for the plume compared to experimental observations. These differences were attributed to the chosen grid resolution and that only a section of the dome was modelled. (Floyd, 2002)

Merci and Vandevelde (2007) considered the different methods of estimating heat and smoke in large compartments including zone models (OZONE and CFAST) and field models (FDS). A generic supermarket (35 x 70 x 4 m) and a sports hall (66 x 95 x 11 m) were used as examples. A uniform mesh was used with grid sizes of 0.5 and 0.25 m. Field model estimates showed general agreement between the results of both mesh sizes, with higher temperatures estimated around the source of the fire. The field model results had varying agreement with the results from the zone models.

3. SCENARIOS MODELLED

3.1 Fire models

3.1.1 Zone model

BRANZFIRE Software Version 2008.1 was used except that for simulations where the 'CFAST vent flow deposition rules' apply then the Version 2008.2 was used. A sample input file is included in Appendix A.1. The example presented is the compartment of dimensions 100 x 25 x 6 m high modelled as a virtual two room simulation.

3.1.2 Computational fluid dynamics model

FDS Version 5.0.7 was used.

A single uniform grid was used in each scenario modelled. Grid sizes of 0.25 m and 0.5 m were considered to assess the impact of the grid size for the smallest of the compartment sizes considered. A grid size of 0.5 m was selected for the analysis of each of the scenarios considered in this study.

Details of the fire specification are described in Section 3.2.2.

Devices were located evenly spaced at 5 m intervals at the ceiling height of the compartment to represent heat detectors and smoke detectors. Temperatures were recorded for the planes at every 5 m interval in the x- and y-directions and at every 1 m interval in the z-direction. The radiant intensity was also recorded for the planes at 1 m and 2 m heights above the floor level. Temperatures were recorded for a virtual thermocouple tree located in the centre of each 25 x 25 m section (or cell) of the compartment, with temperatures recorded at 0.5 m intervals from the floor to the ceiling. For additional comparison with the zone model results, the inbuilt FDS function for integrating over the height of the compartment at specific locations to calculate an effective layer height, upper layer temperature and lower layer temperature was used at 5 m intervals in the x- and y-directions.

An ambient temperature of 20°C and 60% relative humidity was assumed within and outside of the building. Building materials were also assumed to have an initial temperature of 20°C throughout.

A sample input file is included in Appendix A.2. The example presented is for the compartment of dimensions 25 x 25 x 6 m high.

3.2 Scenario description and common features

3.2.1 Enclosure construction and ventilation

The enclosures were all assumed to be of rectangular shape with a flat ceiling. Sheet steel was assumed for the walls and ceiling/roof with a concrete floor. The sheet metal was assumed to have the emissivity (1.0), density (7850 kg/m³), thermal conductivity (45.8 W/m.°C) and specific heat (0.46 kJ/kg.°C) of mild steel. The sheet metal was assumed to be thermally thin, with a thickness of 5 mm.

A fully open vent (door) measuring 1 m wide x 2 m high were included in the wall for each 625 m^2 (25 x 25 m) of floor area i.e. there was only one vent for the

25 x 25 m enclosure, while there were eight vents for the 100 x 50 m enclosure. There were no ceiling/roof vents included.

3.2.2 Design fire

In all cases the same design fire was used. The HRR of the fire followed a fast-t^2 curve reaching a 10 MW peak after 461 seconds and constant thereafter as shown in Figure 2. The fire area was taken as 2 x 2 m located at floor level, with the plume centreline located near the corner of the compartment at a horizontal distance of 5 m from each wall. This location was chosen to maximise the smoke travel paths without introducing significant wall effects. However, while FDS allows the fire to be precisely located in the compartment, BRANZFIRE only allows a centre location in the room of fire origin for entrainment to take place on all sides.

The fuel was assigned the following properties.

Heat of combustion	41.2 kJ
Radiant loss fraction	0.33
Carbon monoxide yield	0.006 kg/kg
Soot yield	0.015 kg/kg

The exact parameters for the design fire were not considered to be critical since this study is primarily of a comparative nature (i.e. the same fire specification was used in both the BRANZFIRE and FDS simulations), although it was intended that the design fire be representative of what might be used in practice for a building of this size.

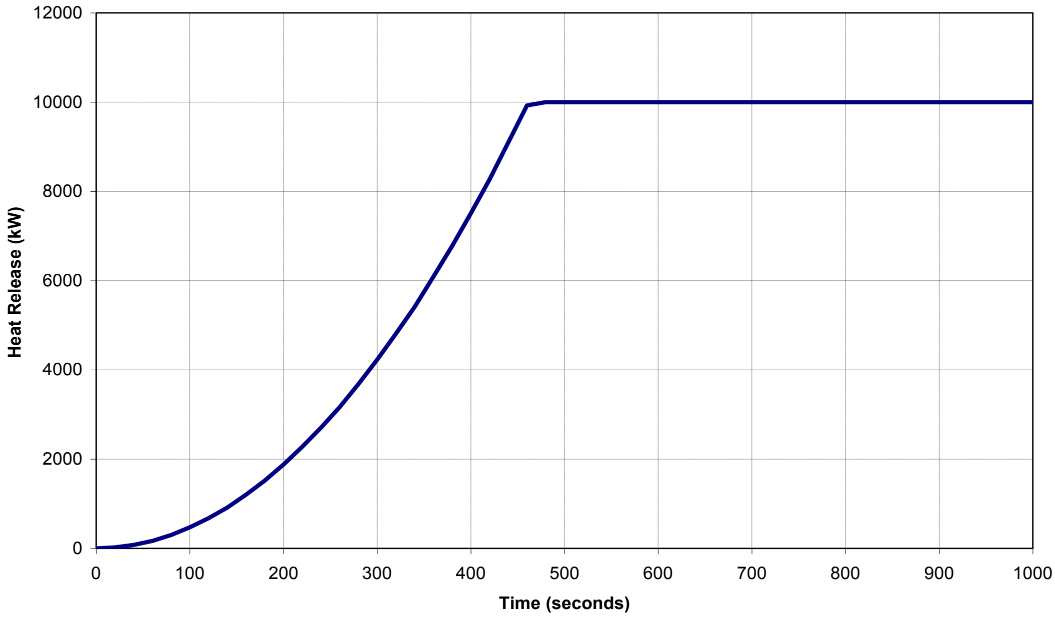

Figure 2. Heat release rate versus time

3.2.3 Explanation of results – terminology

In the following graphs, that compare results obtained using the BRANZFIRE and the FDS models, the FDS results are presented by plots labelled FDS x, y where x and y refer to the coordinates (in metres) in plan view relative to the corner of the enclosure, designating the location of interest within the enclosure. The fire is assumed to be located at a position x= 5 m, y = 5 m from the corner as shown in Figure 3.

Each room is divided into a number of different combinations of virtual rooms or cells. For each room the designation is Z*a*-R*b*, where *a* is the total number of cells used for the particular combination and *b* is the particular cell considered where the numbering is from left to right, starting at the location of the fire.

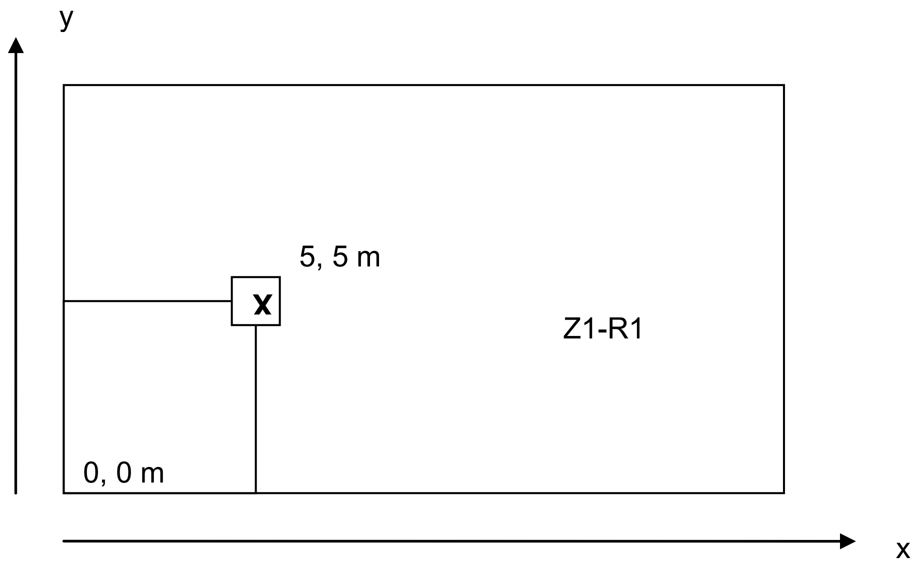

Figure 3. Enclosure schematic and label notation (plan view)

3.2.4 Explanation of FDS effective layer results

CFD results do not automatically include an estimation of an effective layer height. However for purposes of comparison between CFD results and zone model results, the location of the smoke interface can be estimated using the results over the height of the compartment for a specified x- and y-location.

FDS has an inbuilt function that integrates the temperature profile over a specified height at a specified x- and y-location (McGrattan, Klein, et al., 2007). This provides estimates for the layer height and average temperatures for the effective upper and lower layers.

An example is shown in Figure 4 of the comparison of the results for a virtual thermocouple tree located at the centre of the 25 x 25 x 6 m compartment (12.5, 12.5) with the results for the four surrounding points at which estimates of layer height and average upper and lower layer temperatures were calculated.

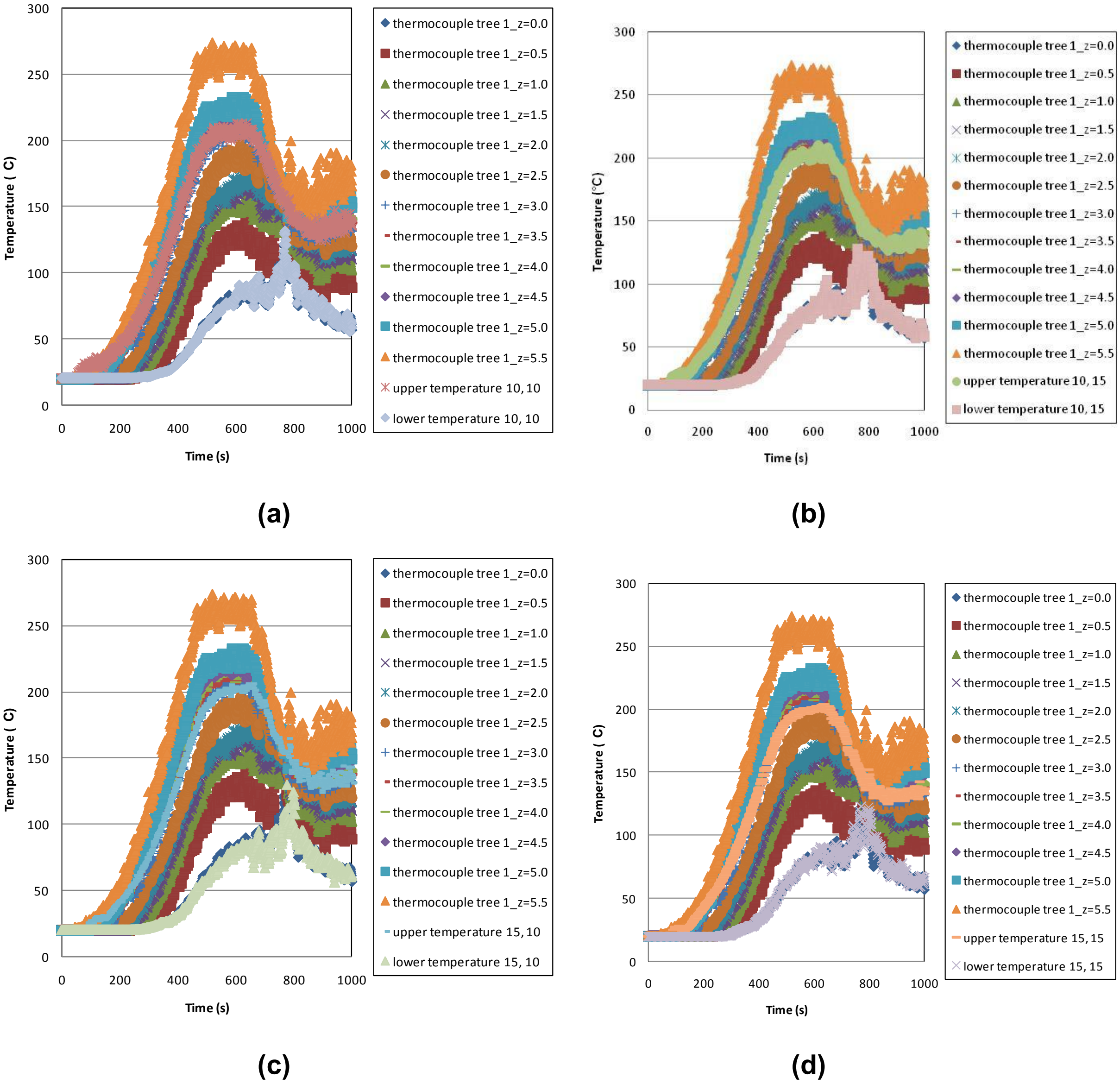

Figure 4. Thermocouple tree temperatures compared with upper and lower layer temperatures surrounding the thermocouple tree position for the 0.25 m uniform grid.

3.2.5 FDS grid size

The grid size to be used for the FDS modelling approach was considered initially, in order to determine the grid size to be used for all the runs using FDS. Uniform grid sizes of 0.25 m and 0.5 m were considered. The 25 x 25 x 6 m scenario was used for comparison of estimated layer height and upper- and lower-layer temperatures and the temperatures in the middle of the compartment.

The results for the two grid sizes had good agreement remote from the fire (i.e. in the far field) for the layer height (Figure 5(a)), upper layer temperature (Figure 5(b)) and lower layer temperature (Figure 5(c)). The largest differences between the results for each of the grid sizes occurred at the central location of the fire, i.e. the location denoted as (5,5). This is expected, since there is a relatively large variation in the values for each of these parameters at this location for both grid sizes considered (e.g. Figure 118 and Figure 121 for layer height, Figure 119 and Figure 122 for upper layer temperature, and Figure 120 and Figure 123 for lower layer temperature). Variation in parameters is expected directly over the location of the fire.

The virtual thermocouple tree temperatures had a maximum of 40% difference between the grid sizes considered. However the majority of thermocouple tree temperatures were within 20%. Considering that the thermocouple tree temperatures represent temperatures at individual points in space, variation in the local conditions is expected and the difference between the results for each of the grid sizes is reasonable.

More detailed results are included in Appendix B.

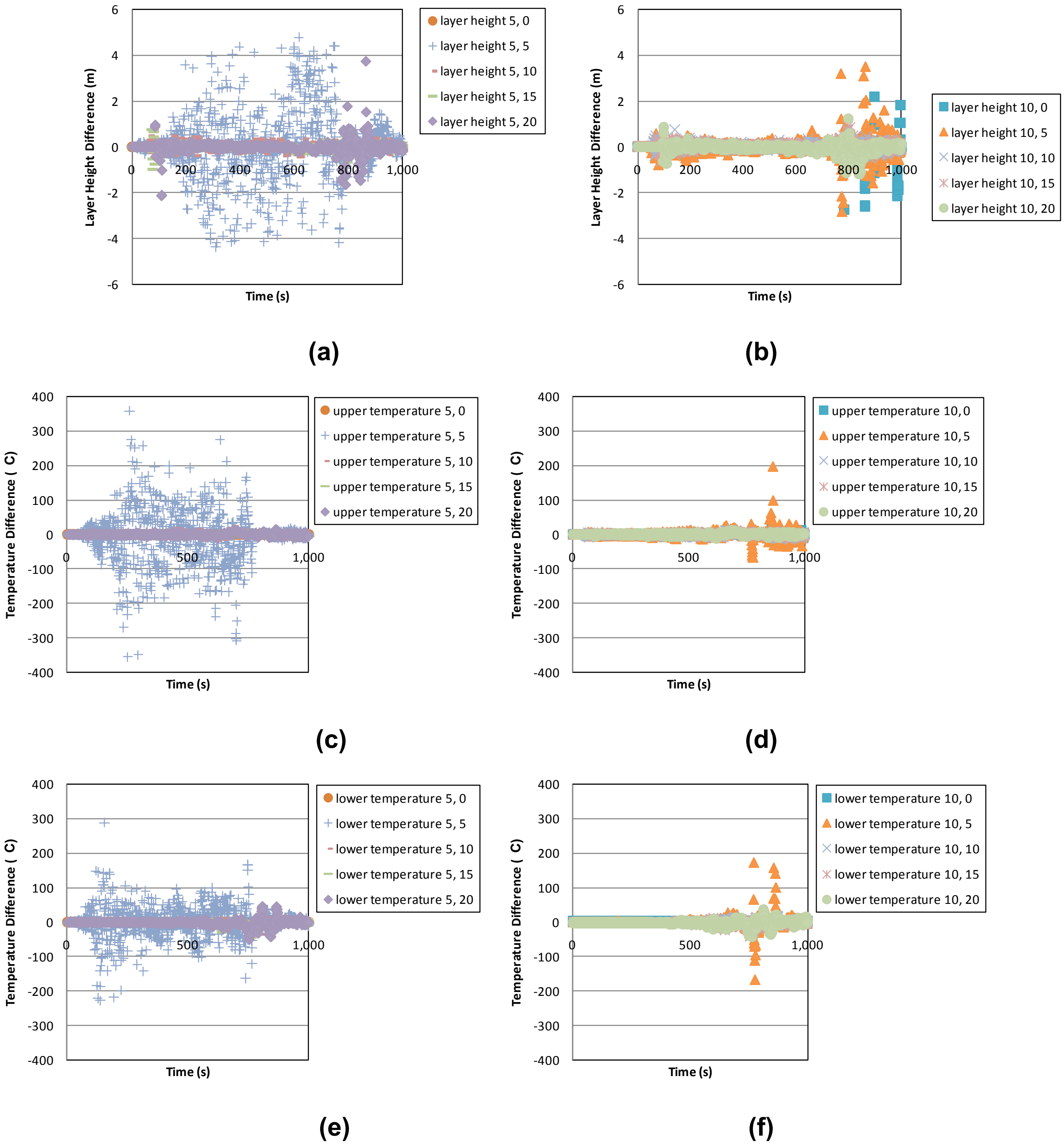

Figure 5. Examples of the comparison of results for the 0.25 and 0.5 m uniform grids for (a) & (b) layer height, (c) & (d) upper layer temperature, (e) & (f) lower layer temperature.

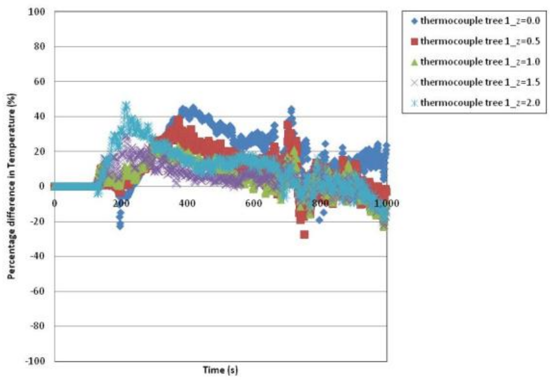

(a)

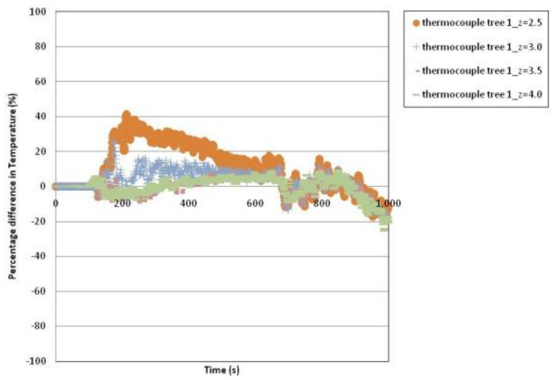

(b)

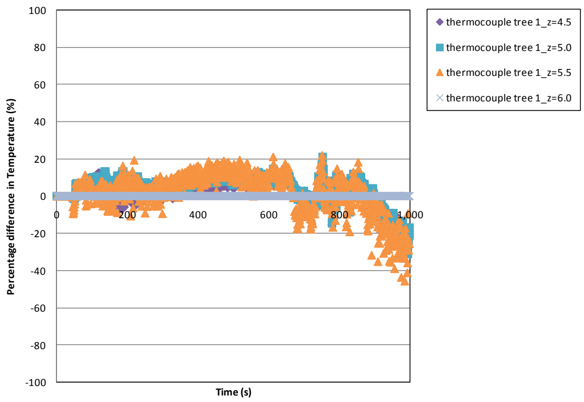

(c)

Figure 6. Examples of the comparison of results for the 0.25 and 0.5 m uniform grids for thermocouple tree temperatures, using the percentage difference between the results for the two grid sizes.

3.3 Results

3.3.1 Enclosure 25 x 25 x 6 m

BRANZFIRE and FDS were used to simulate smoke filling in a single room 25 x 25 x 6 m high with a single vent 2 m high x 1 m wide as illustrated in Figure 7. The FDS data was reduced to an equivalent upper and lower layer by integration of the temperature data over the height of the compartment at the location of interest using functionality provided within the FDS program. This enabled easier comparison of the results from both models.

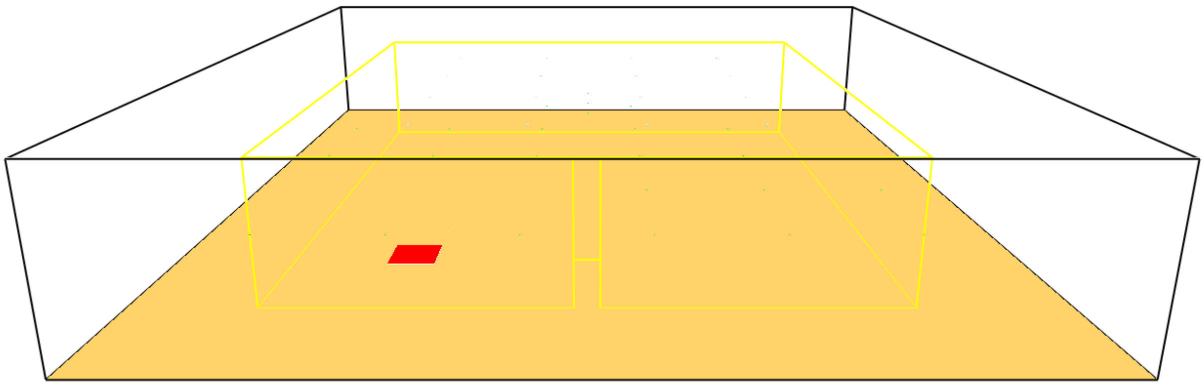

Figure 7. Smokeview representation of 25 x 25 x 6 m compartment showing fire location (in red) and one vent

Figure 8 shows the resulting upper layer temperature as generated by FDS to not vary greatly around the room and it also compares well with the BRANZFIRE prediction of average upper layer temperature.

Gas temperature predictions from FDS at different elevations at the centre of the compartment were compared with the average upper layer temperature from BRANZFIRE, as shown in Figure 9.

The closeness of the upper layer temperature across the enclosure justifies the use of a zone model in this case, provided that the temperature variation over the height of the compartment is not a critical parameter.

Both BRANZFIRE and FDS indicate ventilation-limited conditions as represented by the decay in the upper layer temperature, but it can be seen to occur later with the zone model when compared to FDS.

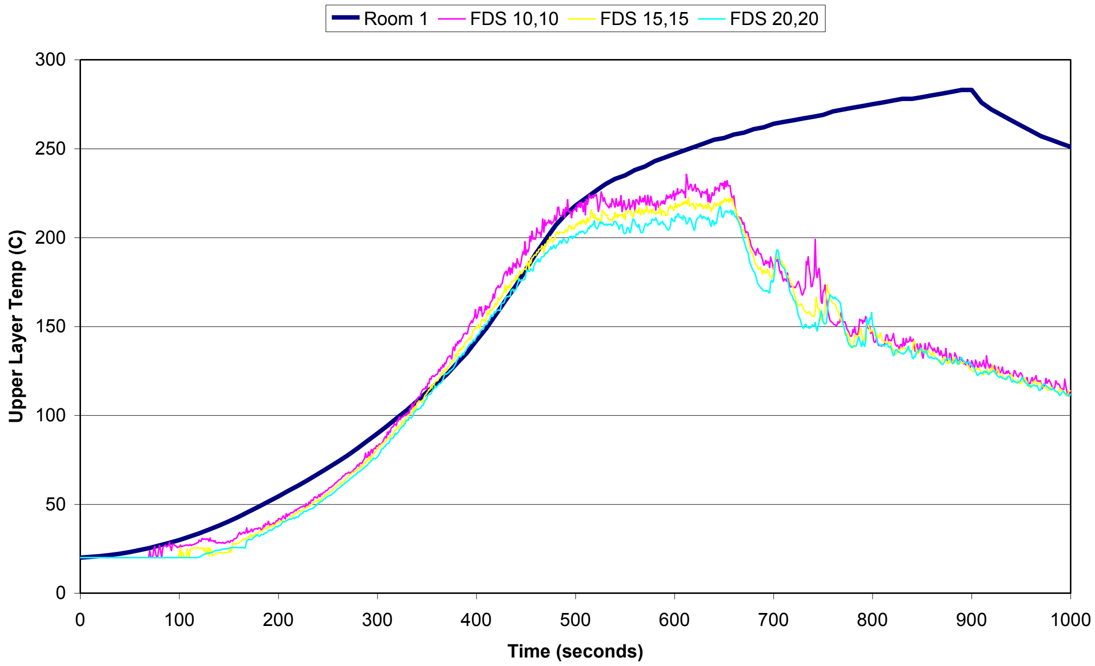

Figure 8. BRANZFIRE upper layer temperature using one room model versus FDS prediction at various locations in the compartment 25 x 25 x 6 m

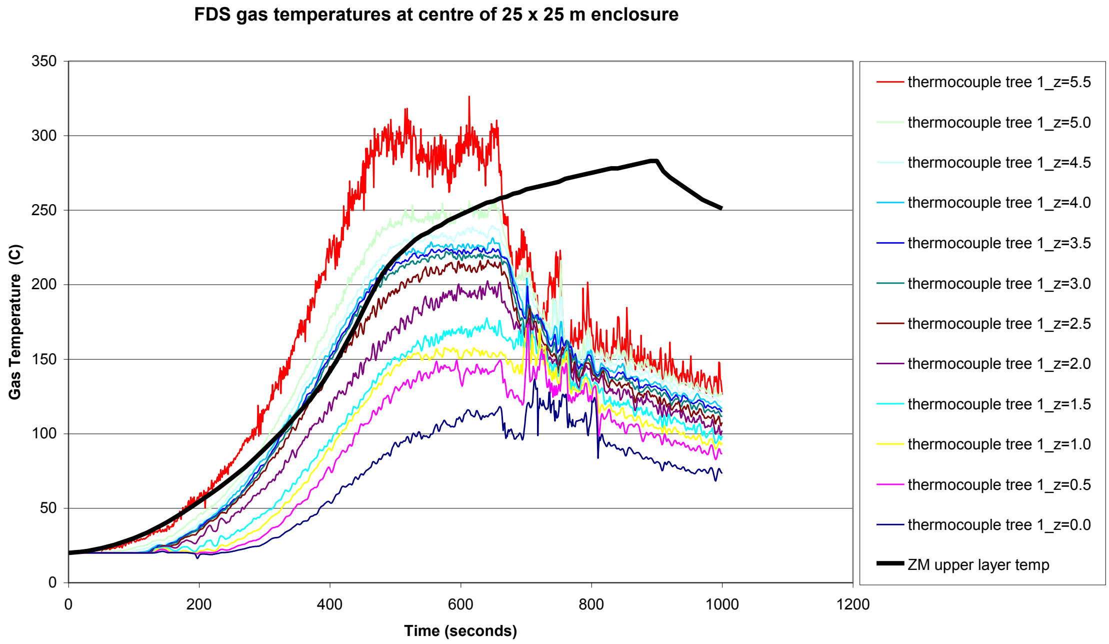

Figure 9. BRANZFIRE upper layer temperature (one room) versus FDS predictions over the height of the enclosure at the centre of the enclosure

Figure 10 shows the predicted height of the layer interface for both models, with the zone model layer almost reaching floor level and well below the layer height determined by FDS. Inspection of the vent flow calculations shows that the zone model calculates a strong outward piston flow through the vent prior to and after the hot layer drops below the top of the vent at 2 m. Two-way 'choked flow' venting is calculated by the zone model to occur after 570 seconds, where the position of the layer interface in the room is below the level of the neutral plane in the vent opening.

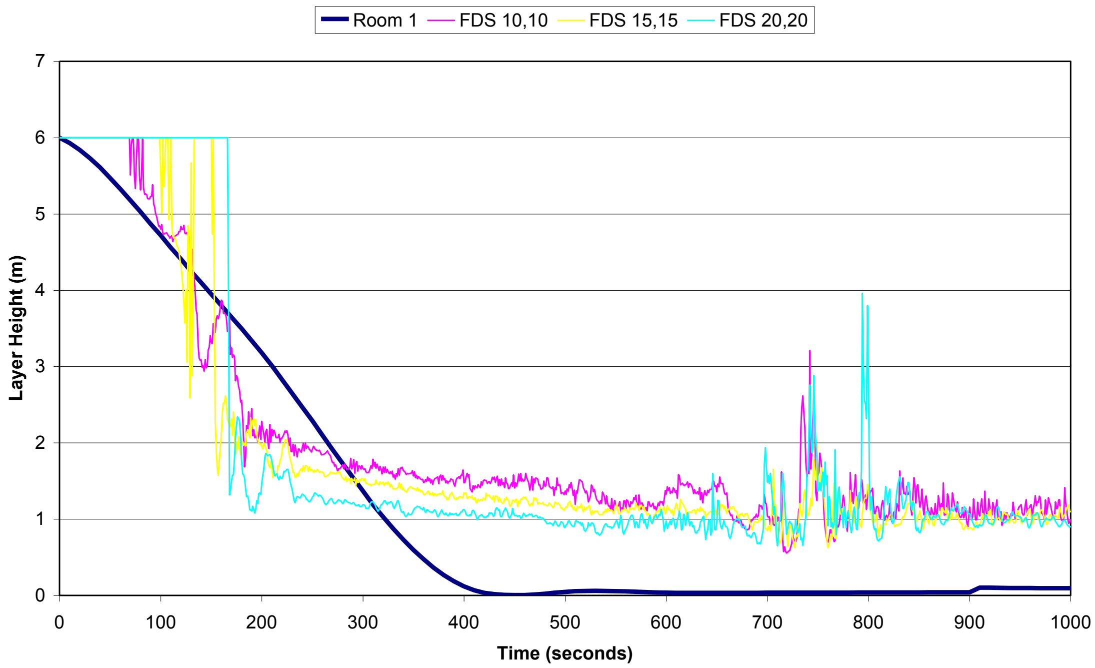

Figure 10. BRANZFIRE layer height using one room model versus FDS prediction at various locations in the compartment 25 x 25 x 6 m

Figure 11 shows the FDS results after 500 and 1000 seconds, using the integrated temperature data to calculate the upper and lower layer temperatures and the layer height. The plots do not cover the complete extent of the compartment area as some of the boundary temperatures were surface rather than gas temperatures. However, the contour colours give a visual indication of the variation around the compartment of the parameter of interest.

Figure 11 confirms the uniformity of conditions around the enclosure and supports the application of a zone model for this case. The relative uniformity around the room, other than over the localised site of the fire, is also observed by the FDS results in Figure 8 and Figure 11.

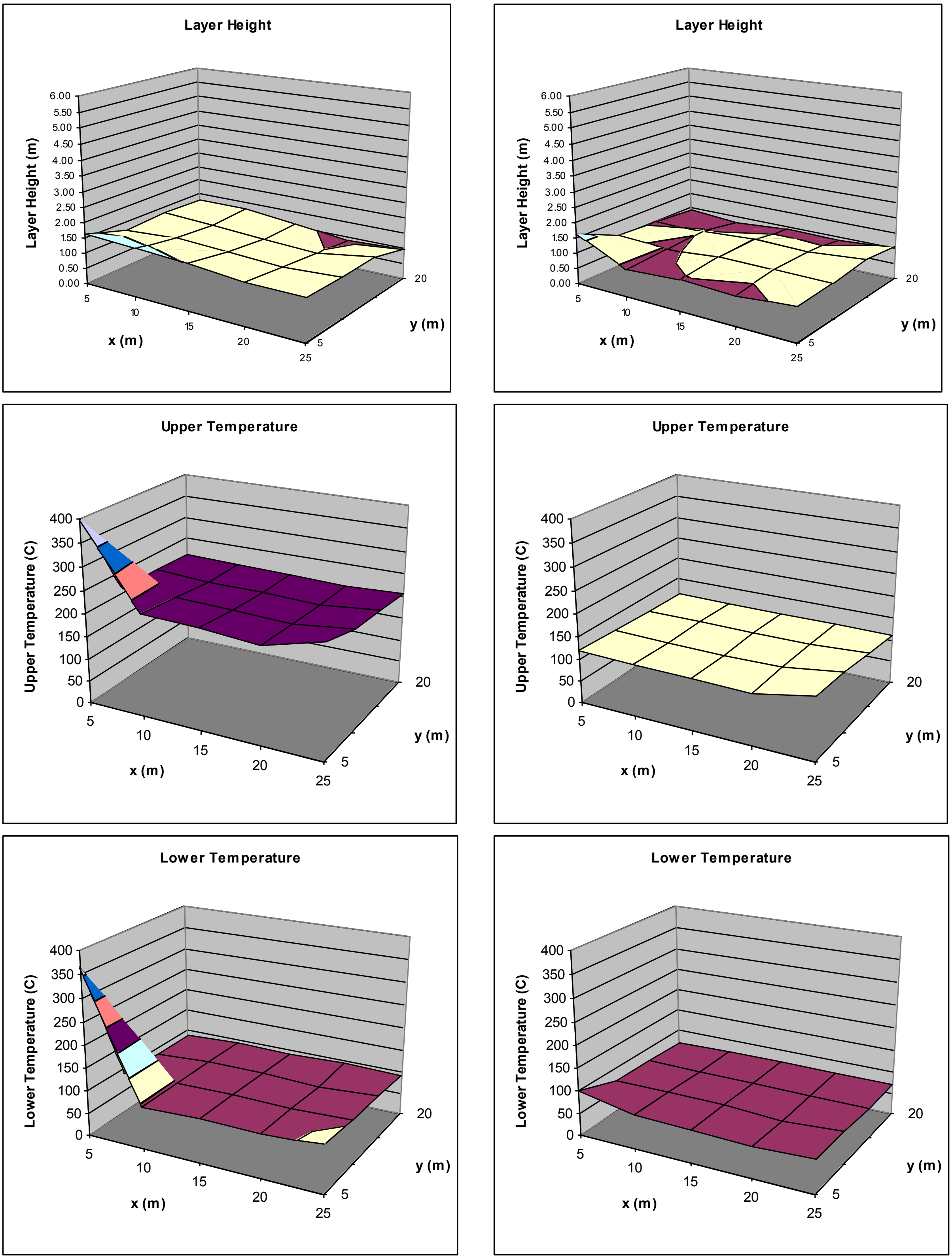

Figure 11. FDS derived predictions of layer height, upper layer temperature and lower layer temperature at 500 seconds (left) and 1000 seconds (right) for 25 x 25 x 6 m high enclosure

3.3.2 Enclosure 50 x 25 x 6 m

BRANZFIRE and FDS were used to simulate smoke filling in a single room 50 x 25 x 6 m high with two openings to the exterior each 2 m high x 1 m wide as illustrated in Figure 12. The FDS data was reduced to an equivalent upper and lower layer, at discrete points around the enclosure, by integration of the temperature data over the height of the compartment at the location of interest using functionality provided within the FDS program. BRANZFIRE was run with the enclosure modelled as one room, and then again as two rooms connected with a full width vent with a 0.6 m transom beneath the ceiling. The transom depth was selected to approximate the depth of the ceiling jet (0.1H). Figure 13 describes the two configurations that were considered.

Figure 12. Smokeview representation of 50 x 25 x 6 m compartment showing fire location (in red) and two vents

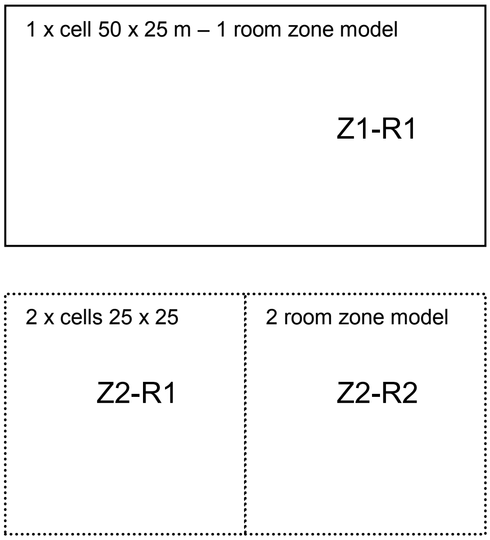

Figure 13. Zone model configurations for 50 x 25 m enclosure (one or two rooms)

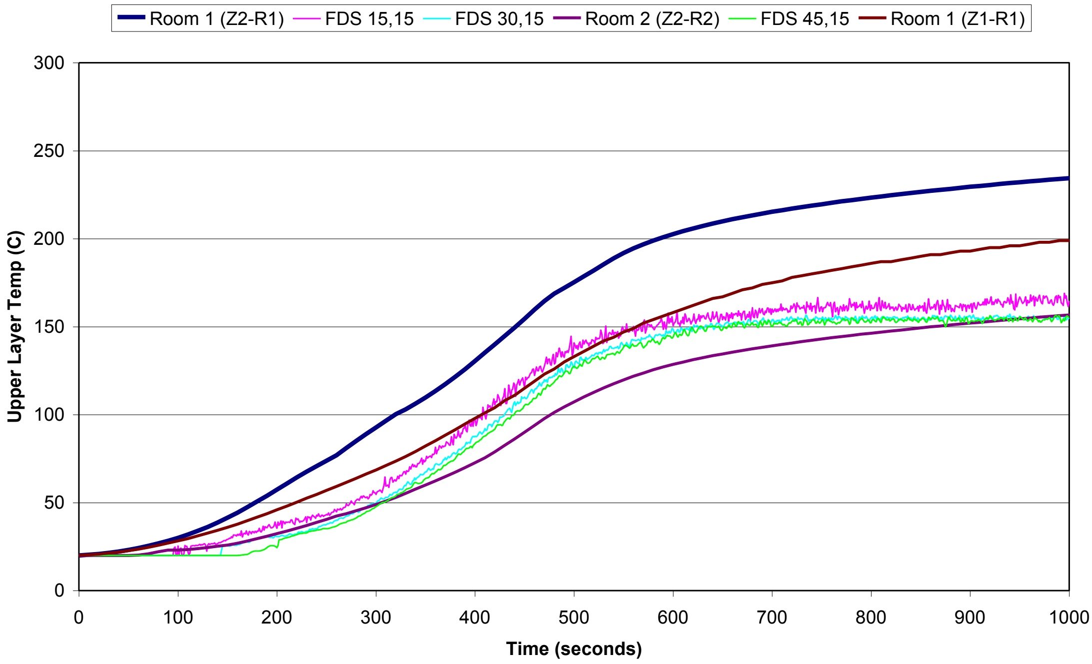

Figure 14. BRANZFIRE (with CCFM rules) upper layer temperatures using one room and two room models versus FDS predictions at various locations in the compartment 50 x 25 x 6 m

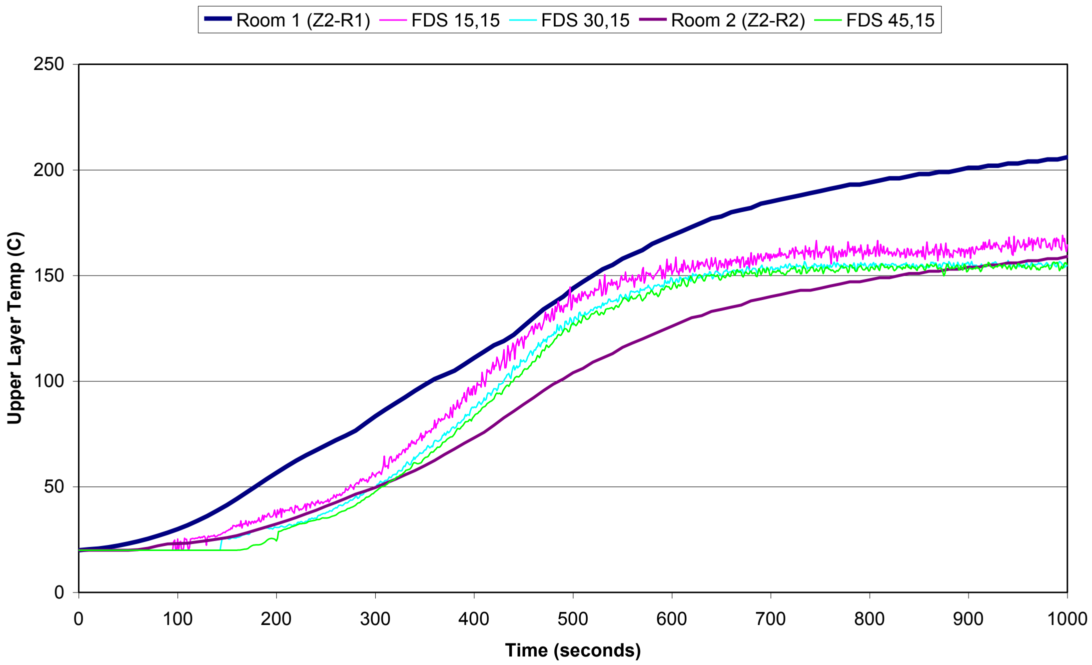

Figure 15. BRANZFIRE (with CFAST rules) upper layer temperatures using two room model versus FDS predictions at various locations in the compartment 50 x 25 x 6 m

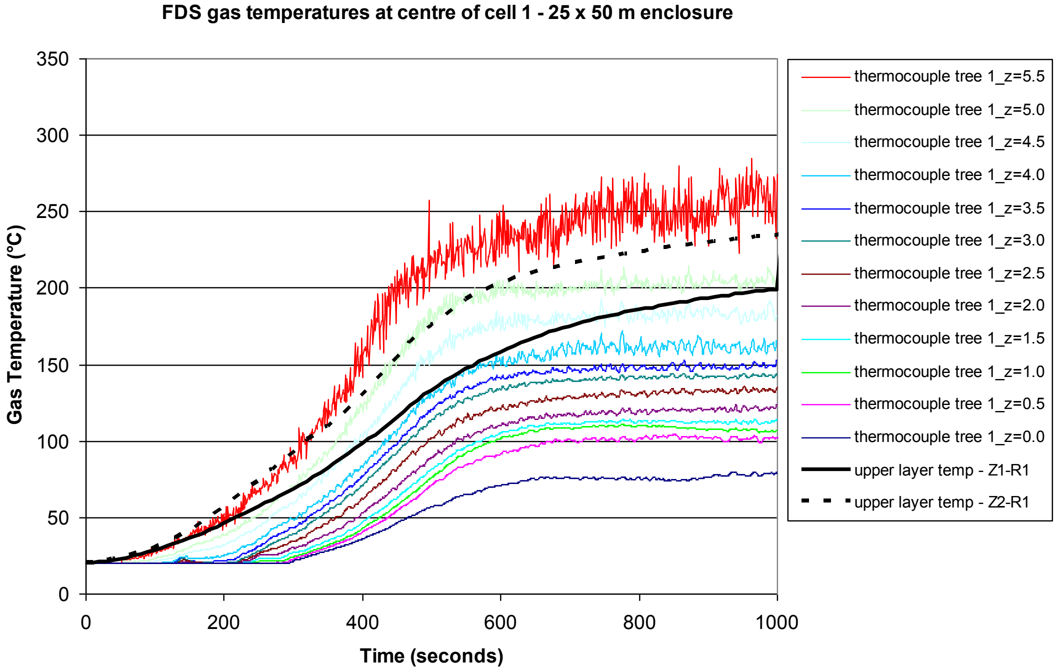

Figure 16. BRANZFIRE (with CCFM rules) upper layer temperatures versus FDS predictions over the height of the enclosure at the centre of compartment Z2-R1

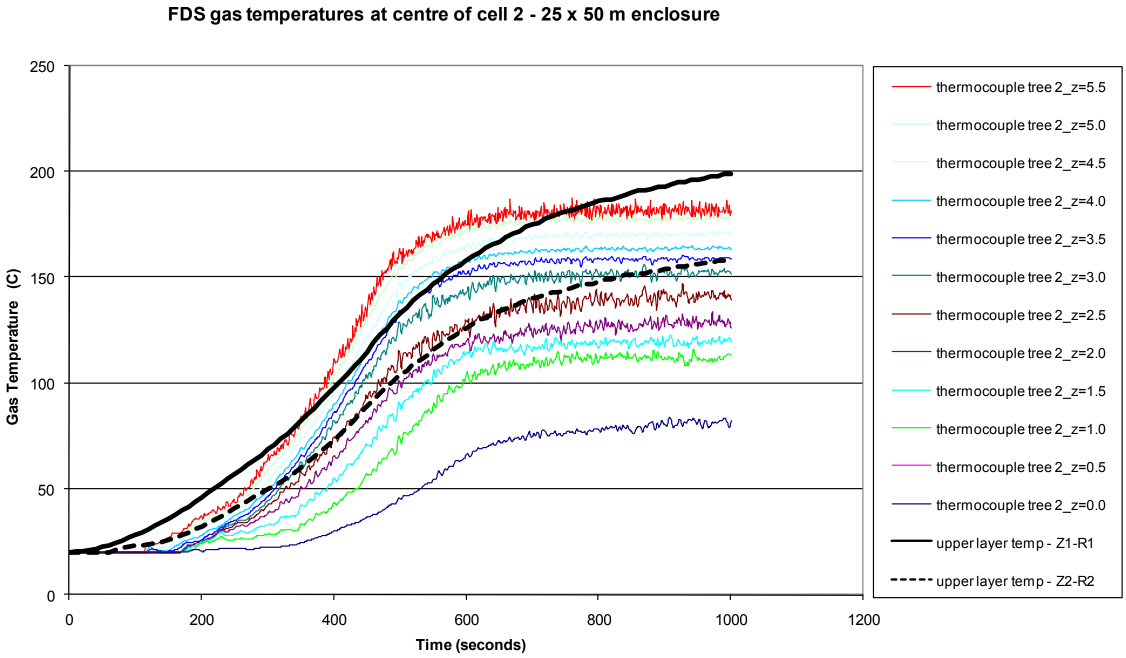

Figure 17. BRANZFIRE (with CCFM rules) upper layer temperatures versus FDS predictions over the height of the enclosure at the centre of compartment Z2-R2

Figure 14 and Figure 15 compare the BRANZFIRE upper layer predictions for the 50 x 25 x 6 m high enclosure using both the one room and two room simulations with FDS upper layer temperatures at various locations around the compartment. On the whole, the single room zone model appears to give the best agreement with the FDS results for average upper layer temperature. However, the two-room results are within the range of temperatures predicted by FDS over the height of the room (see Figure 16 and Figure 17).

Figure 16 compares the FDS predicted gas temperatures at different elevations at the centre of compartment Z2-R1 with: (a) the BRANZFIRE upper layer temperature when the whole compartment is modelled as a single room (solid line) (Z1-R1); and (b) the BRANZFIRE upper layer temperature in the fire compartment when modelled as two rooms (dashed line).

Figure 17 compares the FDS predicted gas temperatures at different elevations at the centre of compartment Z2-R2 with: (a) the BRANZFIRE upper layer temperature when the whole compartment is modelled as a single room (solid line) (Z1-R1); and (b) the BRANZFIRE upper layer temperature in the non-fire compartment when modelled as two rooms (dashed line).

Figure 18 compares the BRANZFIRE layer height predictions for the 50 x 25 x 6 m high enclosure using both the one room and two room simulations with FDS layer height predictions at various locations around the compartment. In the case of the BRANZFIRE simulations, there is much larger divergence between the layer height predictions for the two rooms compared to the FDS predictions. This behaviour is largely driven by the deposition (CCFM) rules for the horizontal flow through the vent.

The zone model simulations shown in Figure 14 and Figure 18 were repeated using the CFAST rules for horizontal vent flow deposition and the results are shown in Figure 15 and Figure 19. This results in BRANZFIRE predicting a slightly lower upper layer temperature in the fire compartment and slightly higher upper layer temperature in the non-fire compartment. However, there is a significant difference in the layer height prediction for the room of fire origin. The behaviour of the layer height in both rooms is now somewhat similar with the layer in both rooms trending toward the floor.

Figure 20 shows the FDS results at 500 and 1000 seconds, using the integrated temperature data to calculate the upper and lower layer temperatures and the layer height. It confirms a drop in the layer interface height with distance from the fire plume.

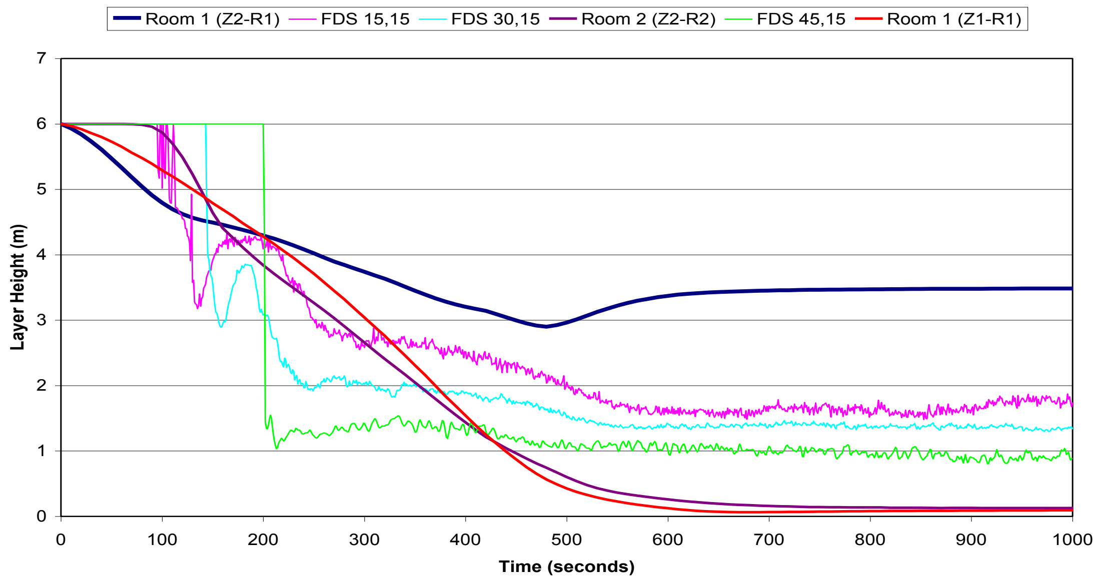

Figure 18. BRANZFIRE (with CCFM rules) layer interface height using one room and two room models versus FDS predictions at various locations in the compartment 50 x 25 x 6 m

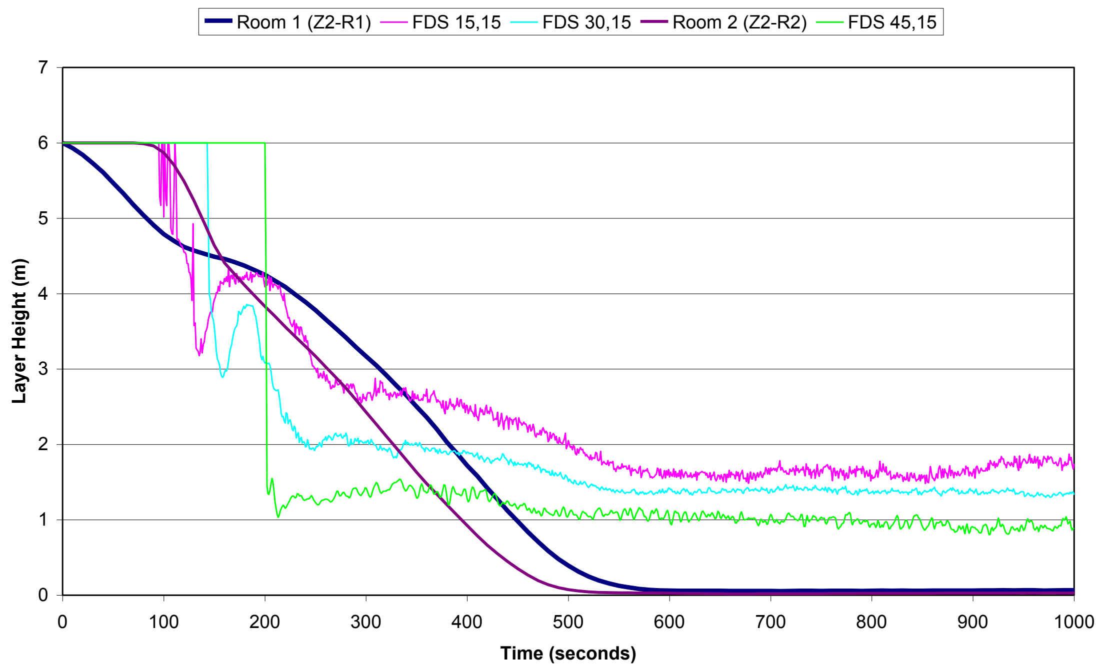

Figure 19. BRANZFIRE (with CFAST rules) layer interface height using two room model versus FDS predictions at various locations in the compartment 50 x 25 x 6 m

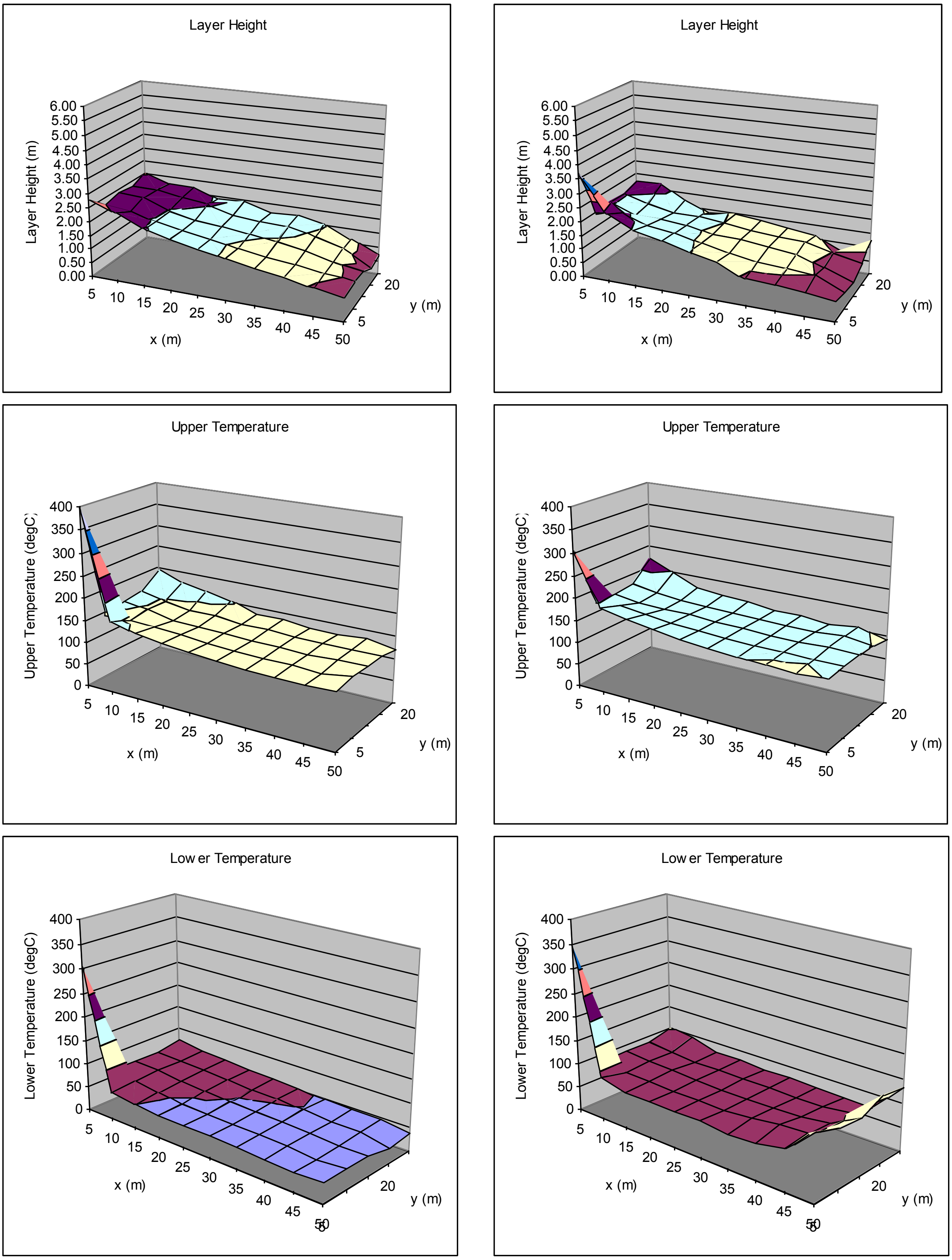

Figure 20. FDS derived predictions of layer height, upper layer temperature and lower layer temperature at 500 seconds (left) and 1000 seconds (right) for 25 x 50 x 6 m high enclosure

3.3.3 Enclosure 75 x 25 x 6 m

BRANZFIRE and FDS were used to simulate smoke filling in a single room 70 x 25 x 6 m high with three openings each 2 m high x 1 m wide as illustrated in Figure 21. The FDS data was reduced to an equivalent upper and lower layer, at discrete points around the enclosure, by integration of the temperature data over the height of the compartment at the location of interest using functionality provided within the FDS program. BRANZFIRE was run with the enclosure modelled as one room, and then again as two rooms and three rooms connected with a full width vents with a 0.6 m transom beneath the ceiling. Figure 22 describes the three configurations that were considered.

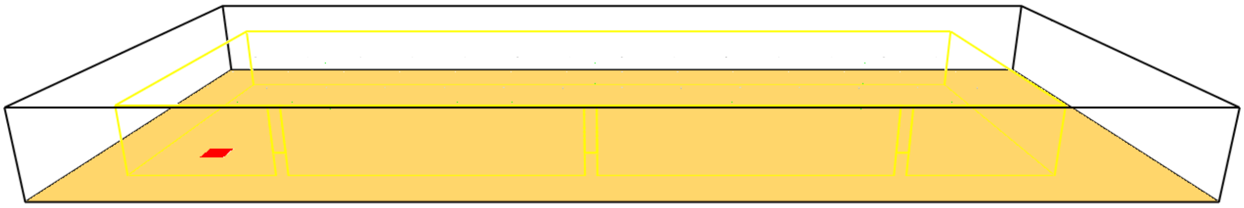

Figure 21. Smokeview representation of 75 x 25 x 6 m compartment showing fire location (in red) and three vents

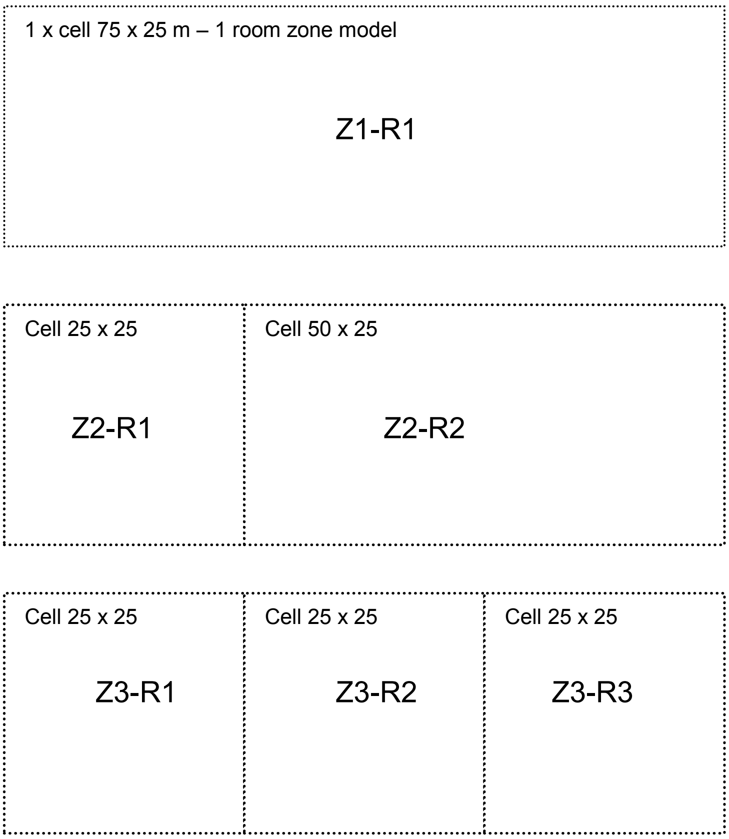

Figure 22. Zone model configurations for 75 x 25 m enclosure (one, two or three rooms)

Figure 23 compares the upper layer temperatures using a single room zone model with average upper layer temperatures from FDS at various locations in the enclosure. The zone model prediction is within the range of upper layer temperatures predicted by FDS but would not necessarily be conservative for design purposes.

Figure 24 compares the upper layer temperatures using a two room zone model with average upper layer temperatures from FDS at various locations in the enclosure. The zone model predictions provide a conservative (higher) estimate of the average upper layer temperatures when compared to those predicted by FDS for the room of fire origin. The average upper layer prediction for the adjacent room is also in close agreement with FDS.

Figure 28 compares the FDS predicted gas temperatures at different elevations at the centre of cell Z3-R1 with: (a) the BRANZFIRE upper layer temperature when the whole compartment is modelled as a single room (solid line) (Z1-R1); (b) the BRANZFIRE upper layer temperature in the fire compartment when modelled as two rooms (dashed line) (Z2-R1), and (c) the BRANZFIRE upper layer temperature in the fire compartment when modelled as three rooms (dotted line) (Z3-R1).

Figure 29 compares the FDS predicted gas temperatures at different elevations at the centre of cell Z3-R2 with: (a) the BRANZFIRE upper layer temperature when the whole compartment is modelled as a single room (solid line) (Z1-R1); and (b) the BRANZFIRE upper layer temperature in the non-fire compartment when modelled as two rooms (dashed line) (Z2-R2), and (c) the BRANZFIRE upper layer temperature in the first non-fire compartment when modelled as three rooms (dashed line) (Z3-R2).

Figure 30 compares the FDS predicted gas temperatures at different elevations at the centre of cell Z3-R3 with: (a) the BRANZFIRE upper layer temperature when the whole compartment is modelled as a single room (solid line) (Z1-R1); and (b) the BRANZFIRE upper layer temperature in the non-fire compartment when modelled as two rooms (dashed line) (Z2-R2), and (c) the BRANZFIRE upper layer temperature in the second non-fire compartment when modelled as three rooms (dashed line) (Z3-R3). The single-cell approach provided an average upper layer temperature that was more conservative than the highest FDS-predicted temperature at the centre of the third cell.

Figure 31 compares the layer height for the same case. The zone model predicts a slower initial descent of the layer compared to FDS, but then is ultimately closer to the floor in the latter stage.

Figure 32 compares the layer height for the same two room case. The zone model predicts a slower initial descent of the layer compared to FDS, but then is ultimately closer to the floor in the latter stage. Again, in the case of the BRANZFIRE simulations, there is significant divergence between the layer height predictions for the two rooms compared to the FDS predictions resulting from the application of the CCFM deposition rules for the horizontal flow through the vent.

Figure 25 and Figure 33 show the comparison again for the two room zone model using the CFAST deposition rules. Overall these show better (and more conservative) agreement with the FDS predictions than for the one room model.

Figure 26, Figure 27, Figure 34 and Figure 35 compare the three room zone model results using CCFM and CFAST deposition rules with FDS predictions. Compared to the FDS-estimated upper layer temperatures, the 3-cell approach provided a conservative estimate for the first cell, but an underestimate for the third cell. Therefore there appears to be no advantage to using the three room model over the two room model for the arrangements considered here.

Figure 36 shows the FDS results after 500 and 1000 seconds, using the integrated temperature data to calculate the upper and lower layer temperatures and the layer height. It clearly shows the increasing layer thickness across the enclosure in the far field. As expected the gradient in the layer height is more pronounced at 500 seconds compared to that at 1000 seconds.

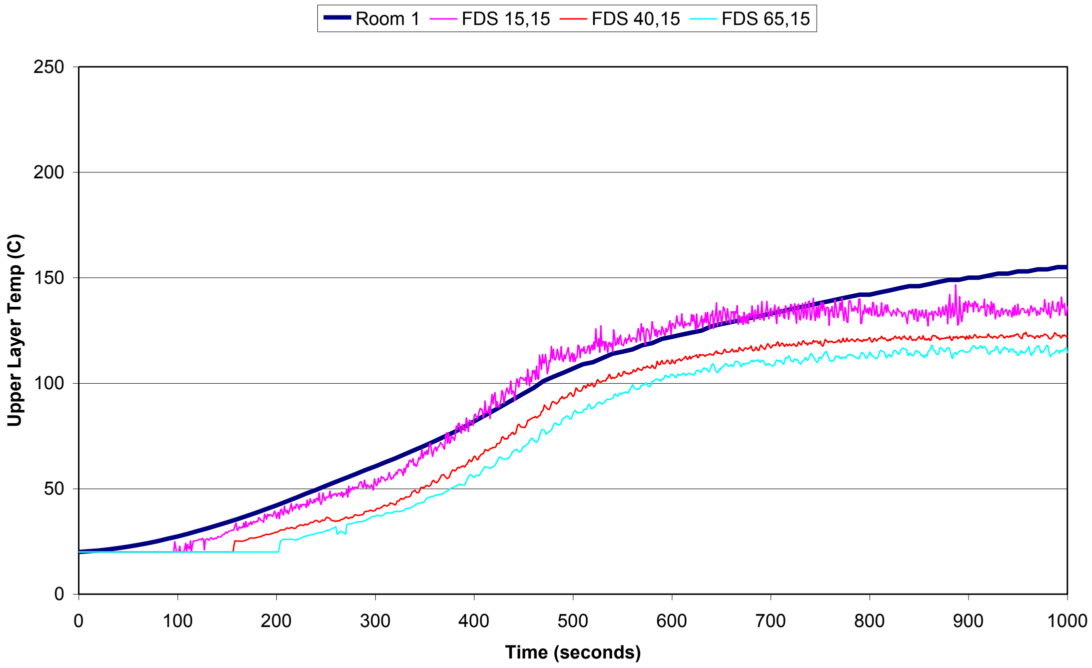

Figure 23. BRANZFIRE upper layer temperatures using one room model versus FDS upper layer predictions at various locations in the compartment 75 x 25 x 6 m

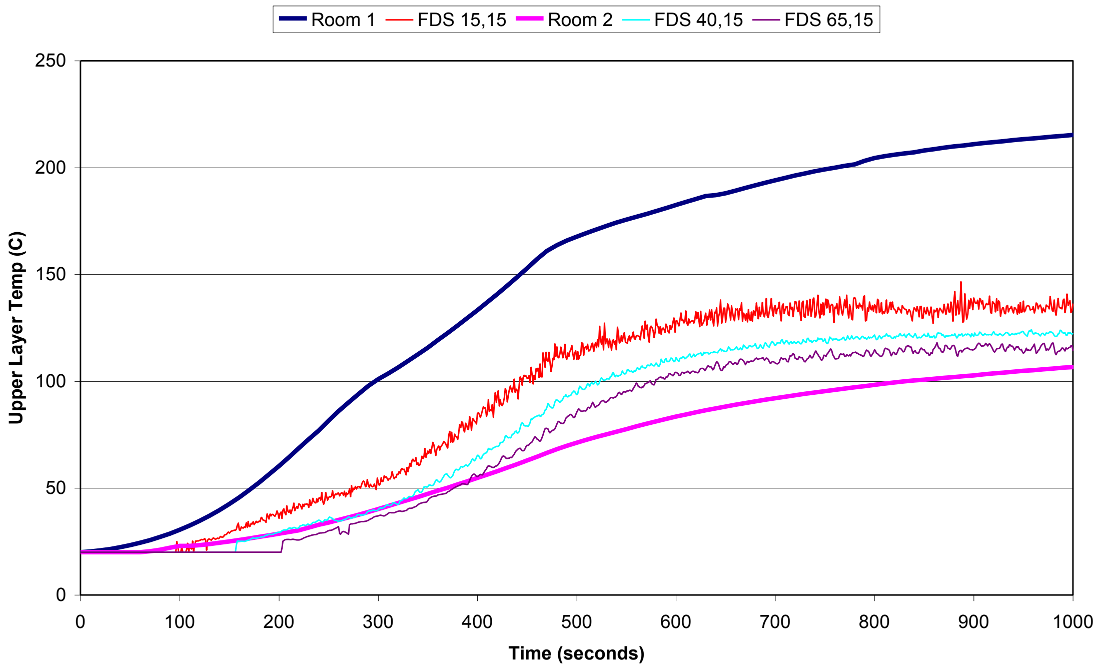

Figure 24. BRANZFIRE (with CCFM rules) upper layer temperatures using two room model versus FDS upper layer predictions at various locations in the compartment 75 x 25 x 6 m

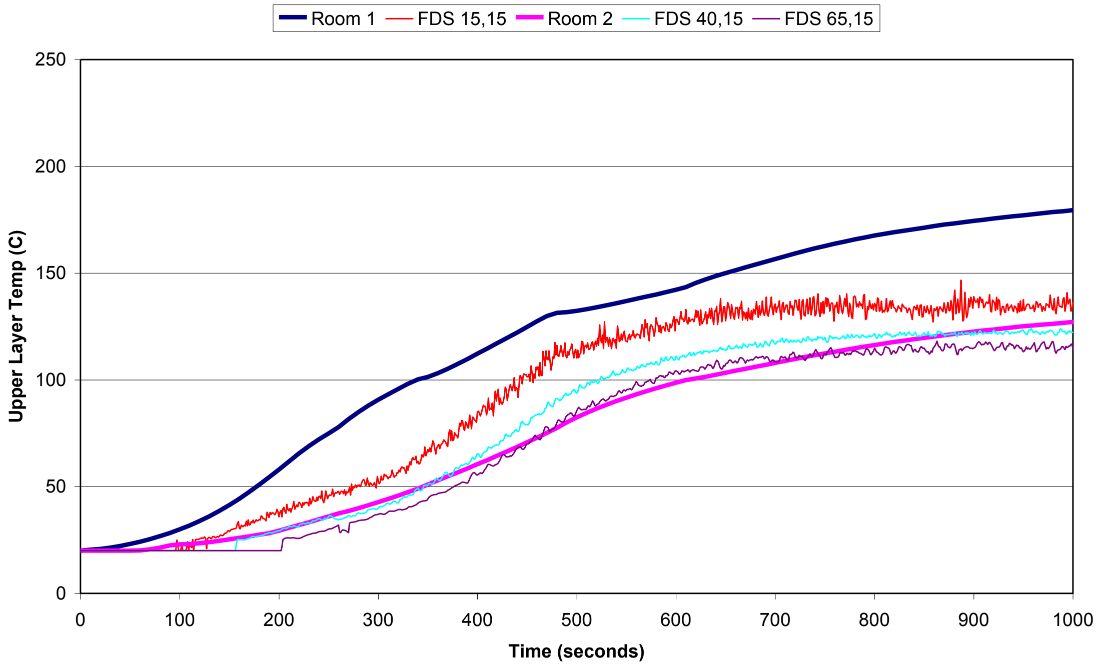

Figure 25. BRANZFIRE (with CFAST rules) upper layer temperatures using two room model versus FDS upper layer predictions at various locations in the compartment 75 x 25 x 6 m

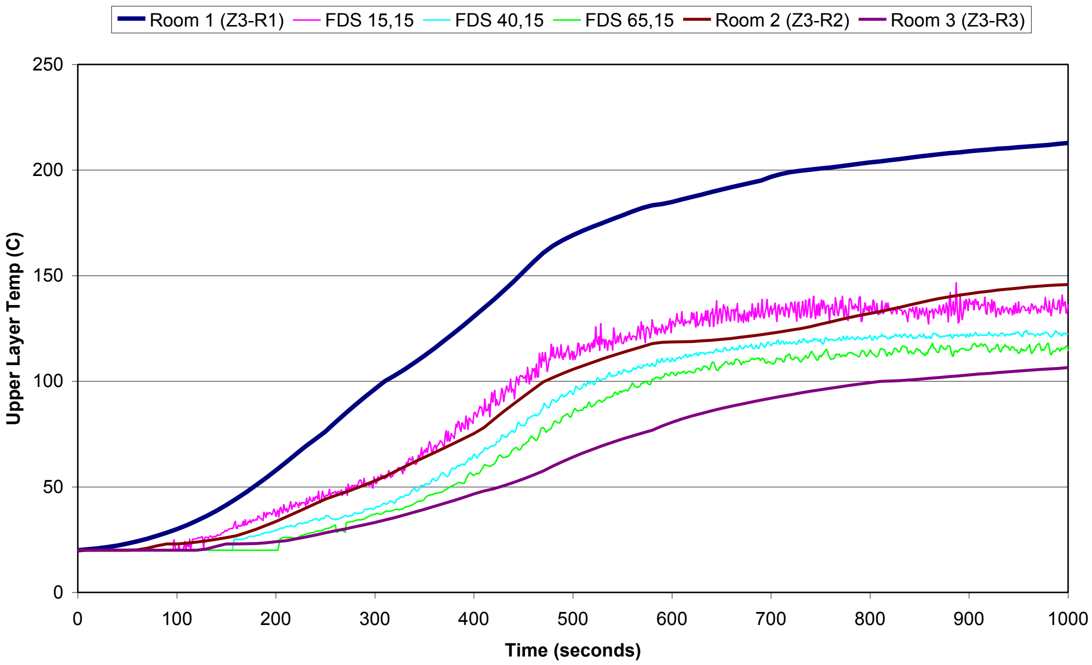

Figure 26. BRANZFIRE (with CCFM rules) upper layer temperatures using three room model versus FDS upper layer predictions at various locations in the compartment 75 x 25 x 6 m

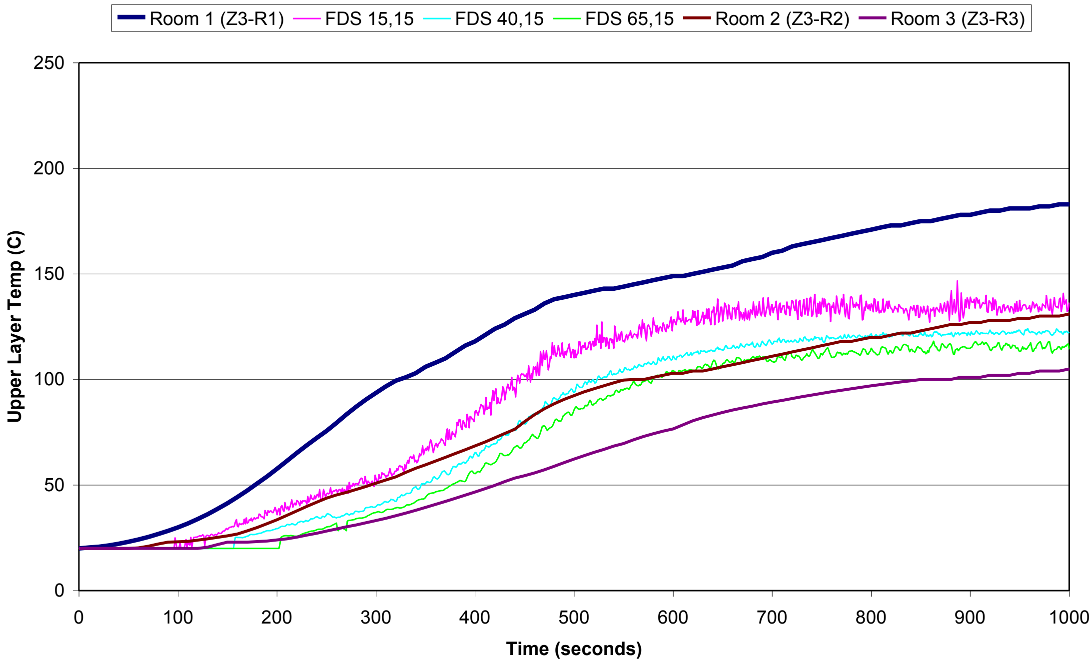

Figure 27 BRANZFIRE (with CFAST rules) upper layer temperatures using three room model versus FDS upper layer predictions at various locations in the compartment 75 x 25 x 6 m

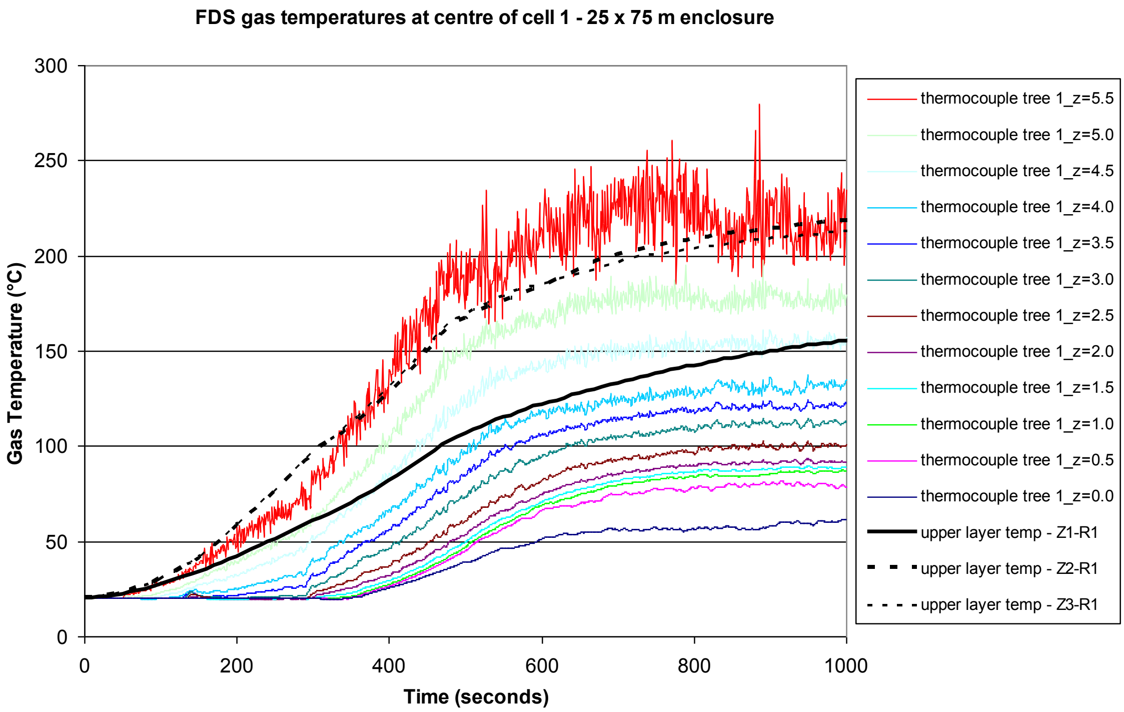

Figure 28. BRANZFIRE (with CCFM rules) upper layer temperatures versus FDS predictions over the height of the enclosure at the centre of compartment Z3-R1

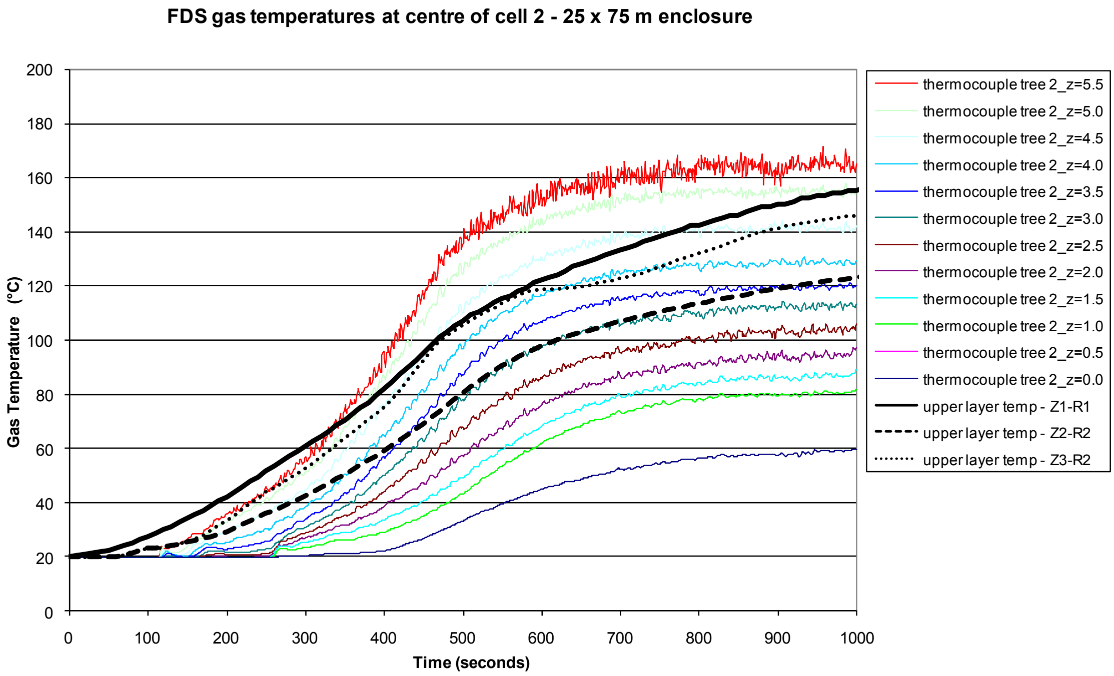

Figure 29. BRANZFIRE (with CCFM rules) upper layer temperatures versus FDS predictions over the height of the enclosure at the centre of compartment Z3-R2

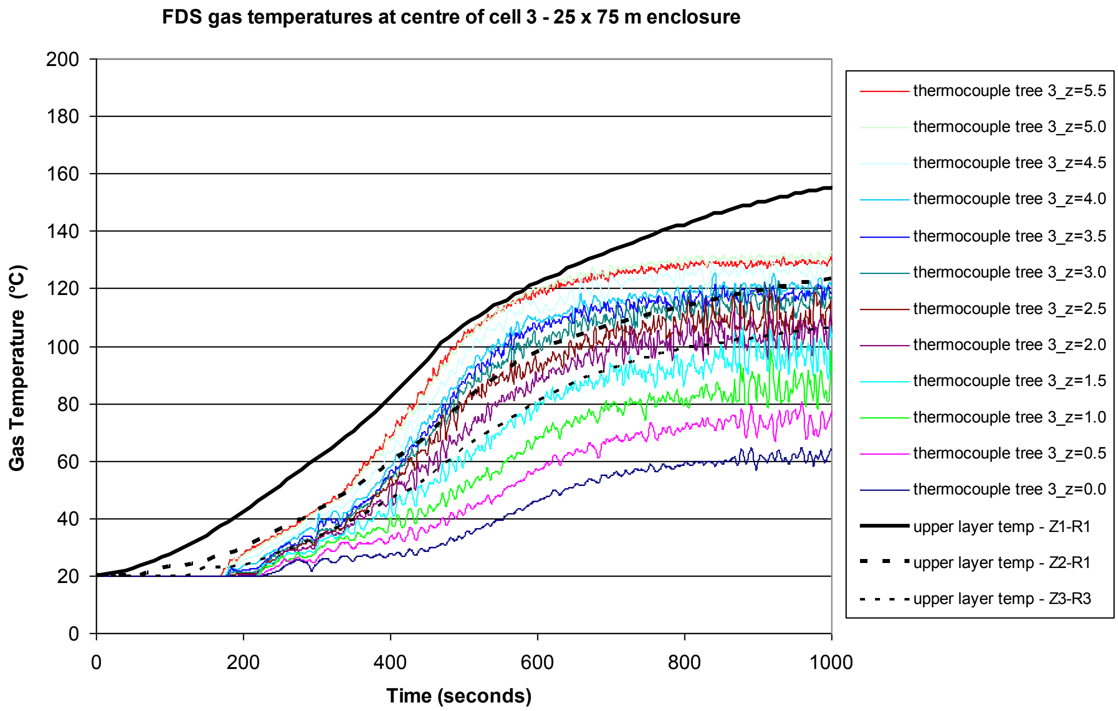

Figure 30. BRANZFIRE (with CCFM rules) upper layer temperatures versus FDS predictions over the height of the enclosure at the centre of compartment Z3-R3

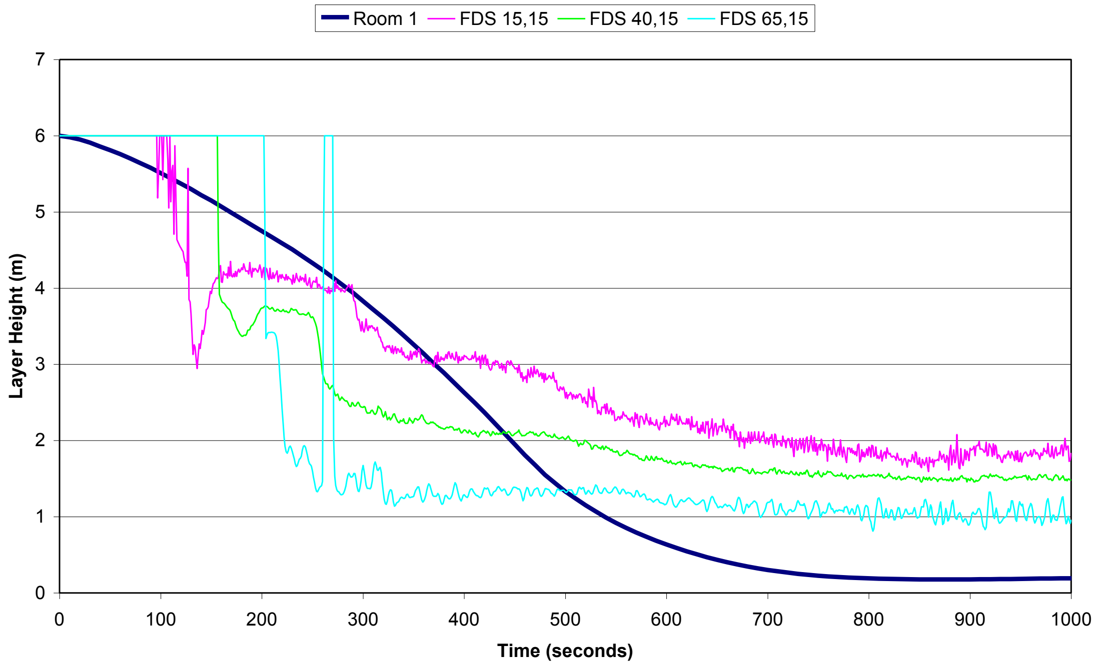

Figure 31. BRANZFIRE layer height using one room model versus FDS upper layer predictions at various locations in the compartment 75 x 25 x 6 m

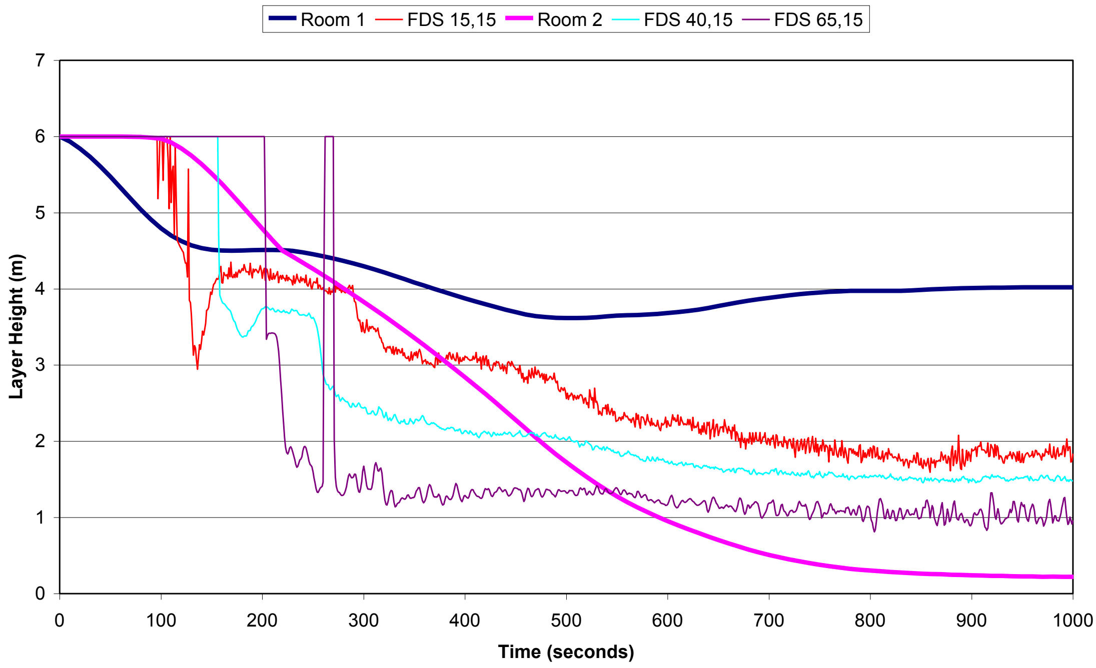

Figure 32. BRANZFIRE (with CCFM rules) layer height using two room model versus FDS upper layer predictions at various locations in the compartment 75 x 25 x 6 m

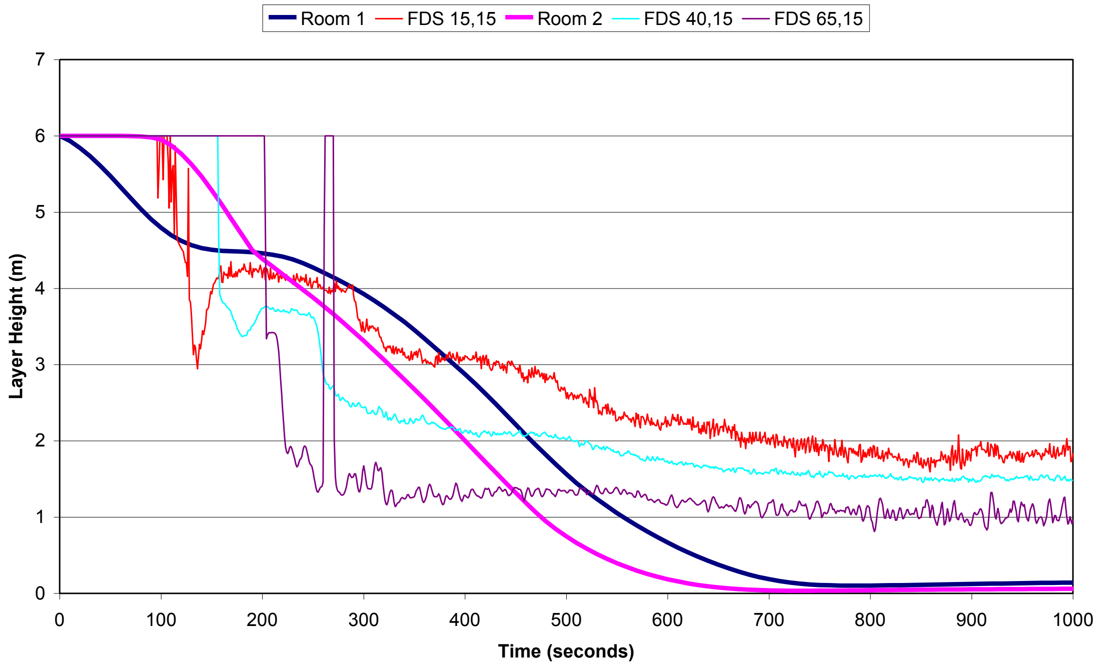

Figure 33. BRANZFIRE (with CFAST rules) layer height using two room model versus FDS upper layer predictions at various locations in the compartment 75 x 25 x 6 m

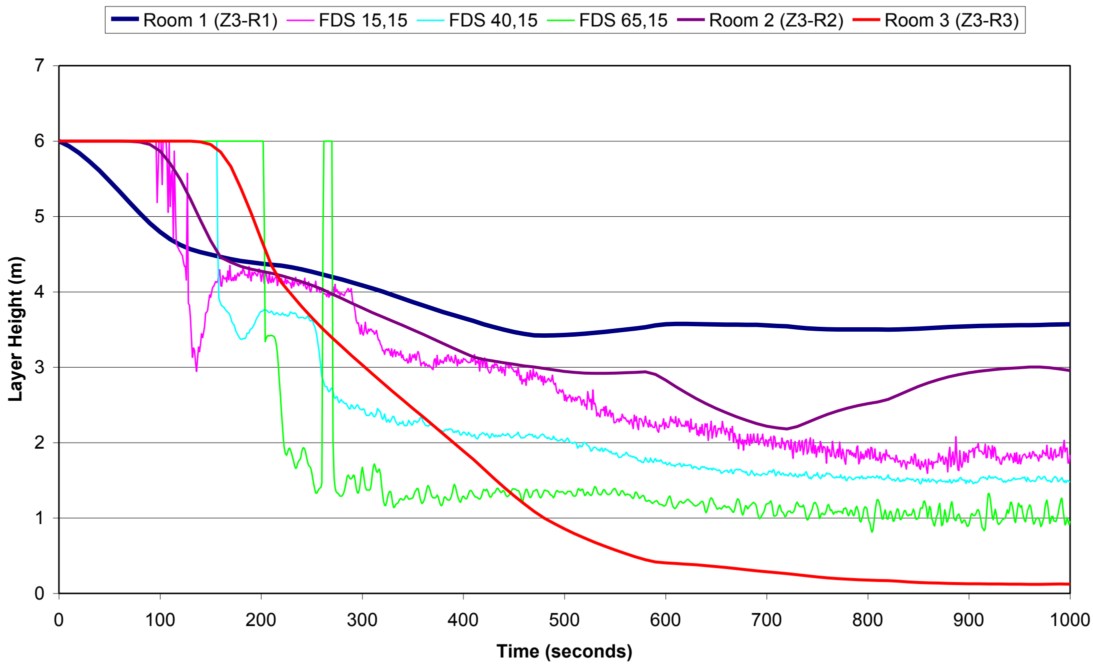

Figure 34. BRANZFIRE (with CCFM rules) layer height using three room model versus FDS upper layer predictions at various locations in the compartment 75 x 25 x 6 m

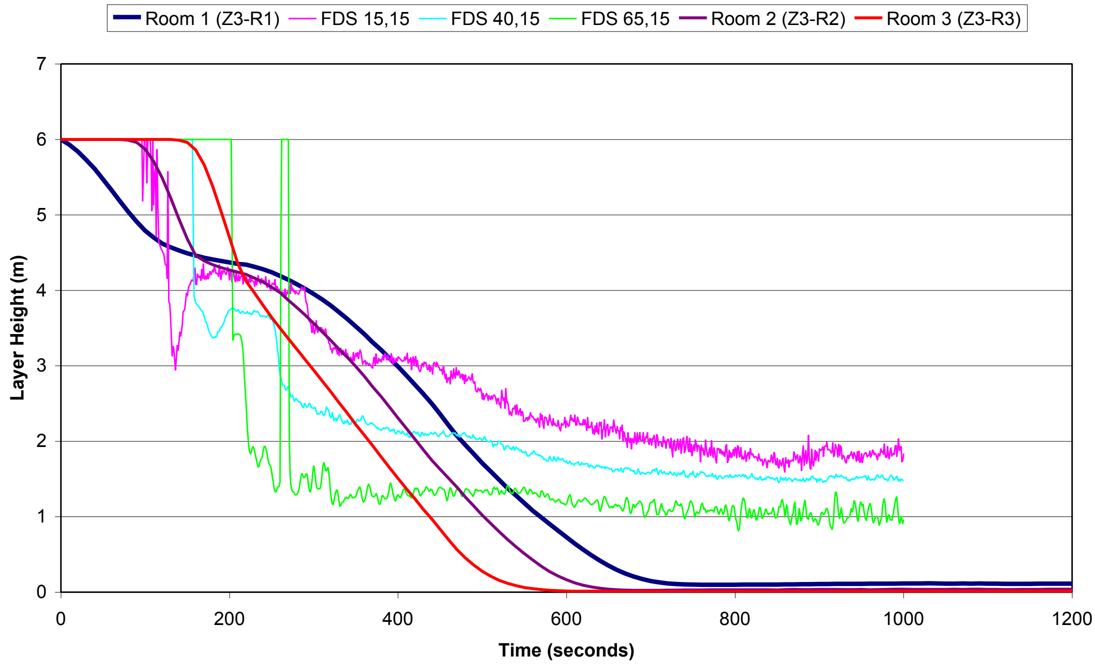

Figure 35 BRANZFIRE (with CFAST rules) layer height using three room model versus FDS upper layer predictions at various locations in the compartment 75 x 25 x 6 m

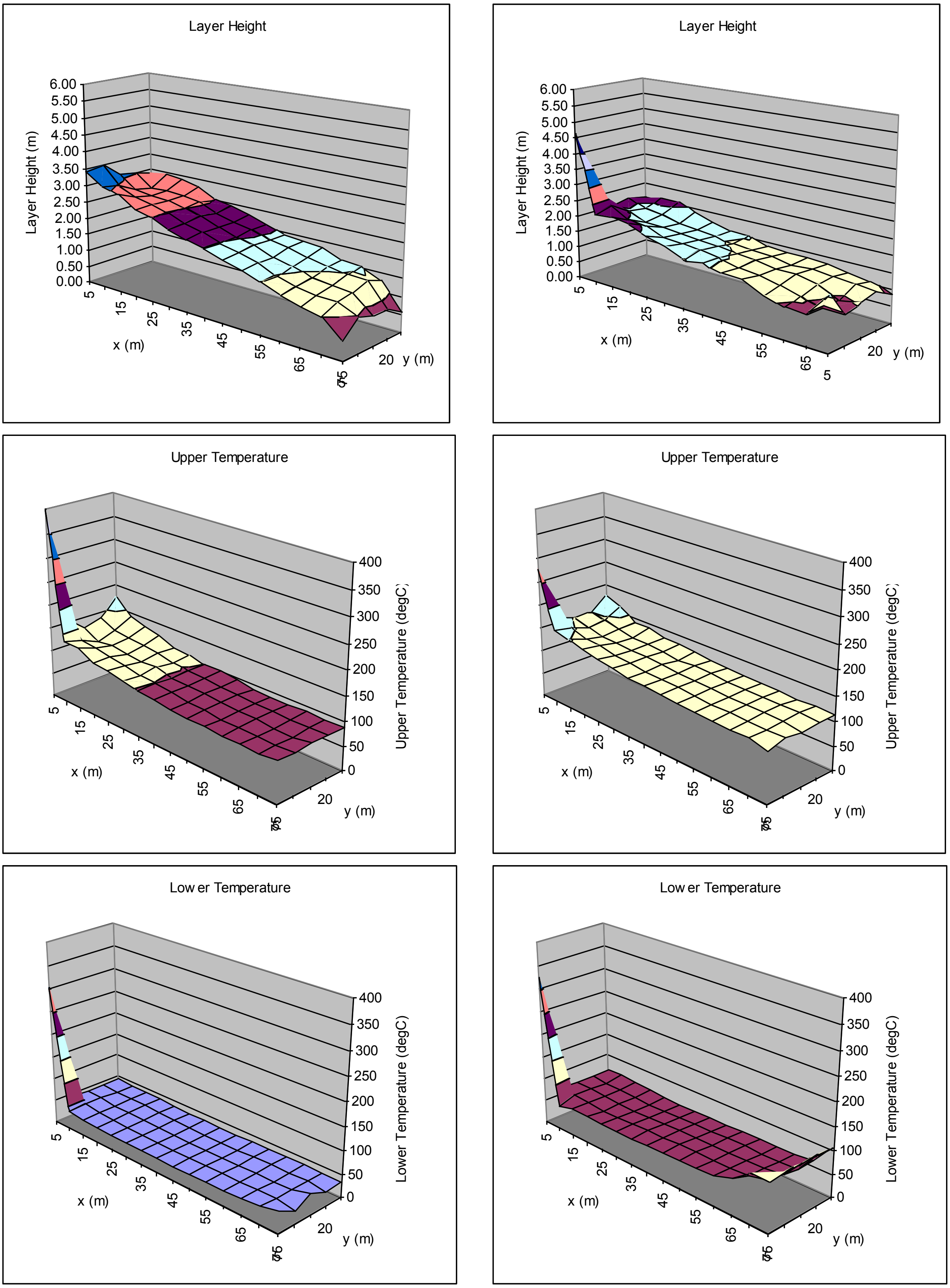

Figure 36. FDS derived predictions of layer height, upper layer temperature and lower layer temperature at 500 seconds (left) and 1000 seconds (right) for 25 x 75 x 6 m high enclosure

3.3.4 Enclosure 100 x 25 x 6 m

BRANZFIRE and FDS were used to simulate smoke filling in a single room 100 x 25 x 6 m high with four openings each 2 m high x 1 m wide as illustrated in Figure 37. The FDS data was reduced to an equivalent upper and lower layer, at discrete points around the enclosure, by integration of the temperature data over the height of the compartment at the location of interest using functionality provided within the FDS program. BRANZFIRE was run with the enclosure modelled as one room, and then again as two rooms and four rooms connected with a full width vents with a 0.6 m transom beneath the ceiling. Figure 38 describes the three configurations that were considered.

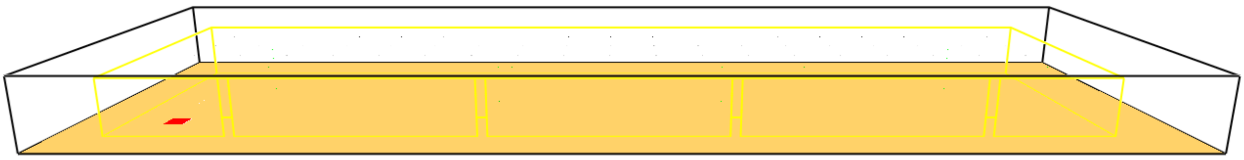

Figure 37. Smokeview representation of 100 x 25 x 6 m compartment showing fire location (in red) and four vents

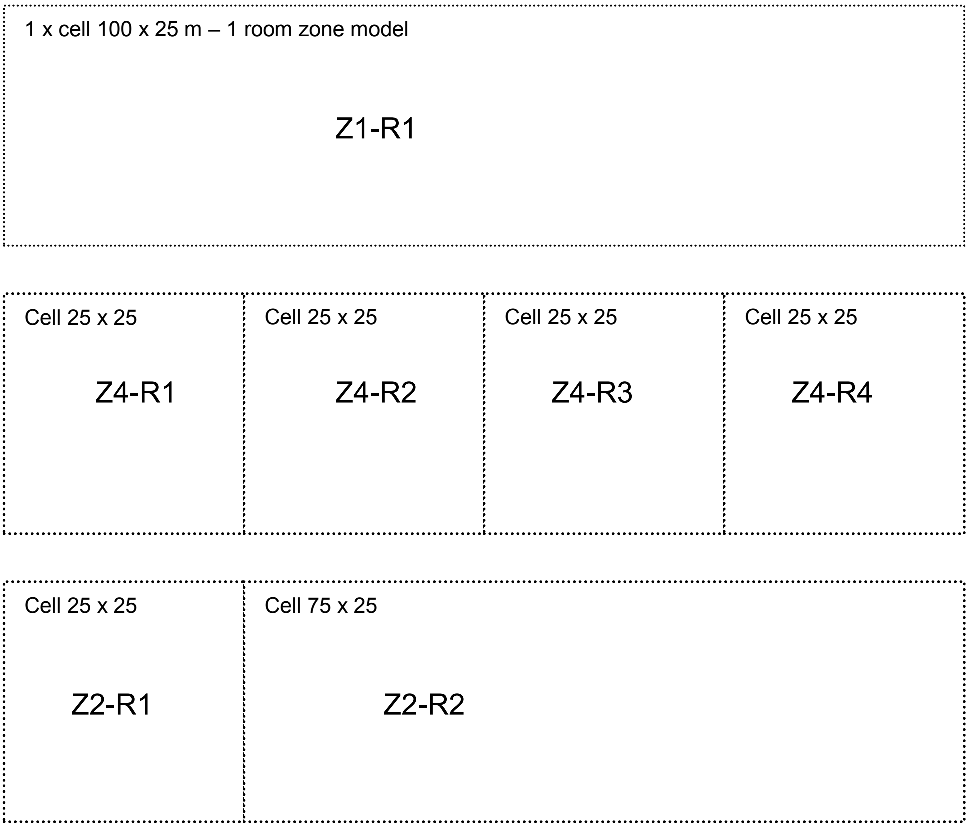

Figure 38. Zone model configurations for 100 x 25 m enclosure

Figure 39 compares the upper layer temperatures using a single room zone model with average upper layer temperatures from FDS at various locations in the enclosure. The zone model prediction is within the range of upper layer temperatures predicted by FDS but would not necessarily be conservative for design purposes.

Figure 42 compares the upper layer temperature for the four cell case. The estimates for cells 2 and 3 are in good agreement with the spread of FDS estimated layer temperatures. However the estimate for cell 1 is highly conservative compared to the FDS results. In addition the results for cell 4 underestimate the lower range of FDS predicted upper layer temperatures.

Figure 44 to Figure 47 compare BRANZFIRE upper layer temperatures with the FDS predicted gas temperatures at different elevations at the centre of each cell of the four-cell arrangement (Z4 of Figure 38).

Figure 48 compares the layer height for the single cell case. The zone model predicts a slower initial descent of the layer compared to FDS, but is ultimately closer to the floor at a later stage. Figure 51 compares the layer height for the four cell case.

Figure 41, Figure 43, Figure 50 and Figure 52 show the results where CFAST rules were used instead of CCFM rules associated with vent flows. The upper layer temperature predictions by the zone model shown in Figure 43 and Figure 41 span the values predicted by FDS, but generally overestimate the temperature in the fire compartment and underestimate the temperature in the compartment furthest from the fire.

Figure 53 shows the FDS results after 500 and 1000 seconds, using the integrated temperature data to calculate the upper and lower layer temperatures and the layer height. It clearly shows the increasing layer thickness and reducing average upper layer temperature across the enclosure in the far field.

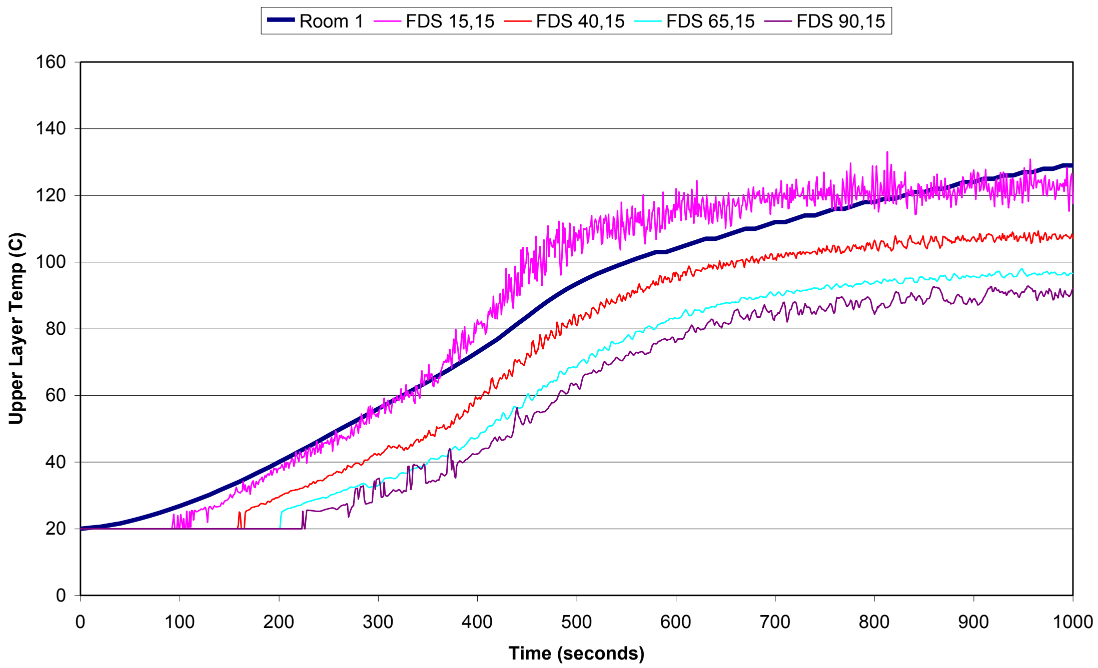

Figure 39. BRANZFIRE upper layer temperatures using one room model versus FDS upper layer predictions at various locations in the compartment 100 x 25 x 6 m

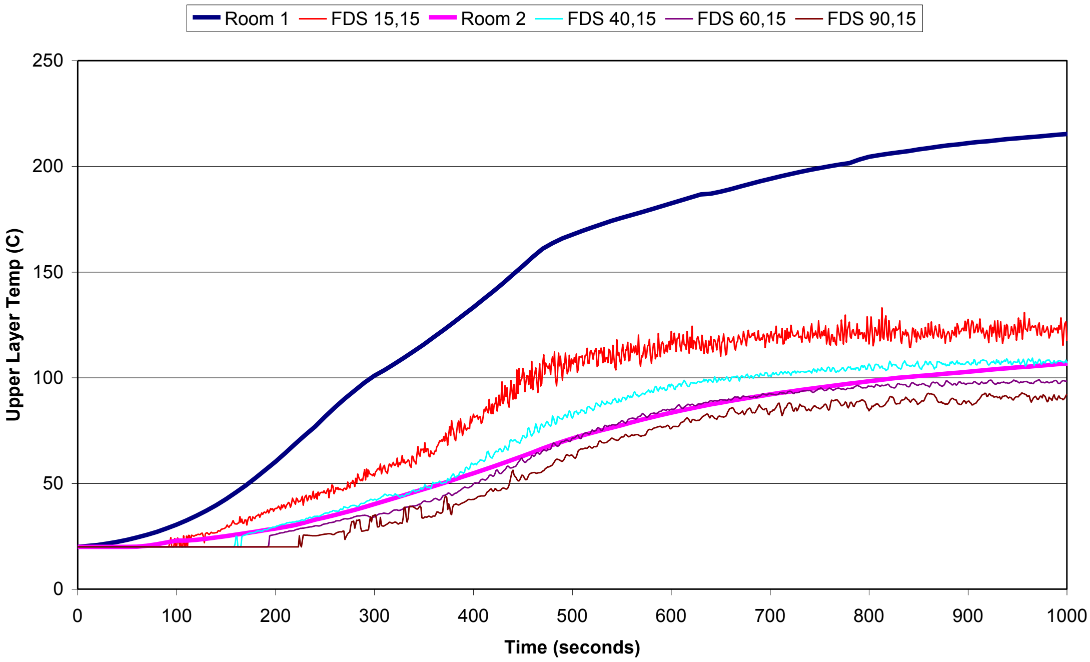

Figure 40. BRANZFIRE (with CCFM rules) upper layer temperatures using two room model versus FDS upper layer predictions at various locations in the compartment 100 x 25 x 6 m

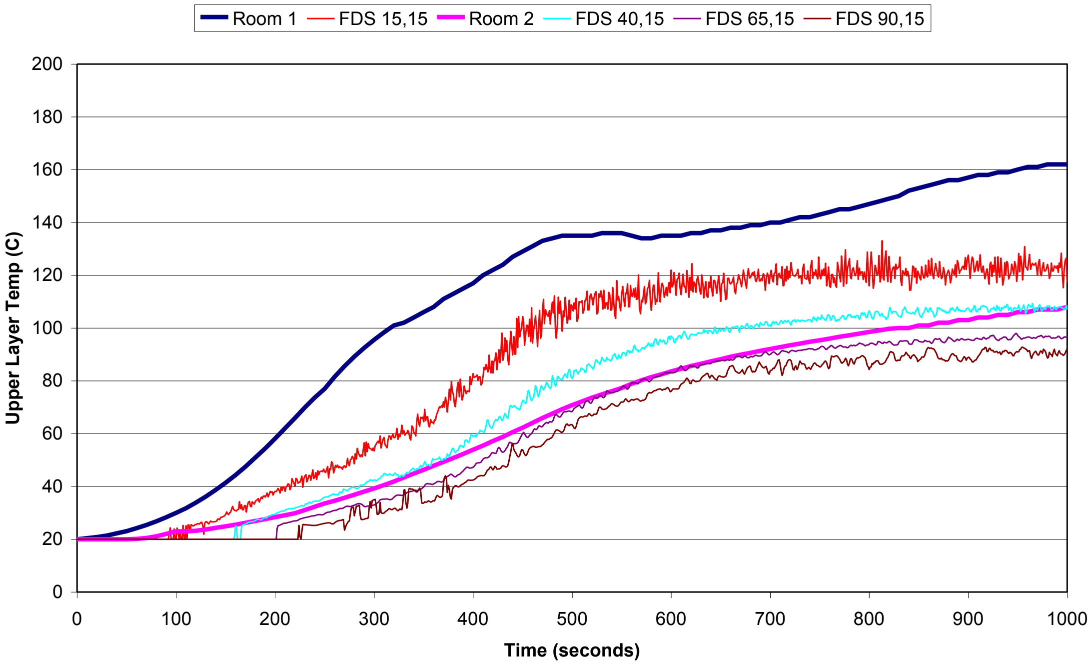

Figure 41. BRANZFIRE (with CFAST rules) upper layer temperatures using two room model versus FDS upper layer predictions at various locations in the compartment 100 x 25 x 6 m

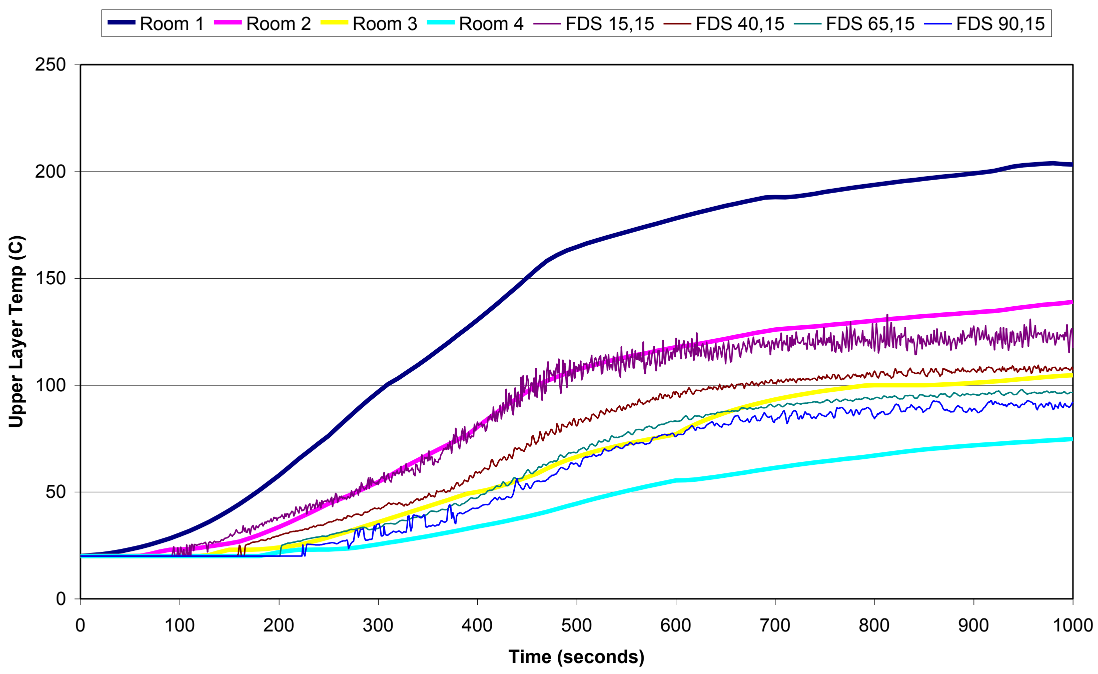

Figure 42. BRANZFIRE (with CCFM rules) upper layer temperatures using four room model versus FDS upper layer predictions at various locations in the compartment 100 x 25 x 6 m

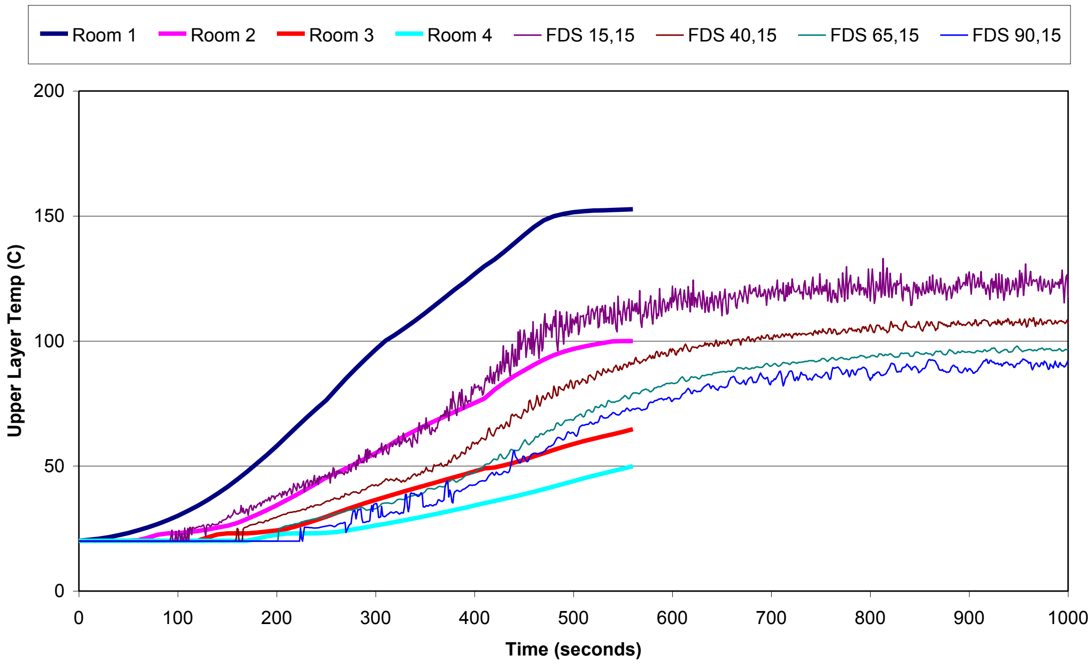

Figure 43. BRANZFIRE* (with CFAST rules) upper layer temperatures using four room model versus FDS upper layer predictions at various locations in the compartment 100 x 25 x 6 m

* Zone model simulation was terminated early due to lack of convergence.

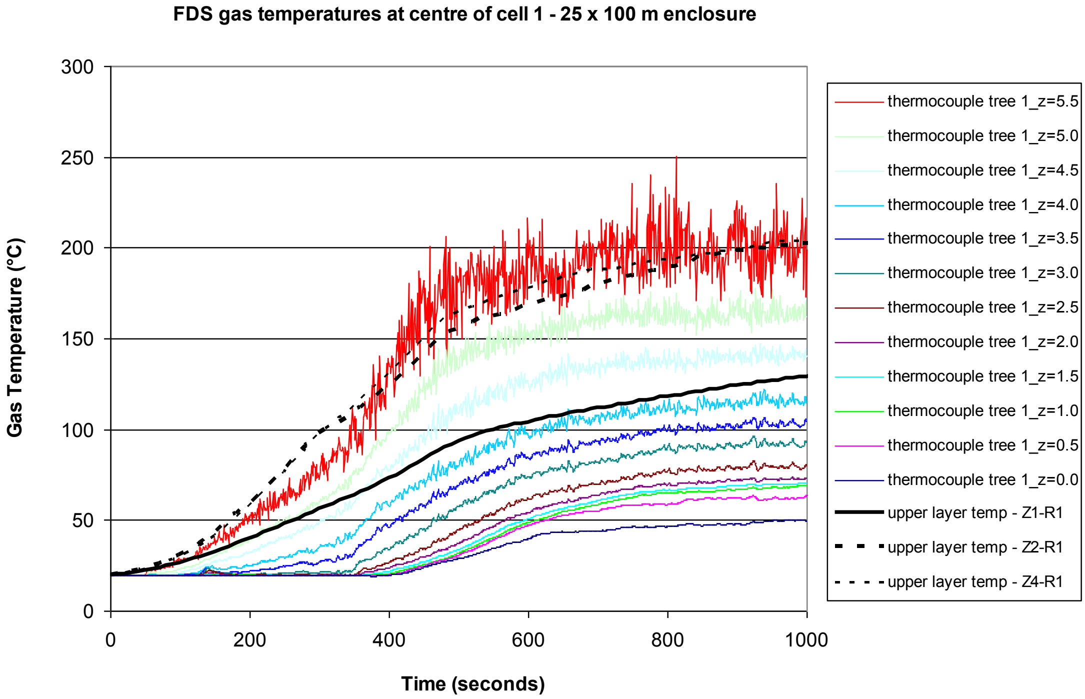

Figure 44. BRANZFIRE (with CCFM rules) upper layer temperatures versus FDS predictions over the height of the enclosure at the centre of compartment Z4-R1

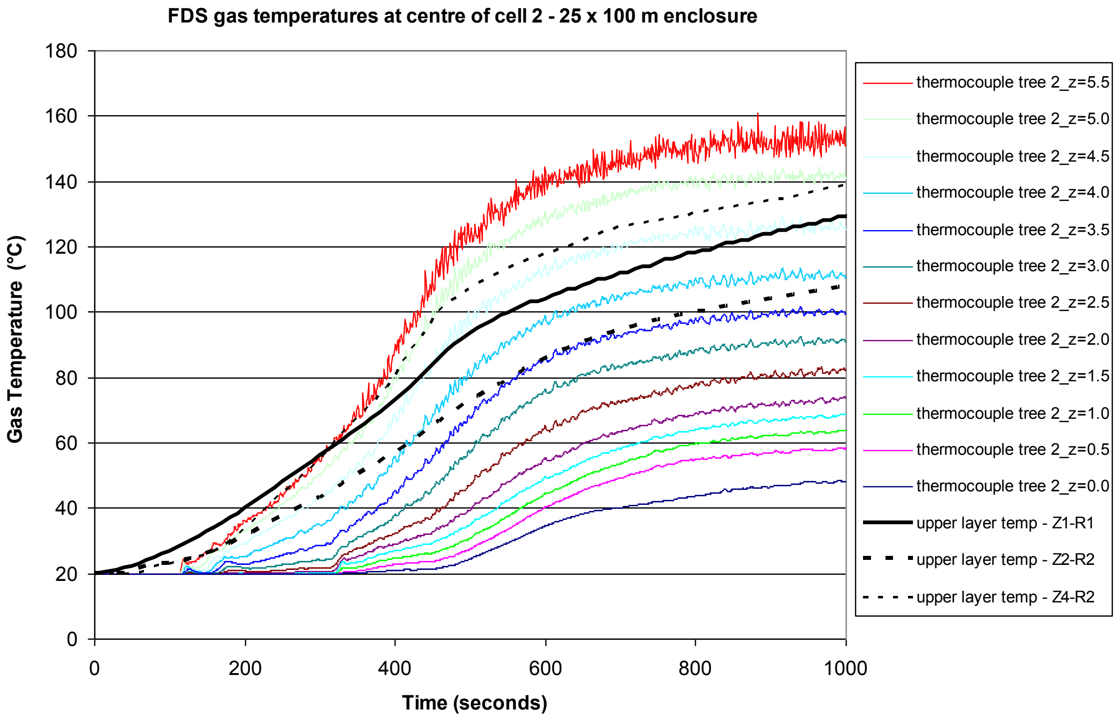

Figure 45. BRANZFIRE (with CCFM rules) upper layer temperatures versus FDS predictions over the height of the enclosure at the centre of compartment Z4-R2

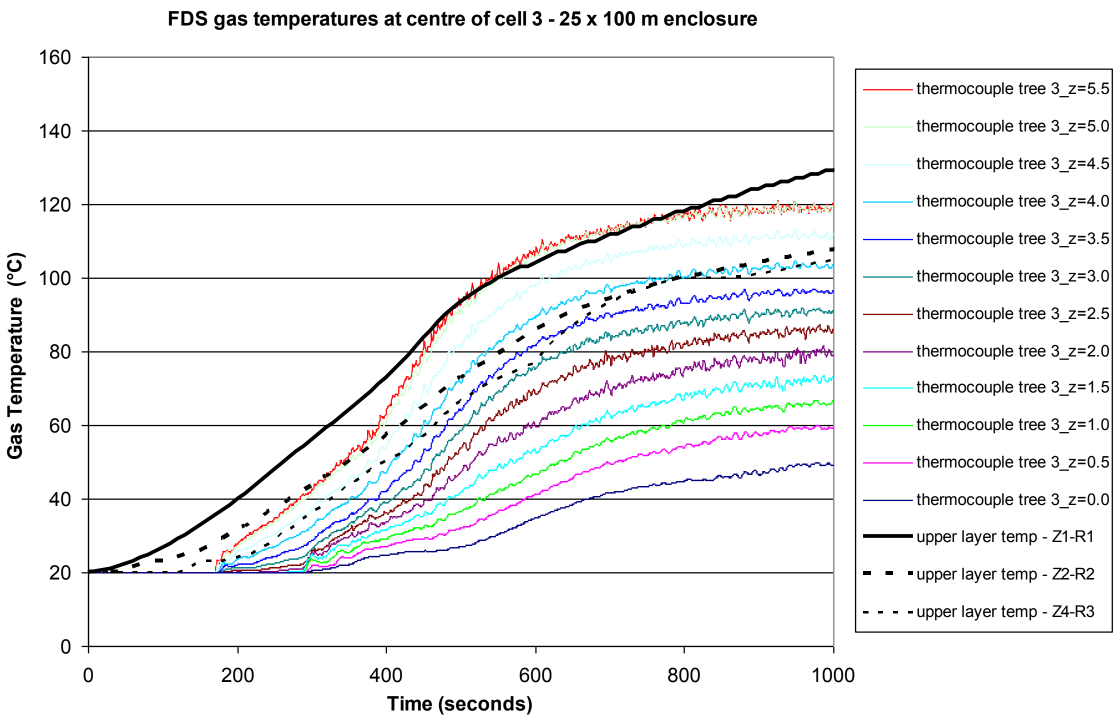

Figure 46. BRANZFIRE (with CCFM rules) upper layer temperatures versus FDS predictions over the height of the enclosure at the centre of compartment Z4-R3

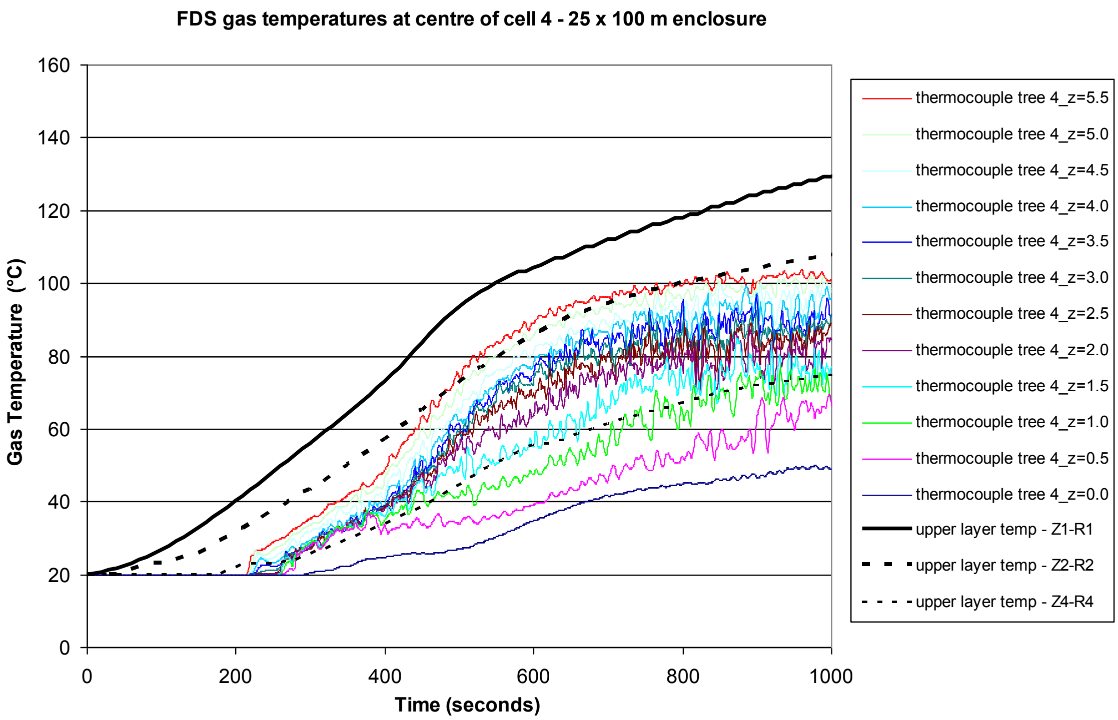

Figure 47. BRANZFIRE (with CCFM rules) upper layer temperatures versus FDS predictions over the height of the enclosure at the centre of compartment Z4-R4

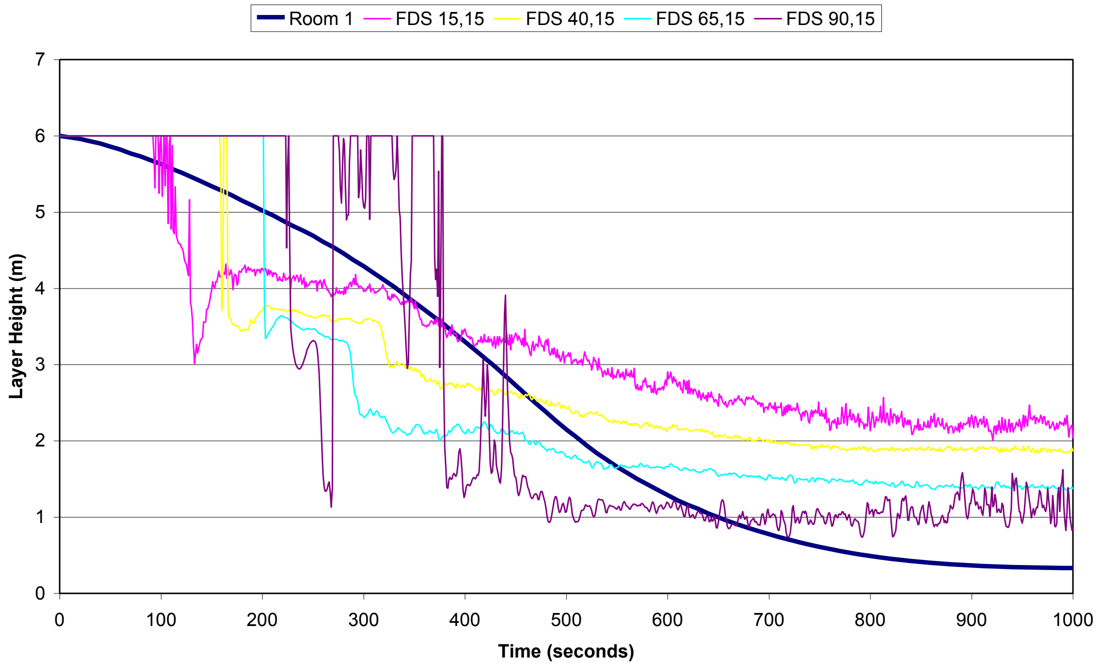

Figure 48. BRANZFIRE layer height using one room model versus FDS upper layer predictions at various locations in the compartment 100 x 25 x 6 m

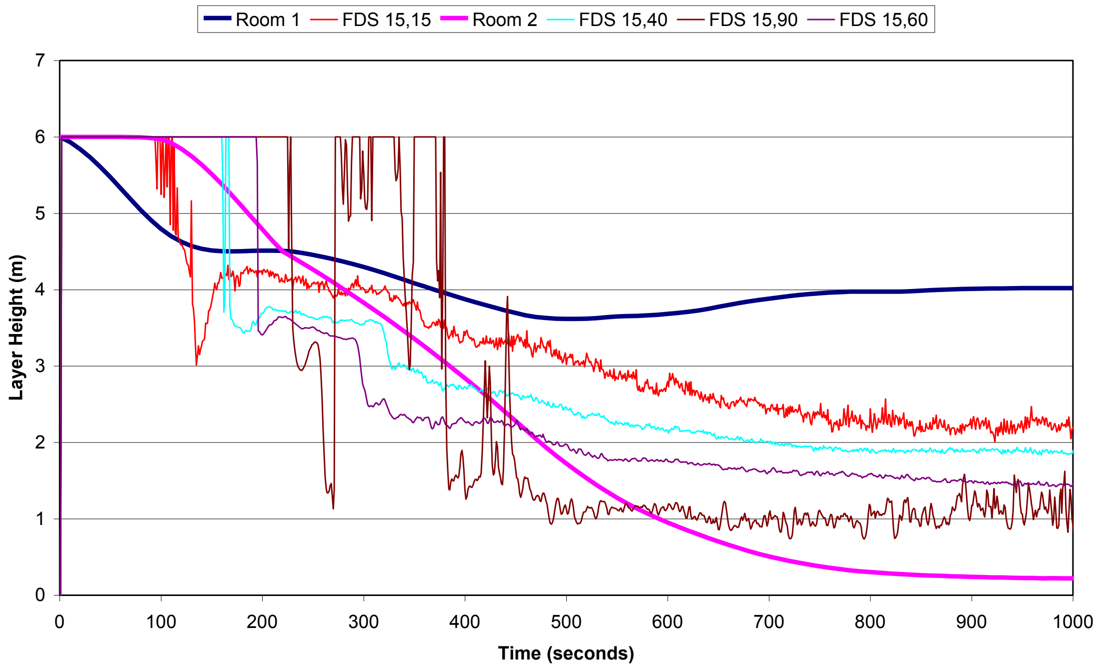

Figure 49. BRANZFIRE (with CCFM rules) layer height using two room model versus FDS upper layer predictions at various locations in the compartment 100 x 25 x 6 m

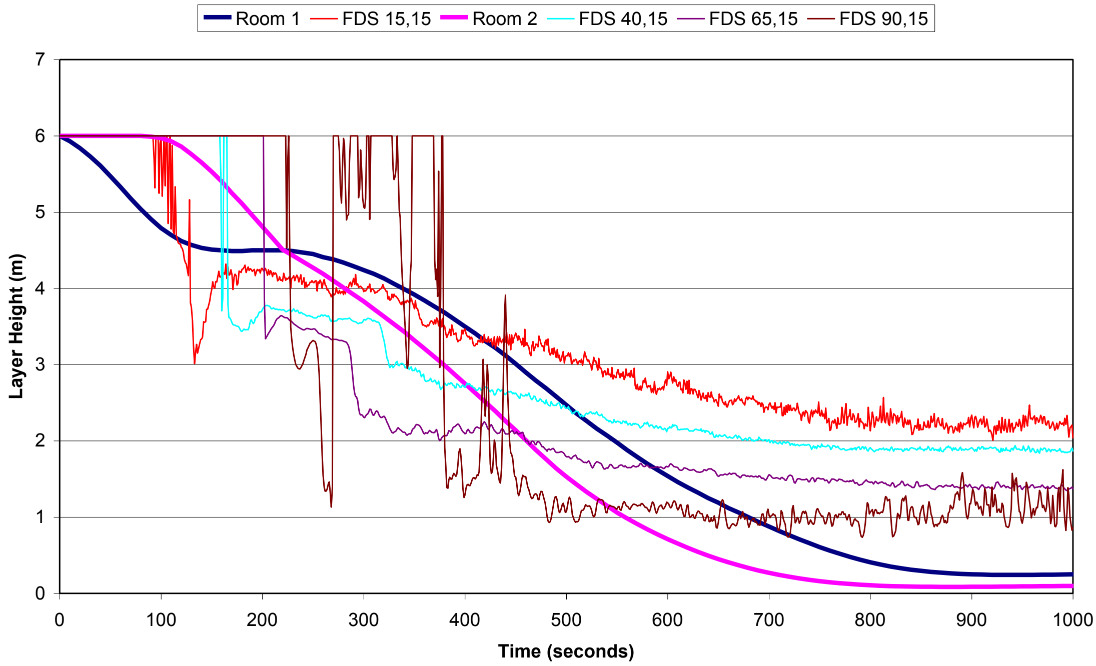

Figure 50. BRANZFIRE (with CFAST rules) layer height using two room model versus FDS upper layer predictions at various locations in the compartment 100 x 25 x 6 m

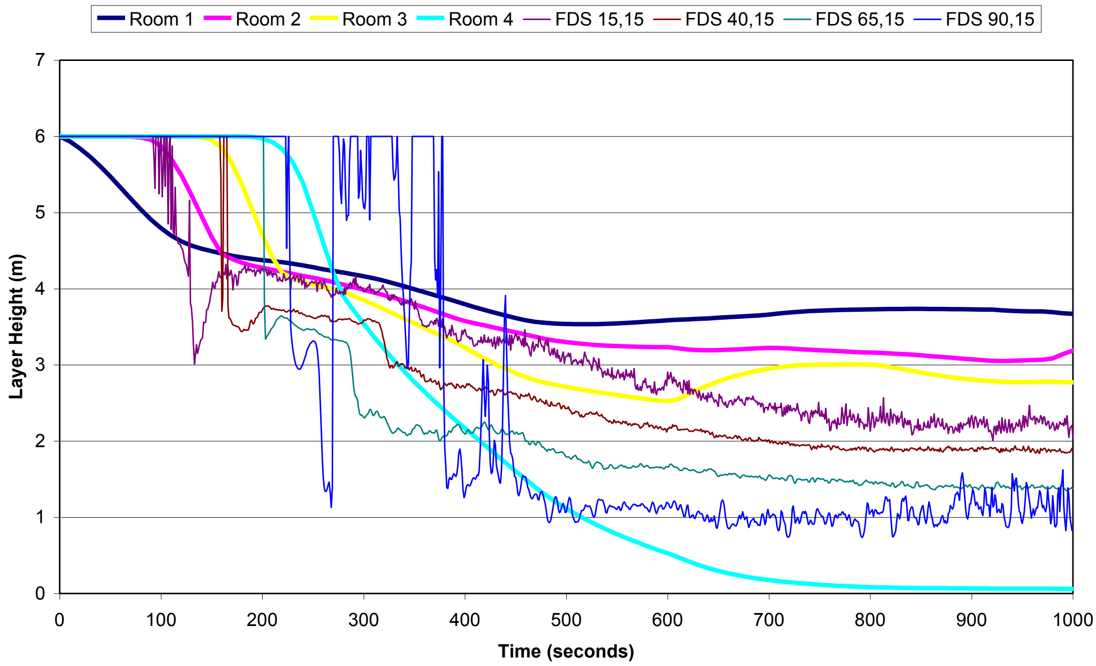

Figure 51. BRANZFIRE (with CCFM rules) layer height using four room model versus FDS upper layer predictions at various locations in the compartment 100 x 25 x 6 m

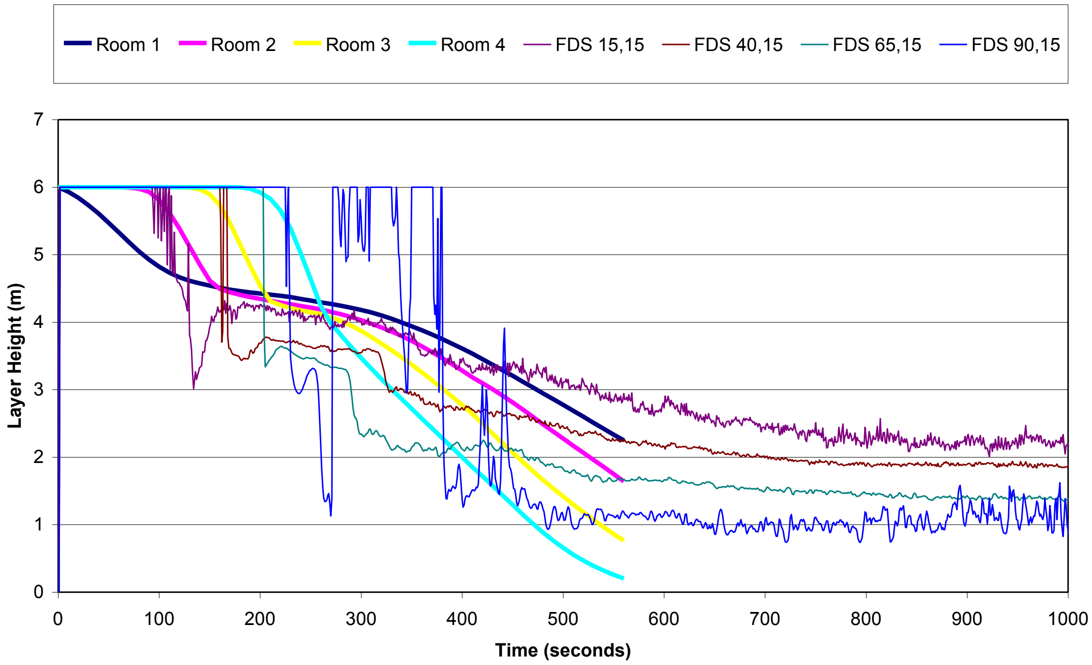

Figure 52. BRANZFIRE† (with CFAST rules) layer height using four room model versus FDS upper layer predictions at various locations in the compartment 100 x 25 x 6 m

† Zone model simulation was terminated early due to lack of convergence.

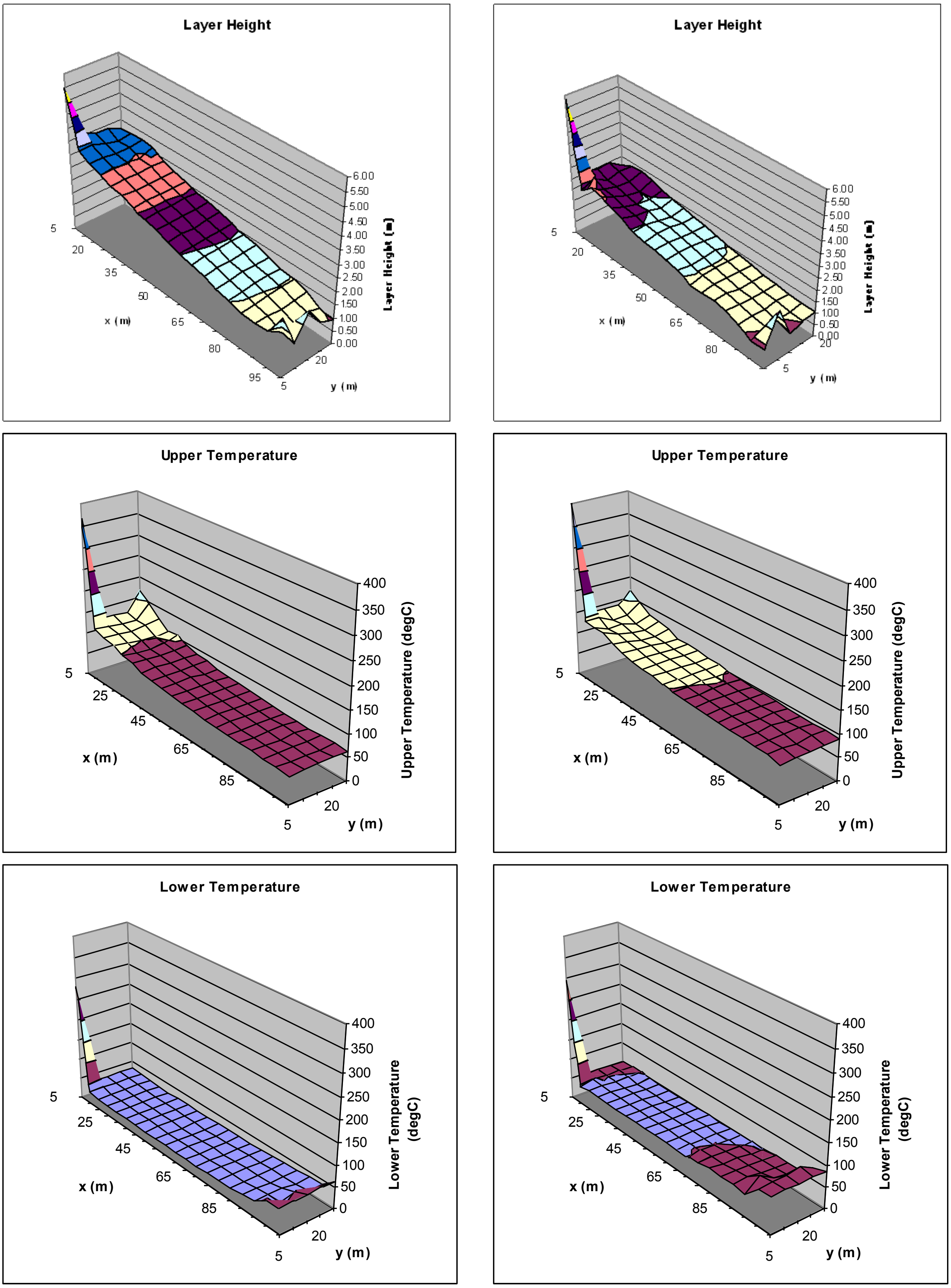

Figure 53. FDS derived predictions of layer height, upper layer temperature and lower layer temperature at 500 seconds (left) and 1000 seconds (right) for 25 x 100 x 6 m high enclosure

3.3.5 Enclosure 100 x 50 x 6 m

BRANZFIRE and FDS were used to simulate smoke filling in a single room 100 x 50 x 6 m high with eight openings each 2 m high x 1 m wide as illustrated in Figure 54. The FDS data was reduced to an equivalent upper and lower layer, at discrete points around the enclosure, by integration of the temperature data over the height of the compartment at the location of interest using functionality provided within the FDS program. BRANZFIRE was run with the enclosure modelled as one room, and then again as two rooms and eight rooms connected with a full width vents with a 0.6 m transom beneath the ceiling. Figure 55 describes the three configurations that were considered.

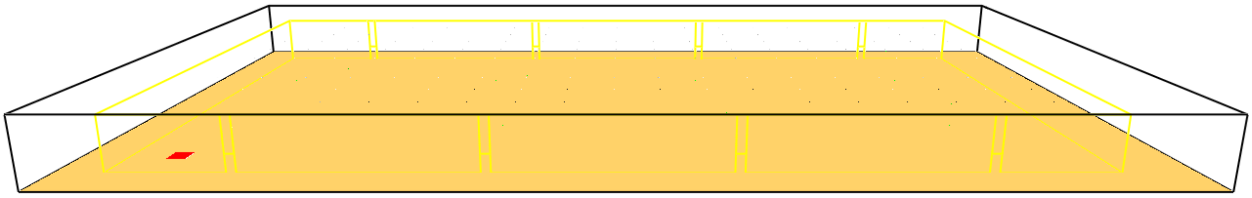

Figure 54. Smokeview representation of 100 x 50 x 6 m compartment showing fire location (in red) and eight vents

Figure 56 compares the upper layer temperatures using a single room zone model with average upper layer temperatures from FDS at various locations in the enclosure. The zone model prediction is within the range of upper layer temperatures predicted by FDS but would not necessarily be conservative for design purposes.

Figure 57 compares the upper layer temperatures for the two room zone model simulation with FDS estimates. These results for the room of fire origin are conservative compared with the FDS simulation results.

Figure 59 compares upper layer temperatures for the eight room zone model simulation with FDS estimates. This simulation provides an underestimate of the upper layer temperature for the cells most remote from the fire (cells 4 and 8).

Figure 58 and Figure 60 compare FDS simulation results with upper layer temperature results using CFAST venting rules for the two cell and eight cell approaches, respectively. In general the results calculated using the CFAST rules provide less of an over prediction of the FDS simulation results and are in generally better agreement overall with the FDS simulation results.

Figure 61 to Figure 68 compare BRANZFIRE upper layer temperatures with the FDS predicted gas temperatures at different elevations at the centre of each cell of the eight-cell arrangement (Z8 of Figure 53).

Figure 69 compares the layer height for the single cell case. The zone model predicts a slower initial descent of the layer compared to FDS, but is ultimately closer to the floor at a later stage.

Figure 57 and Figure 71 show that the two room zone model simulation provides a reasonable prediction of the average upper layer temperature and layer height compared to FDS. This would be satisfactory and conservative for design purposes.

Figure 59 and Figure 72 show that the eight room zone model simulation provides a wider range of upper layer temperatures than predicted by the FDS simulations, where the more remote cells underestimate the FDS predicted temperatures.

Figure 74 shows the FDS results after 500 and 1000 seconds, using the integrated temperature data to calculate the upper and lower layer temperatures and the layer height. It clearly shows the increasing layer thickness and reducing upper layer temperature across the enclosure in the far field.

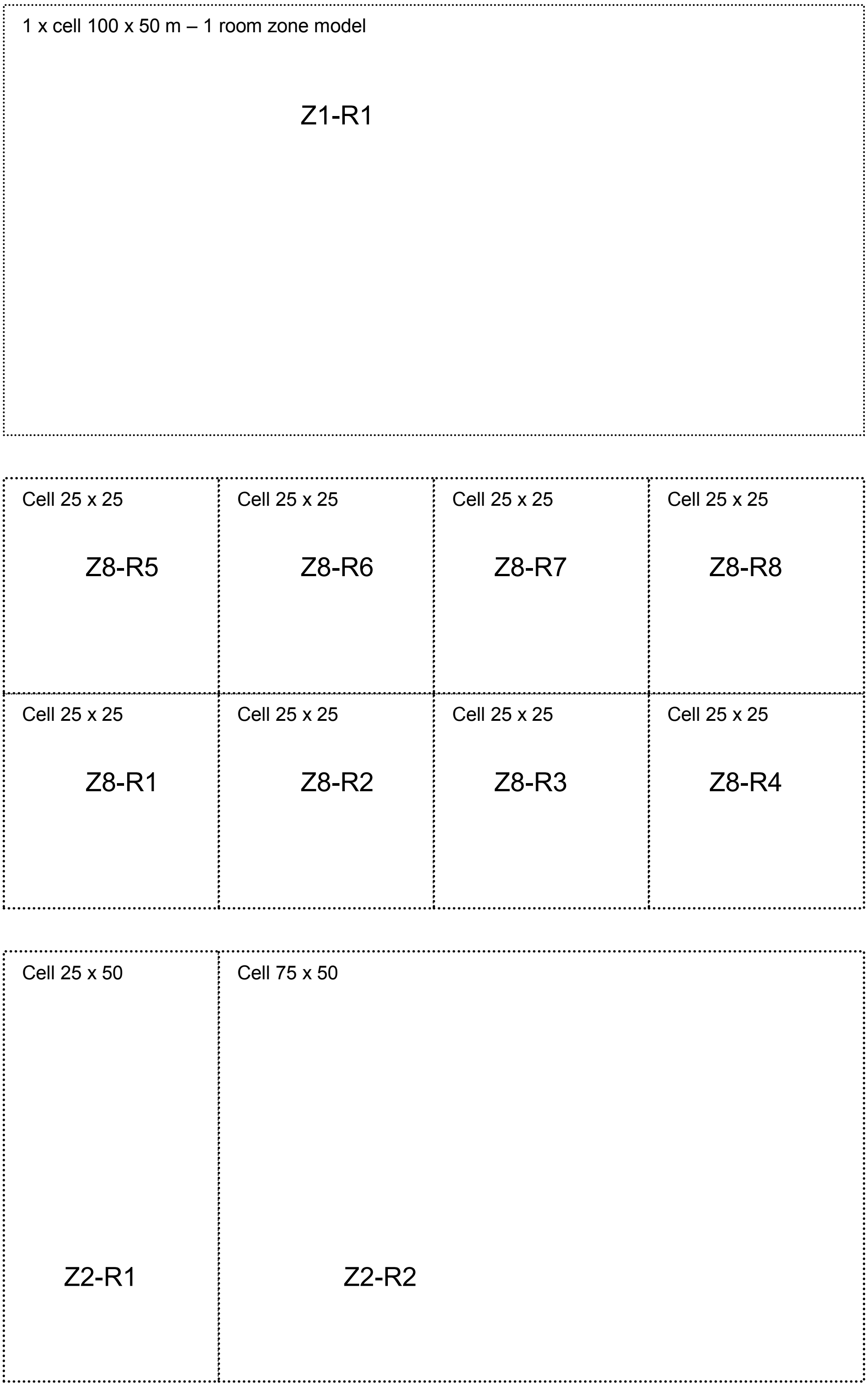

Figure 55. Zone model configurations for 100 x 50 x 6 m enclosure

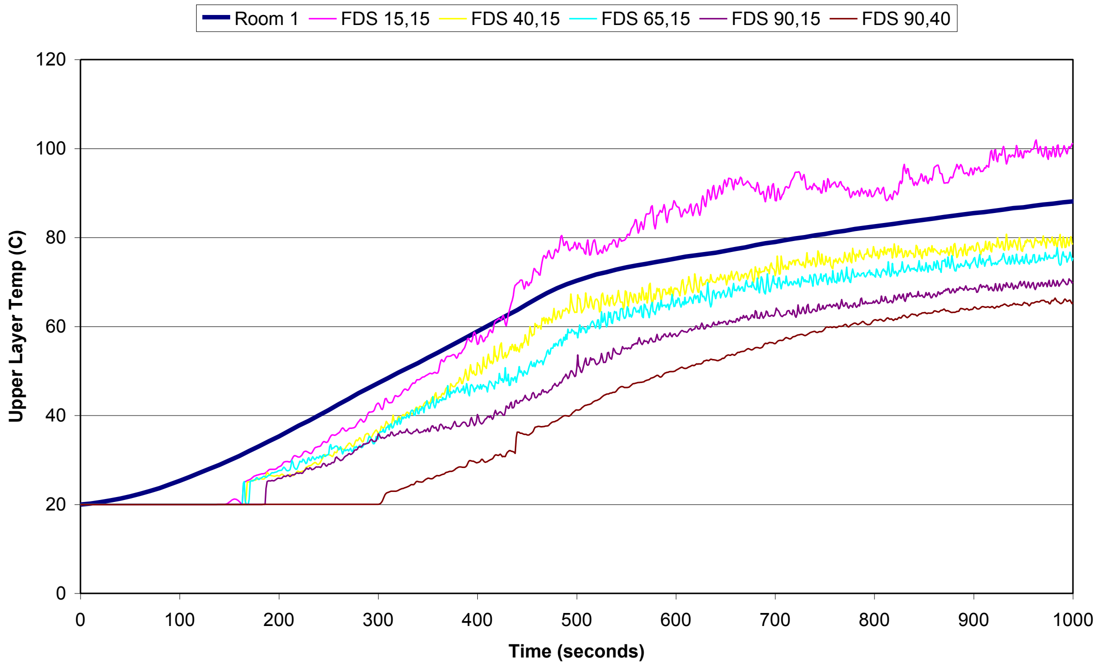

Figure 56. BRANZFIRE upper layer temperatures using one room model versus FDS upper layer predictions at various locations in the compartment 100 x 50 x 6 m

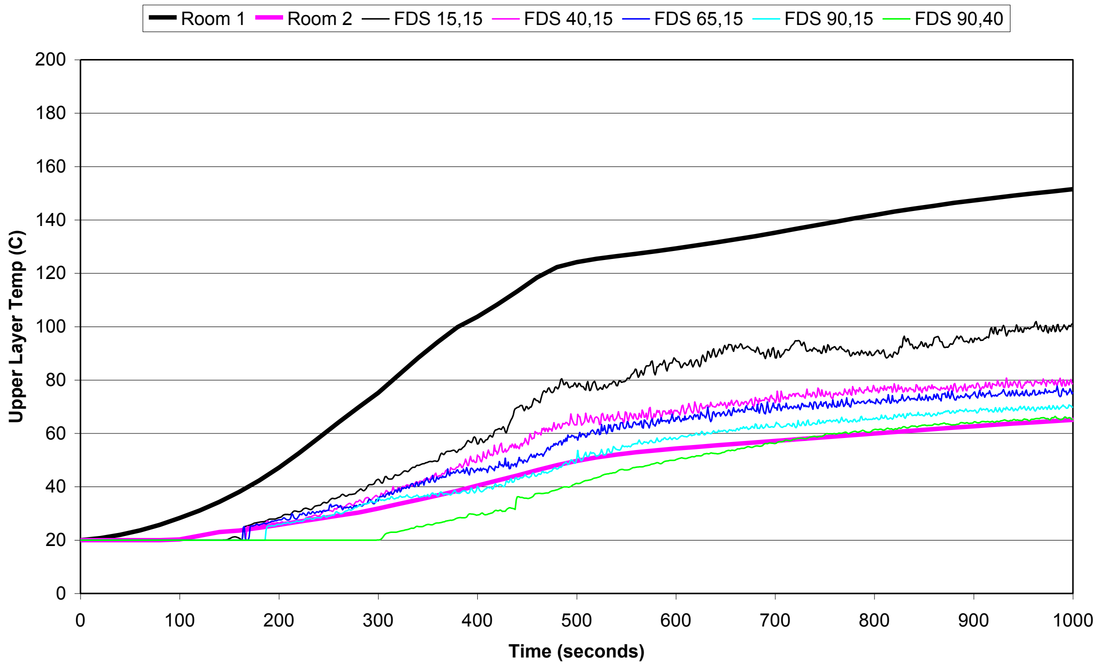

Figure 57. BRANZFIRE (with CCFM rules) upper layer temperatures using two room model versus FDS upper layer predictions at various locations in the compartment 100 x 50 x 6 m

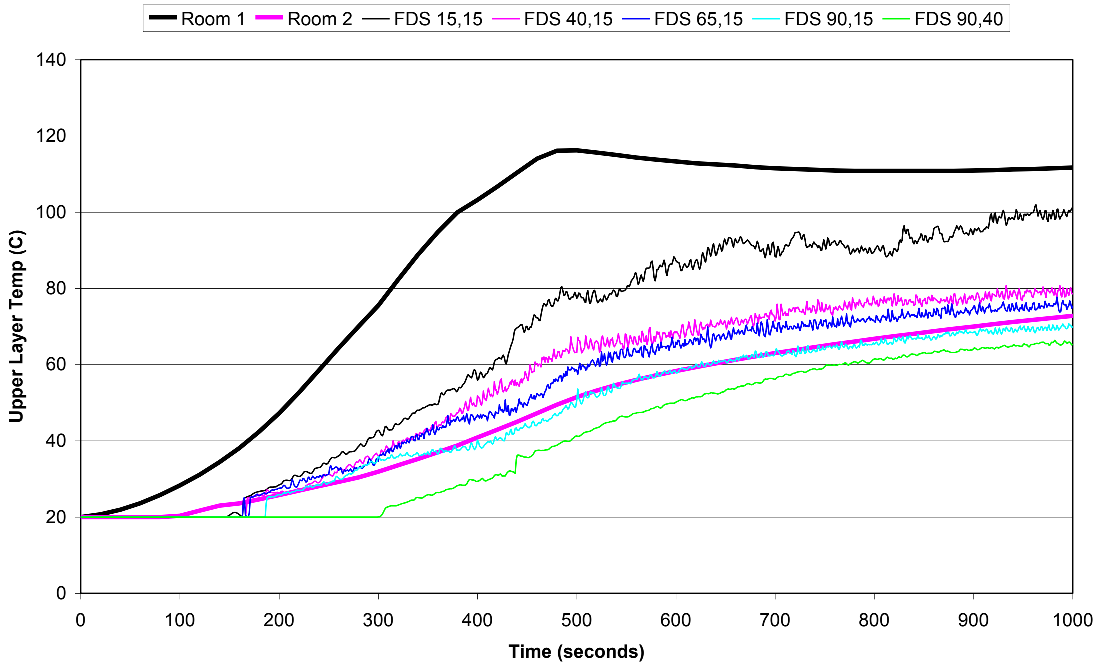

Figure 58. BRANZFIRE (with CFAST rules) upper layer temperatures using two room model versus FDS upper layer predictions at various locations in the compartment 100 x 50 x 6 m

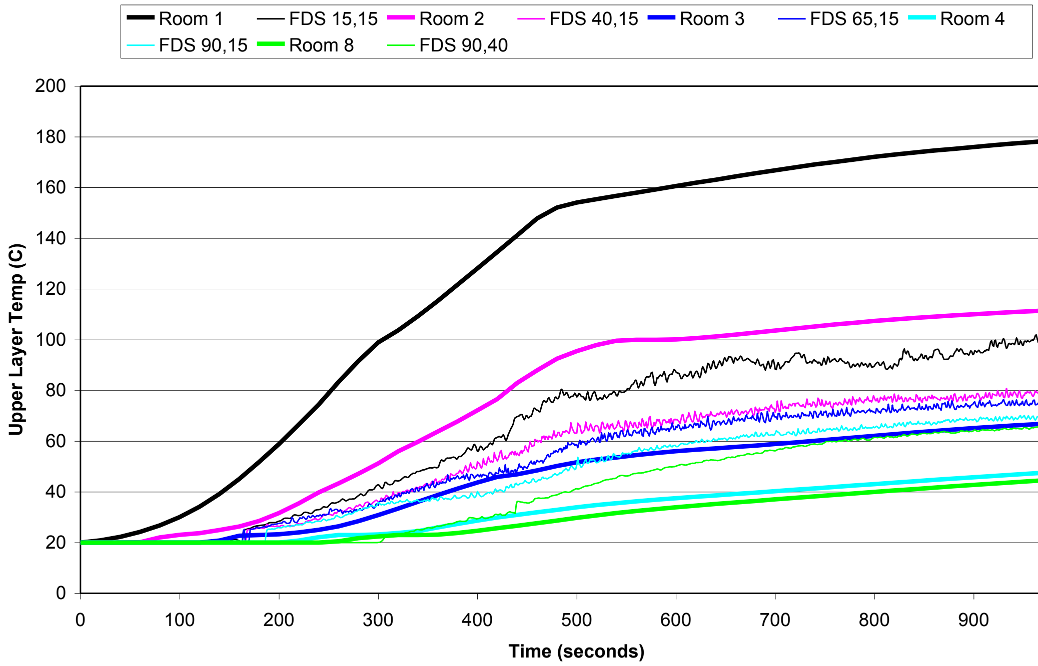

Figure 59. BRANZFIRE (with CCFM rules) upper layer temperatures using eight room model versus FDS upper layer predictions at various locations in the compartment 100 x 50 x 6 m

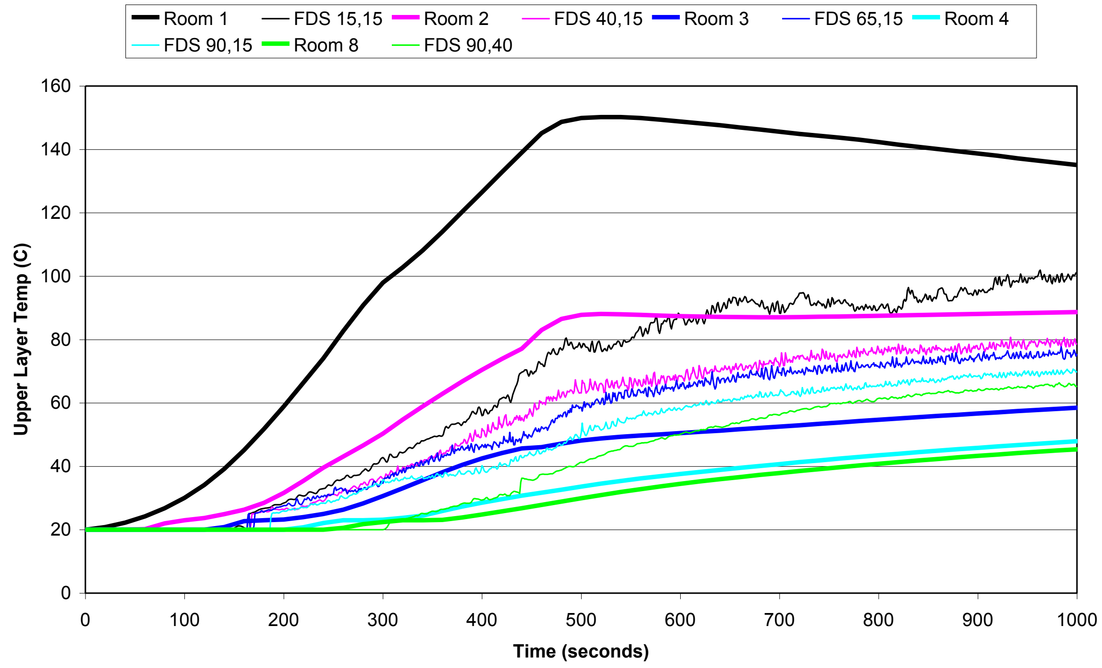

Figure 60. BRANZFIRE (with CFAST rules) upper layer temperatures using eight room model versus FDS upper layer predictions at various locations in the compartment 100 x 50 x 6 m

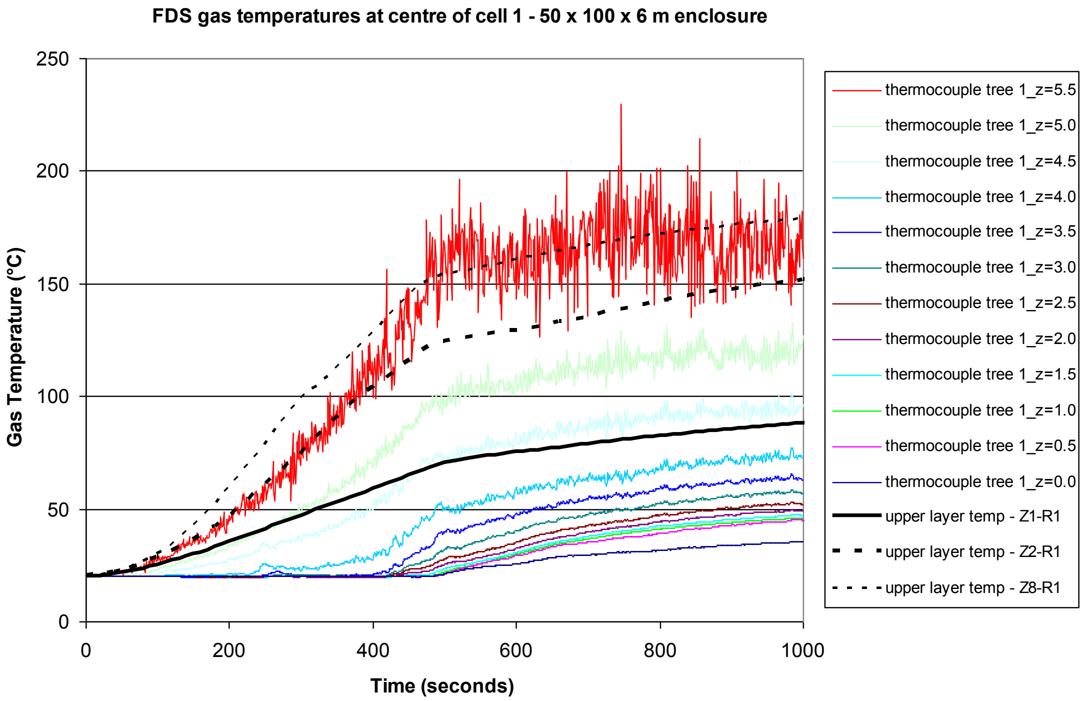

Figure 61. BRANZFIRE (with CCFM rules) upper layer temperatures versus FDS predictions over the height of the enclosure at the centre of compartment Z8-R1

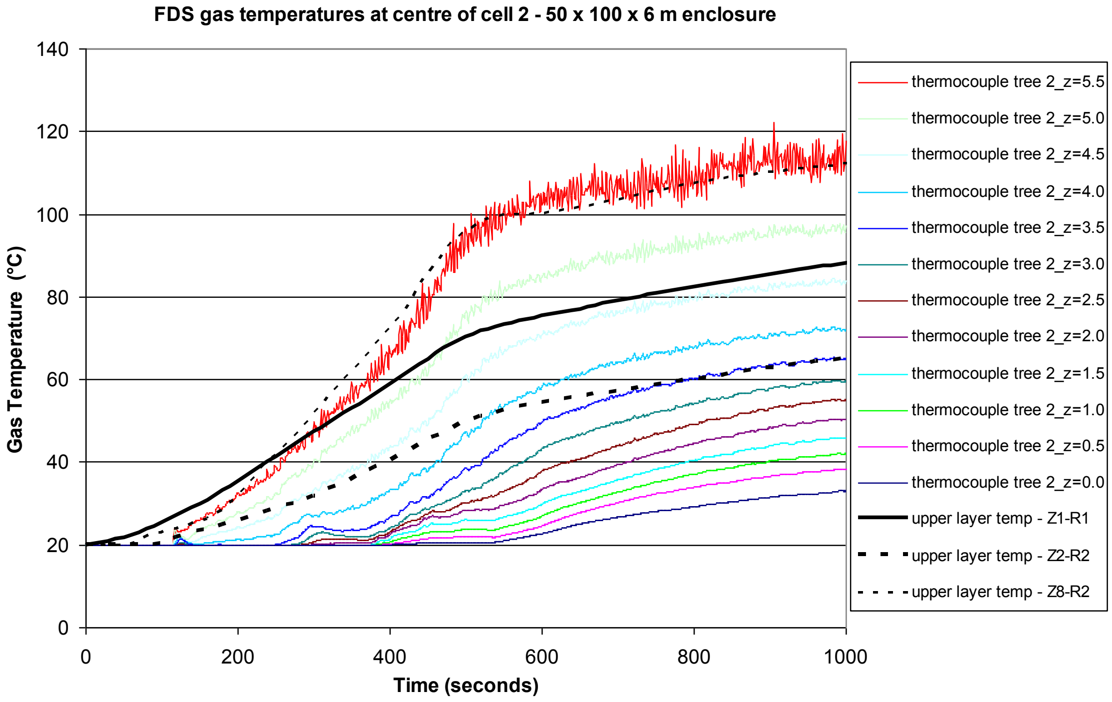

Figure 62. BRANZFIRE (with CCFM rules) upper layer temperatures versus FDS predictions over the height of the enclosure at the centre of compartment Z8-R2

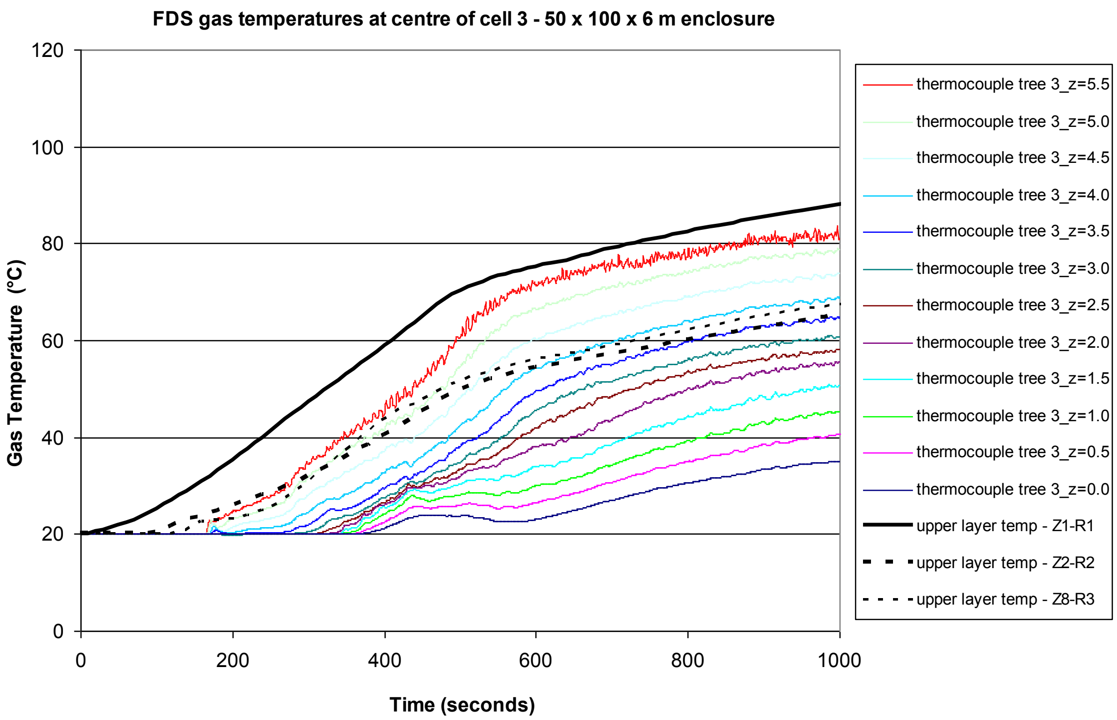

Figure 63. BRANZFIRE (with CCFM rules) upper layer temperatures versus FDS predictions over the height of the enclosure at the centre of compartment Z8-R3

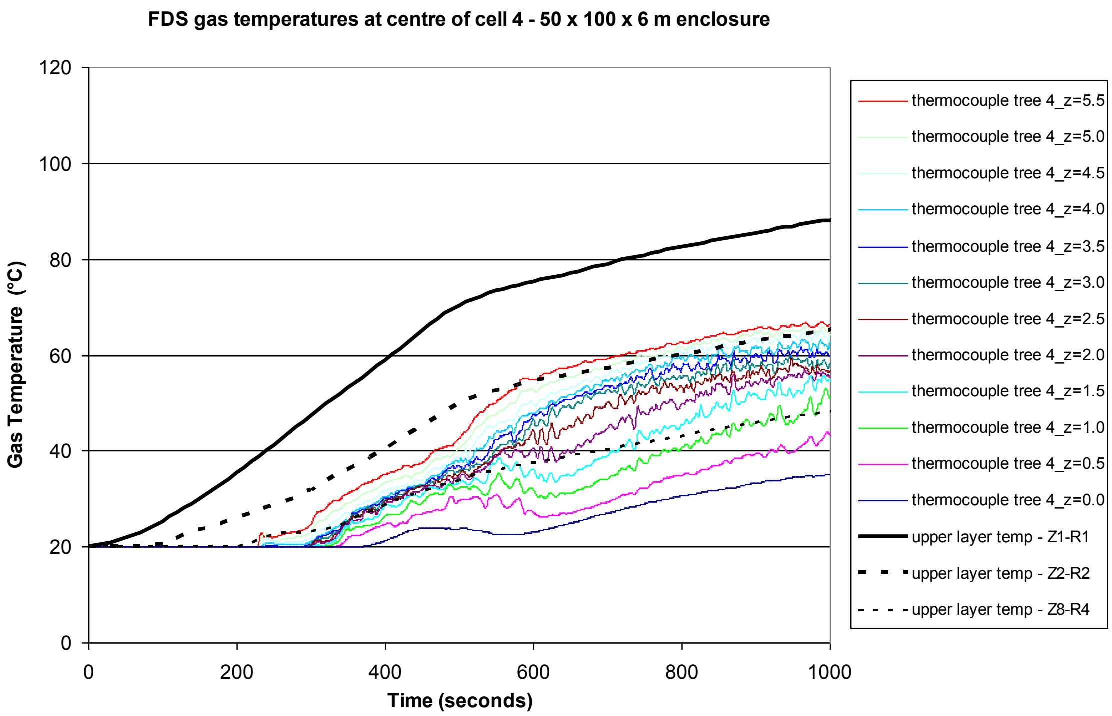

Figure 64. BRANZFIRE (with CCFM rules) upper layer temperatures versus FDS predictions over the height of the enclosure at the centre of compartment Z8-R4

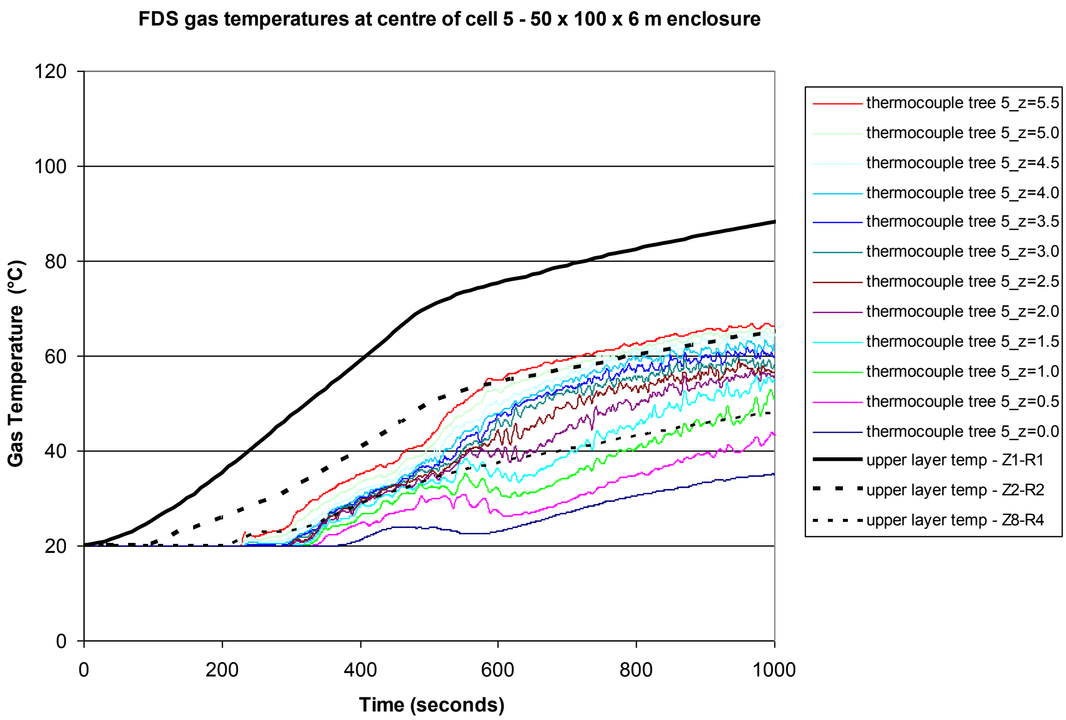

Figure 65. BRANZFIRE (with CCFM rules) upper layer temperatures versus FDS predictions over the height of the enclosure at the centre of compartment Z8-R5

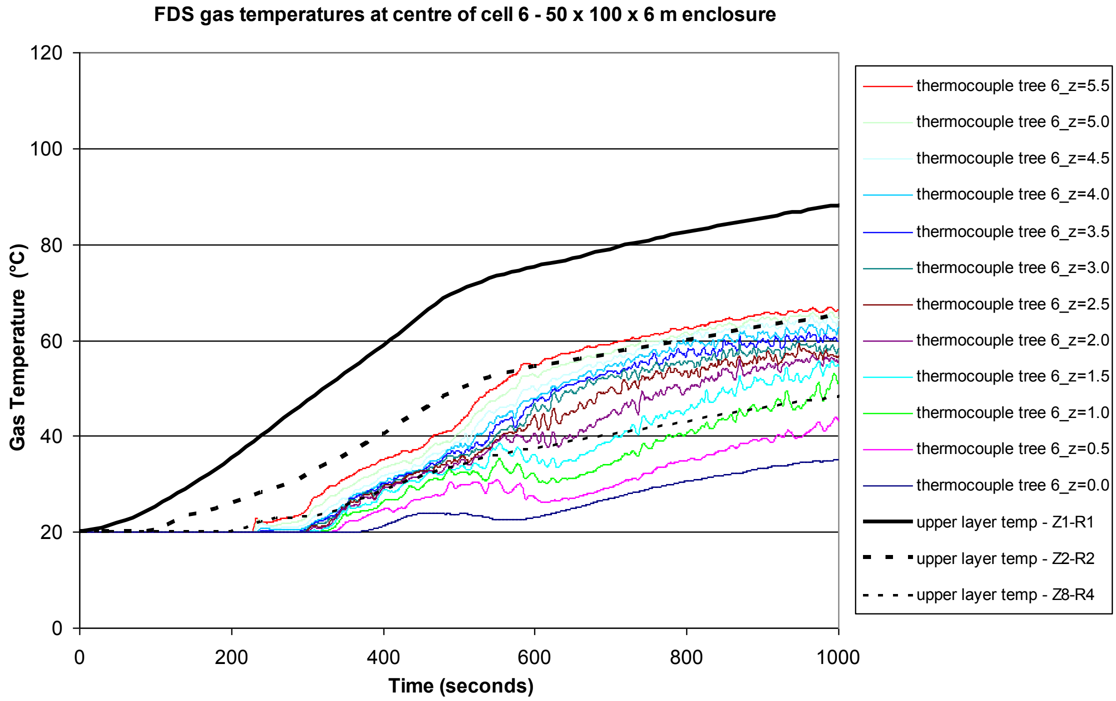

Figure 66. BRANZFIRE (with CCFM rules) upper layer temperatures versus FDS predictions over the height of the enclosure at the centre of compartment Z8-R6

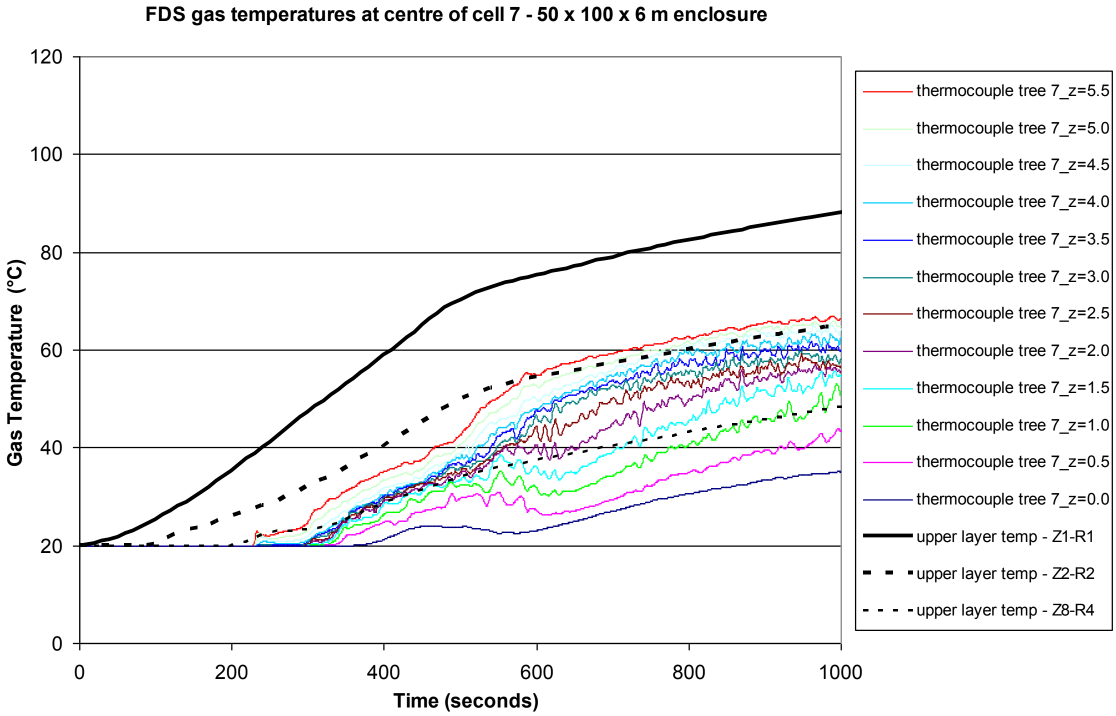

Figure 67. BRANZFIRE (with CCFM rules) upper layer temperatures versus FDS predictions over the height of the enclosure at the centre of compartment Z8-R7

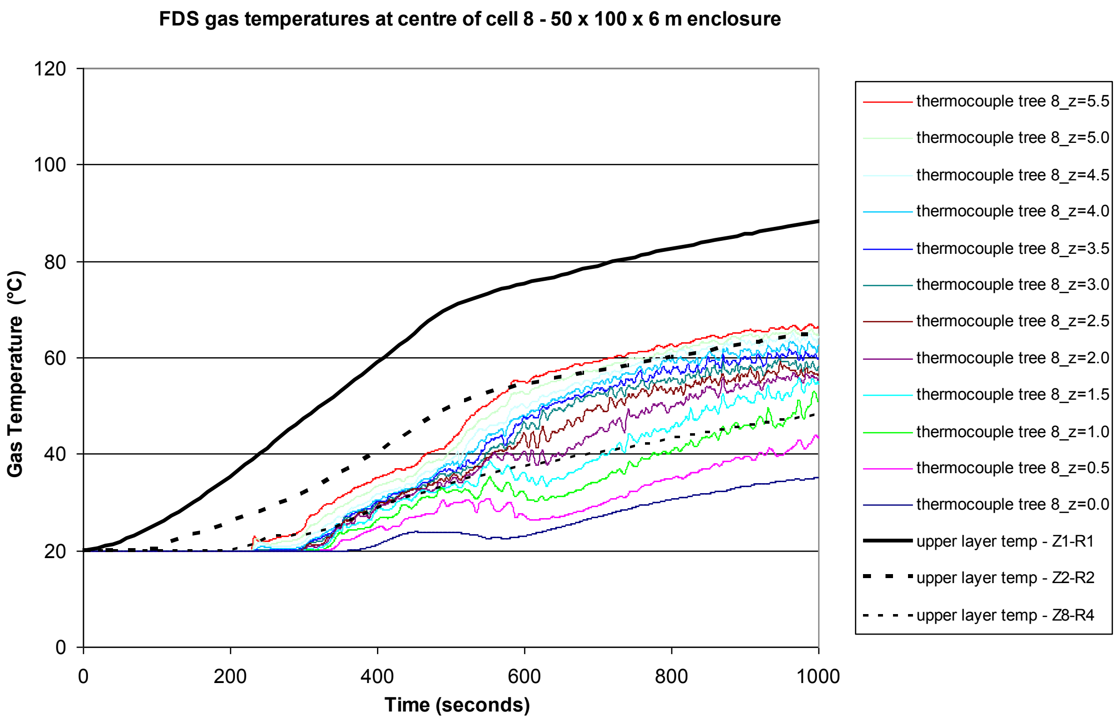

Figure 68. BRANZFIRE (with CCFM rules) upper layer temperatures versus FDS predictions over the height of the enclosure at the centre of compartment Z8-R8

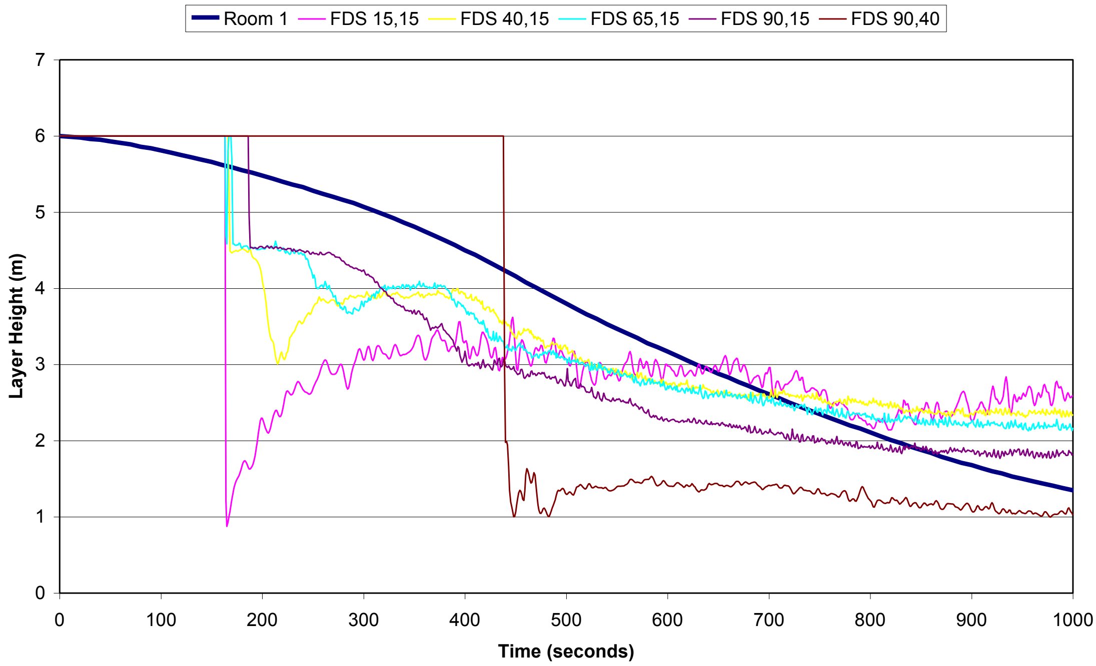

Figure 69. BRANZFIRE layer height using one room model versus FDS upper layer predictions at various locations in the compartment 100 x 50 x 6 m

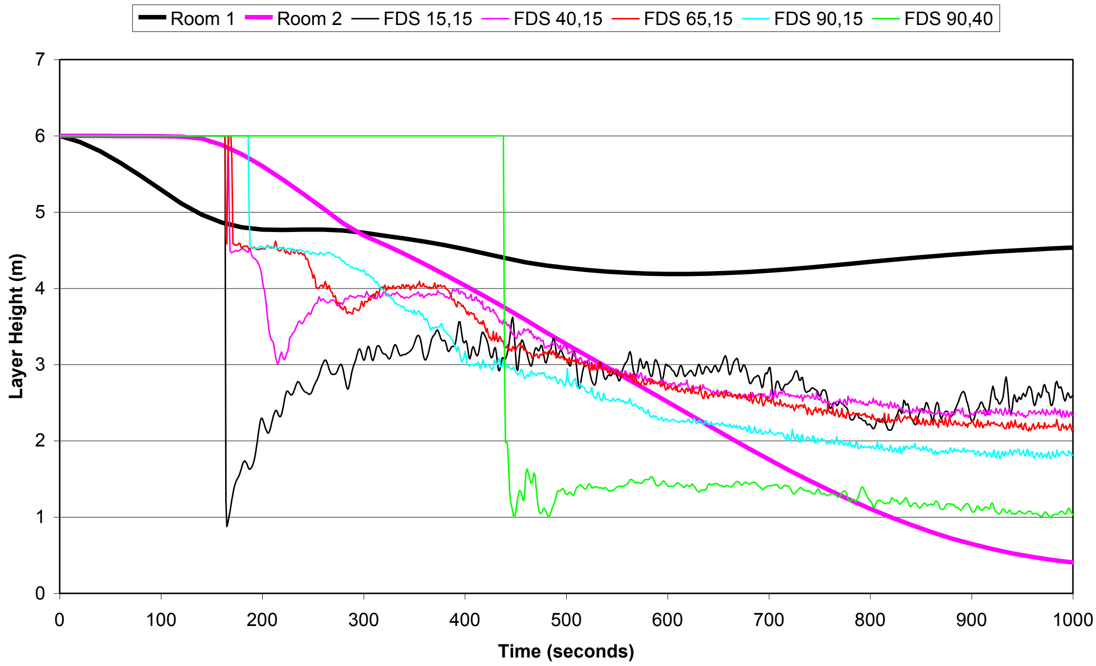

Figure 70. BRANZFIRE (with CCFM rules) layer height using two room model versus FDS upper layer predictions at various locations in the compartment 100 x 50 x 6 m

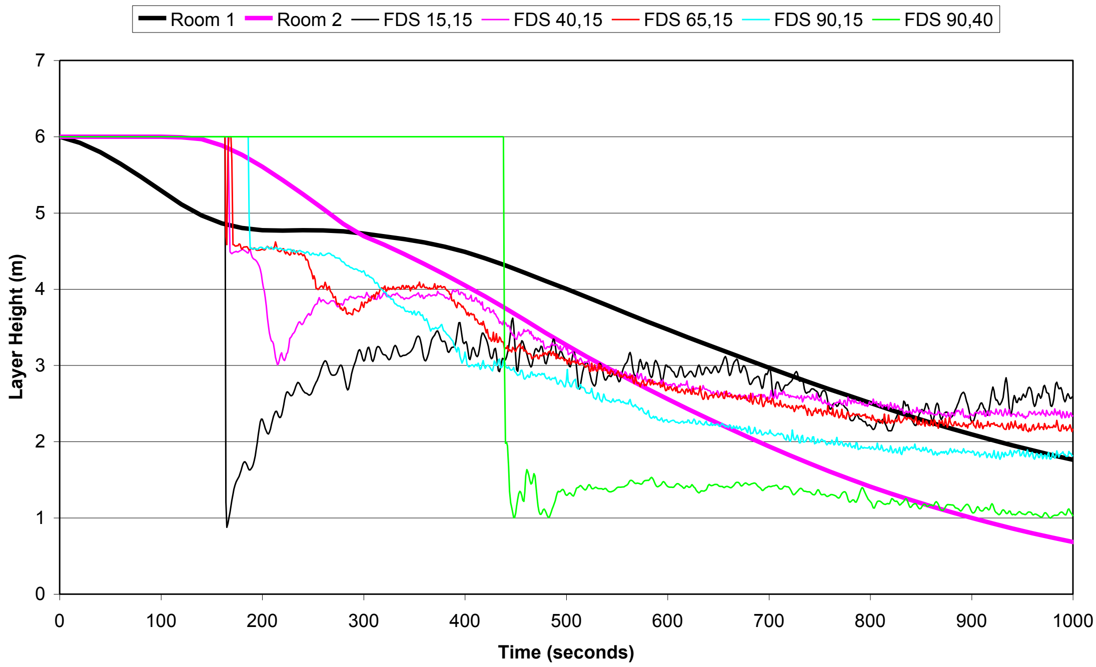

Figure 71. BRANZFIRE (with CFAST rules) layer height using two room model versus FDS upper layer predictions at various locations in the compartment 100 x 50 x 6 m

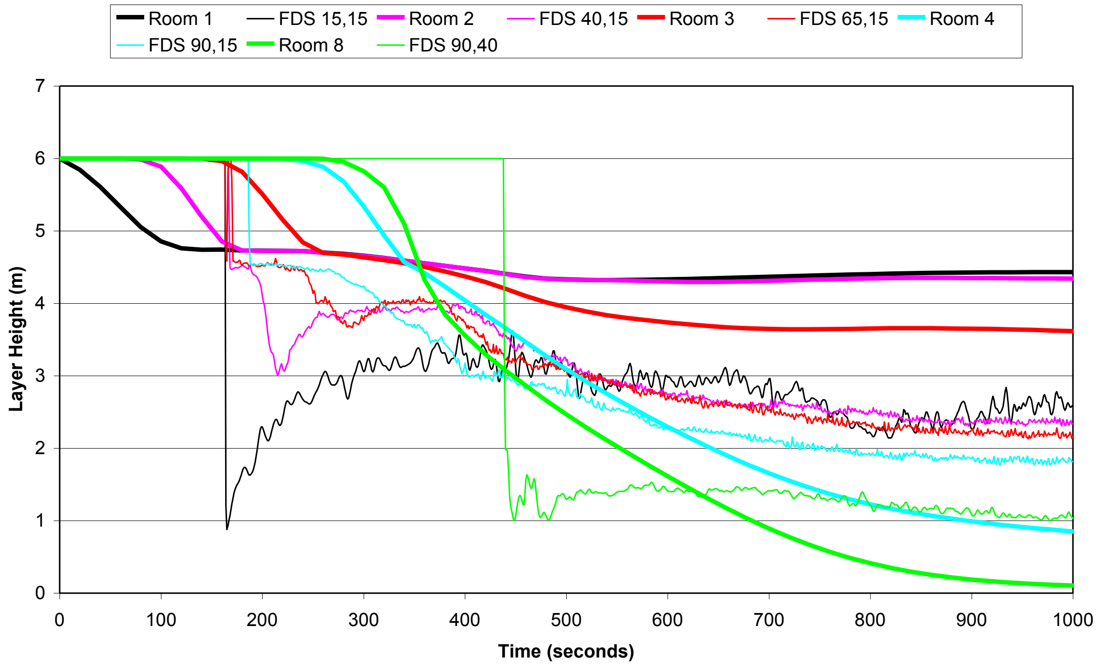

Figure 72. BRANZFIRE (with CCFM rules) layer height using eight room model versus FDS upper layer predictions at various locations in the compartment 100 x 50 x 6 m

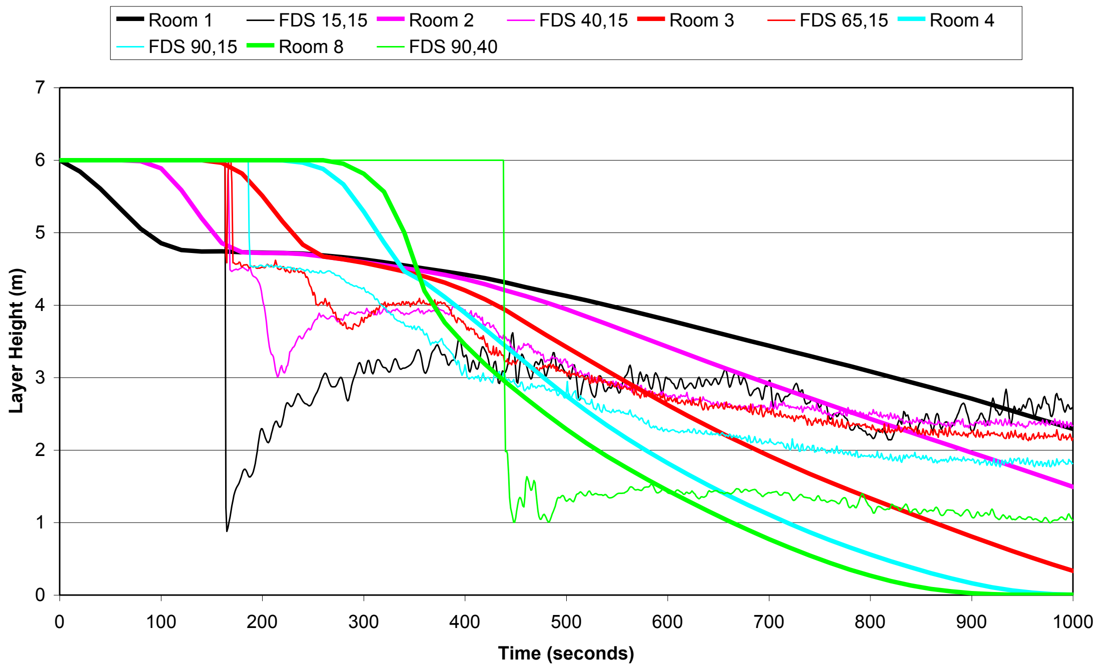

Figure 73. BRANZFIRE (with CFAST rules) layer height using eight room model versus FDS upper layer predictions at various locations in the compartment 100 x 50 x 6 m

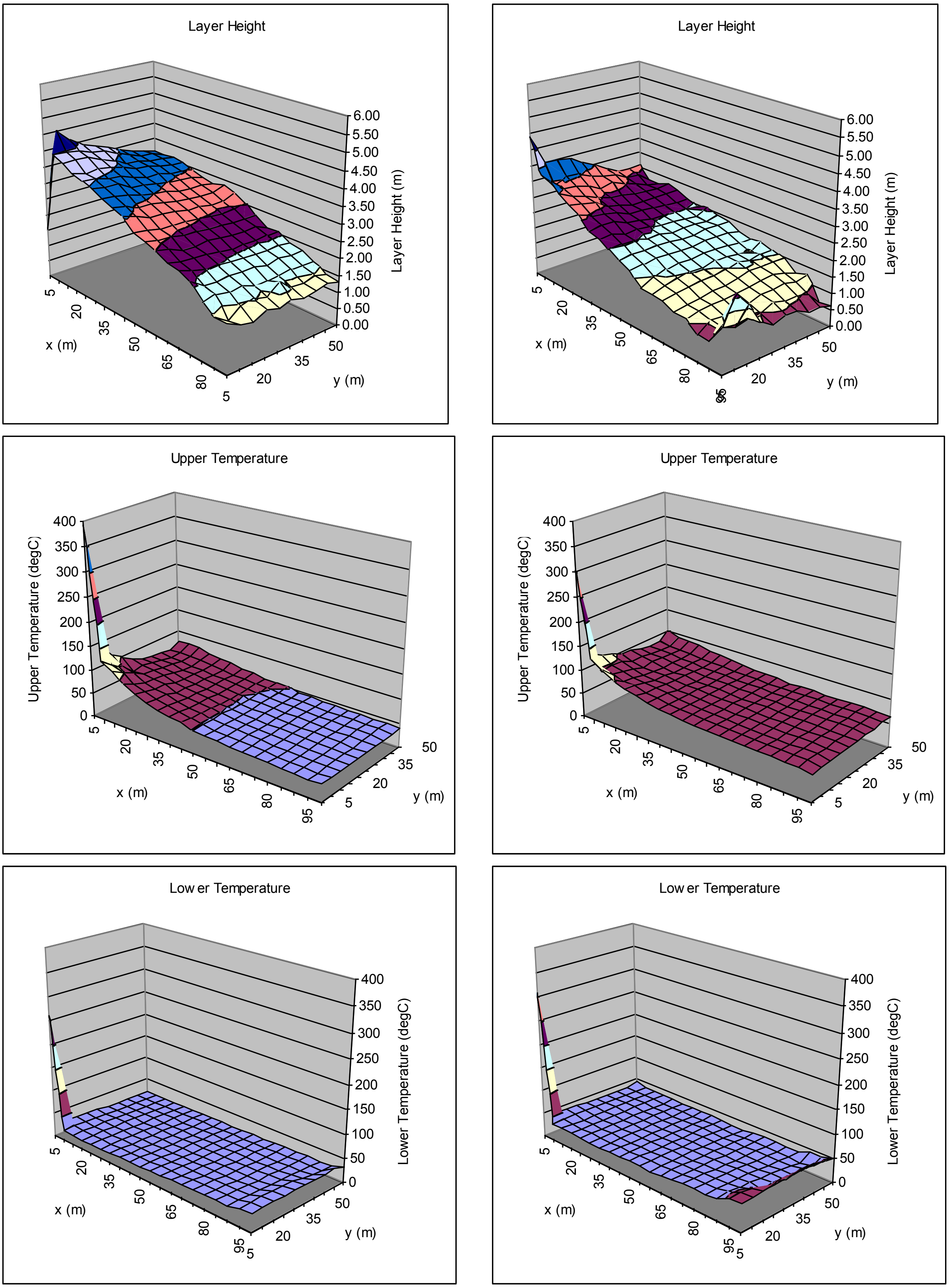

Figure 74. FDS derived predictions of layer height, upper layer temperature and lower layer temperature at 500 seconds (left) and 1000 seconds (right) for 50 x 100 x 6 m high enclosure.

3.3.6 Enclosure 100 x 50 x 9 m

BRANZFIRE and FDS were used to simulate smoke filling in a single room 100 x 50 x 9 m high with eight openings each 2 m high x 1 m wide similar to that illustrated in Figure 54. The FDS data was reduced to an equivalent upper and lower layer, at discrete points around the enclosure, by integration of the temperature data over the height of the compartment at the location of interest using functionality provided within the FDS program. BRANZFIRE was run with the enclosure modelled as one room, and then again as two rooms and eight rooms connected with a full width vents but this time with a minimal 0.1 m transom beneath the ceiling. Figure 55 describes the three configurations that were considered. In this case, only CFAST vent deposition rules were used in the zone model simulations.

Figure 75 compares the upper layer temperatures using a single room zone model with average upper layer temperatures from FDS at various locations in the enclosure. The zone model prediction is within the range of upper layer temperatures predicted by FDS but would not necessarily be conservative for design purposes.

Figure 77 compares the upper layer temperatures using an eight-room zone model with average upper layer temperatures from FDS at various locations in the enclosure.

Figure 78 to Figure 85 compare BRANZFIRE upper layer temperatures with the FDS predicted gas temperatures at different elevations at the centre of each cell of the eight-cell arrangement (Z8 of Figure 53).

Figure 86 compares the BRANZFIRE layer height for the one-room case with selected FDS predictions. The zone model predicts a slower initial descent of the layer compared to FDS, but is ultimately closer to the floor at a later stage.

Figure 87 compares BRANZFIRE layer height, using CFAST rules, for the two-room approach with the FDS estimated layer height for selected locations throughout the enclosure.

Figure 88 compares BRANZFIRE layer height, using CFAST rules, for the eight-room approach with the FDS estimated layer height for selected locations throughout the enclosure.

Figure 89 shows the FDS results after 500 and 1000 seconds, using the integrated temperature data to calculate the upper and lower layer temperatures and the layer height. It clearly shows the increasing layer thickness and reducing upper layer temperature across the enclosure in the far field.

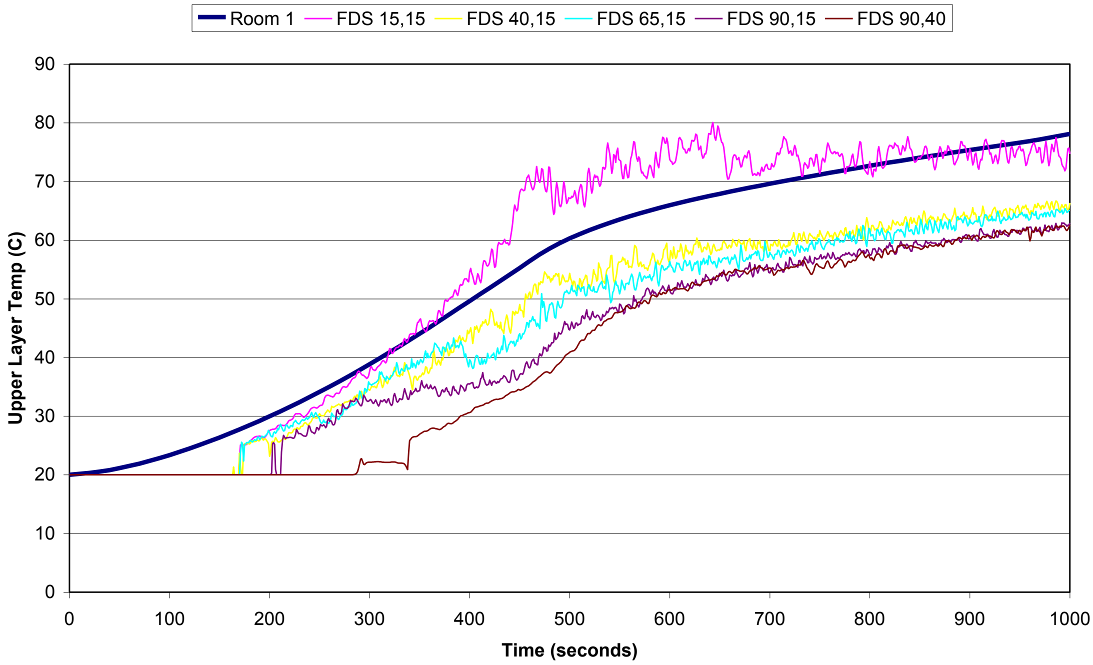

Figure 75. BRANZFIRE upper layer temperatures using one room model versus FDS upper layer predictions at various locations in the compartment 100 x 50 x 9 m

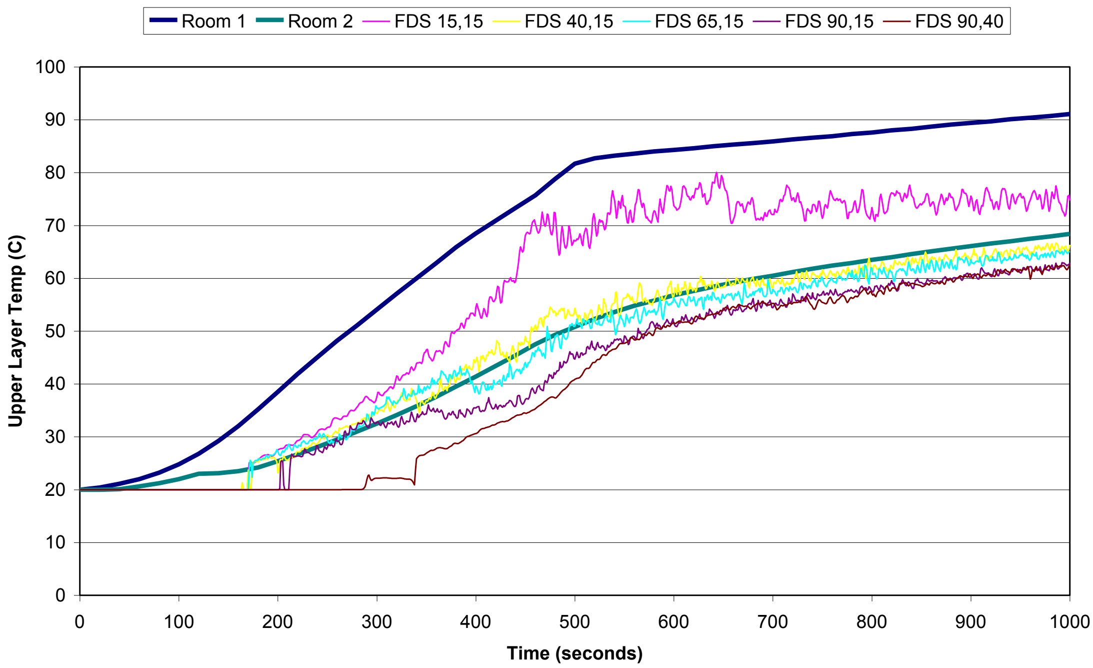

Figure 76. BRANZFIRE upper layer temperatures (with CFAST rules) using two room model versus FDS upper layer predictions at various locations in the compartment 100 x 50 x 9 m

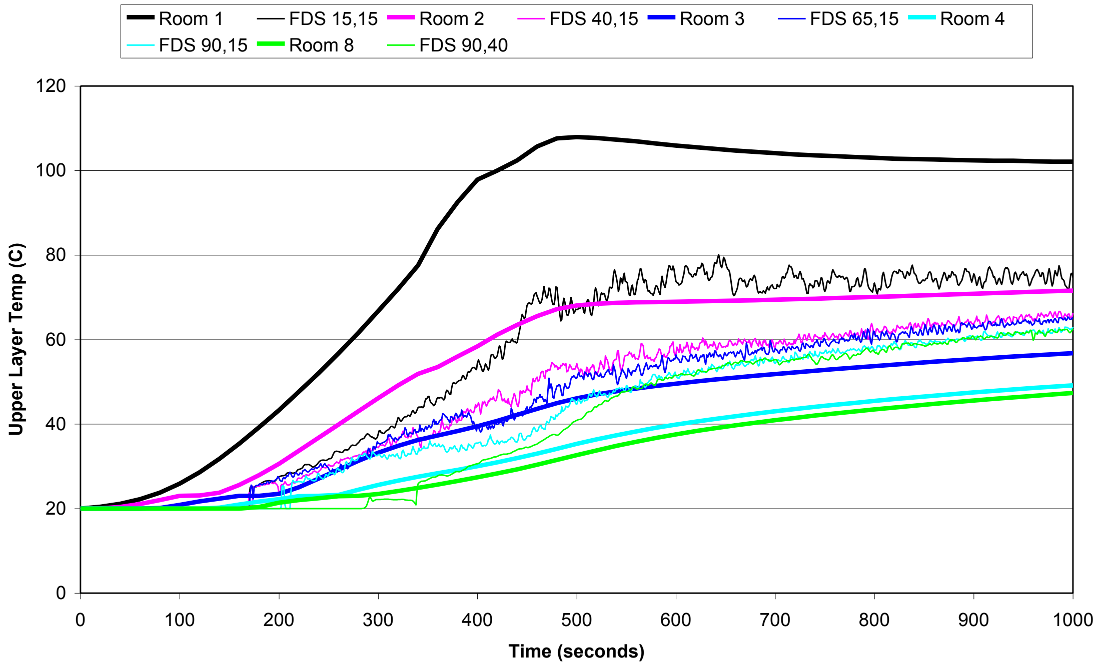

Figure 77. BRANZFIRE (with CFAST rules) upper layer temperatures using eight room model versus FDS upper layer predictions at various locations in the compartment 100 x 50 x 9 m

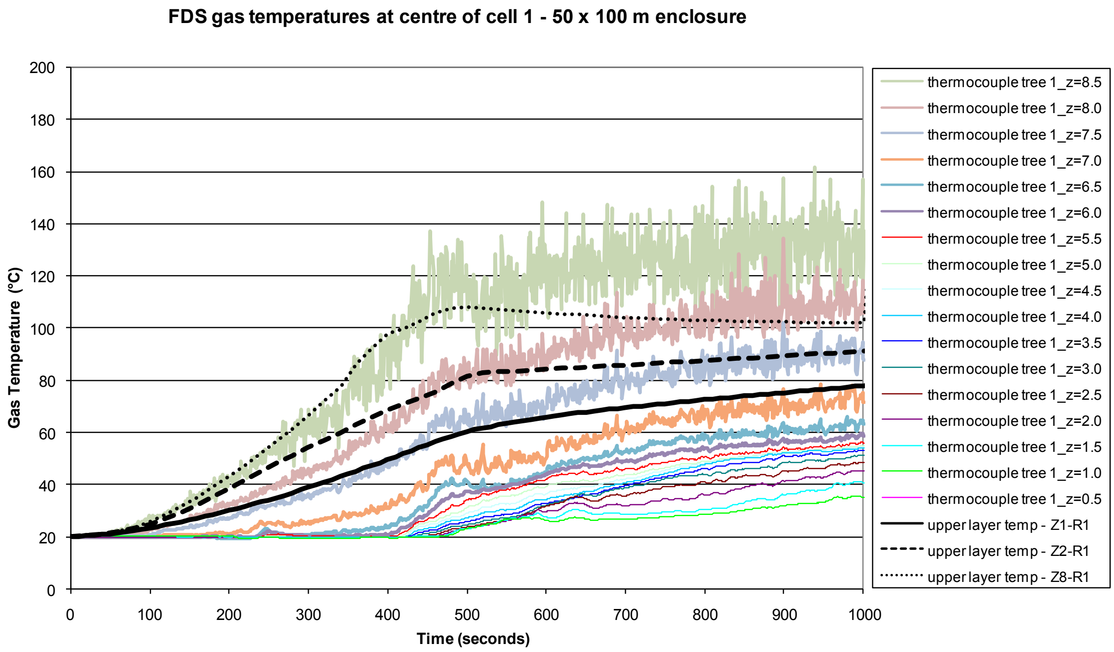

Figure 78. BRANZFIRE (with CFAST rules) upper layer temperatures versus FDS predictions over the height of the enclosure at the centre of compartment Z8-R1

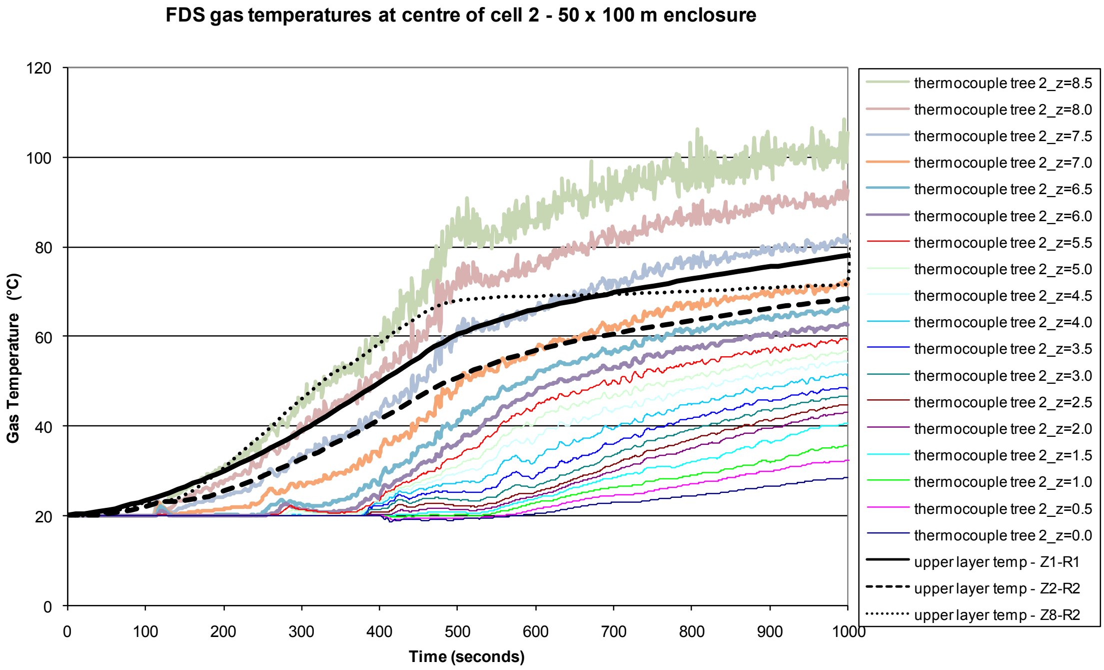

Figure 79. BRANZFIRE (with CFAST rules) upper layer temperatures versus FDS predictions over the height of the enclosure at the centre of compartment Z8-R2

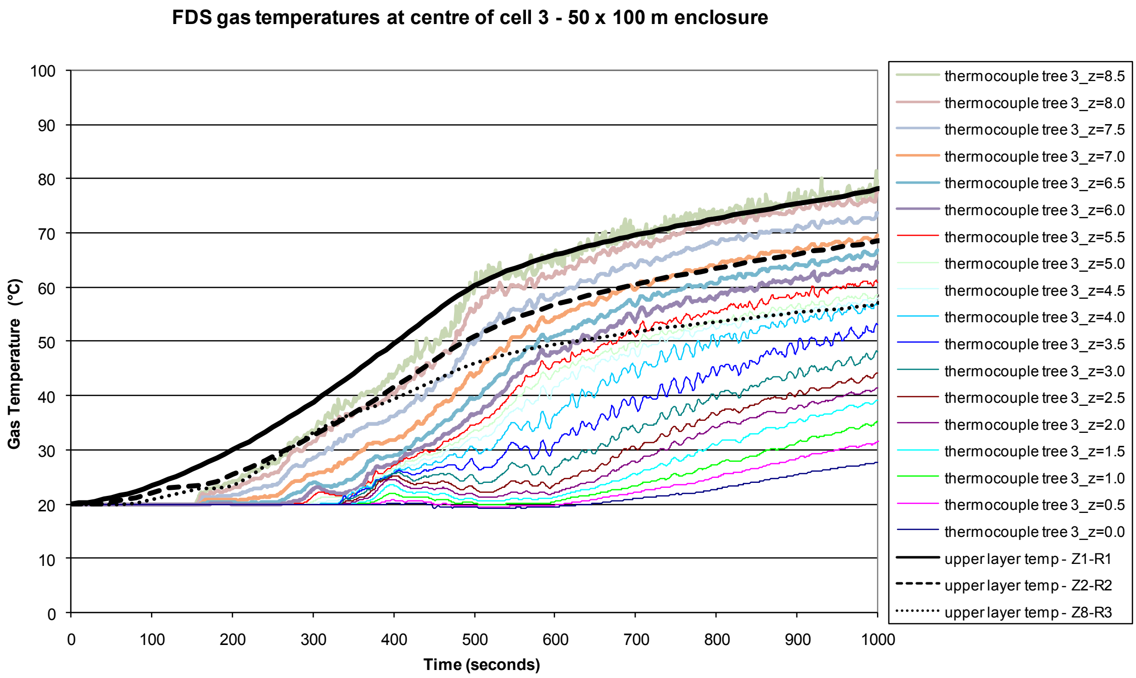

Figure 80. BRANZFIRE (with CFAST rules) upper layer temperatures versus FDS predictions over the height of the enclosure at the centre of compartment Z8-R3

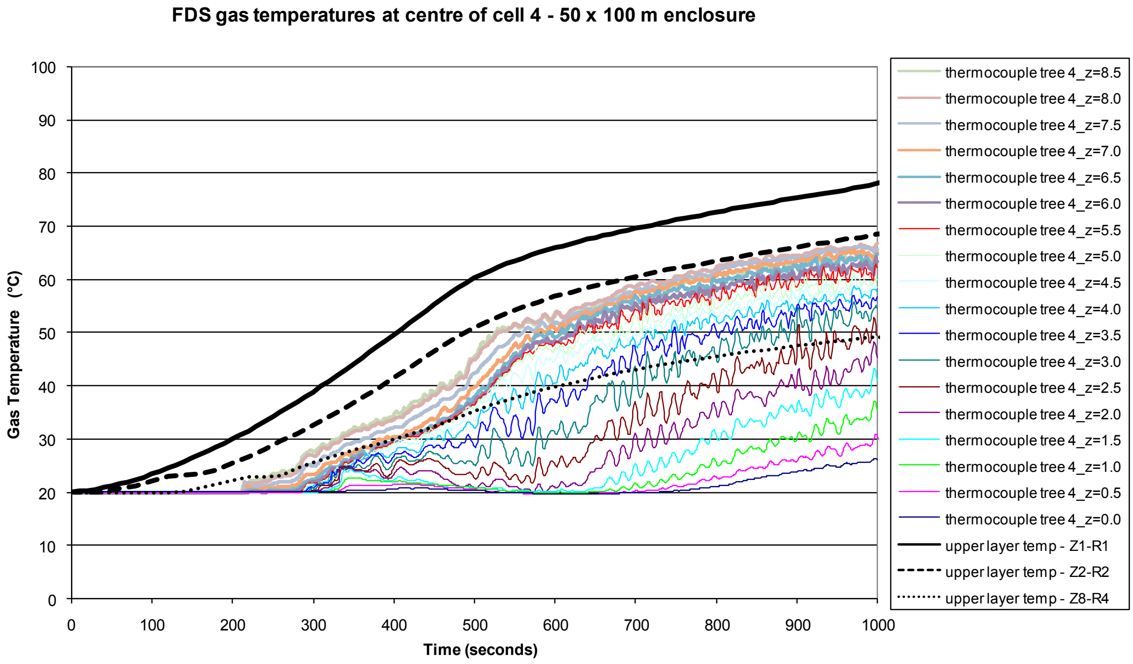

Figure 81. BRANZFIRE (with CFAST rules) upper layer temperatures versus FDS predictions over the height of the enclosure at the centre of compartment Z8-R4

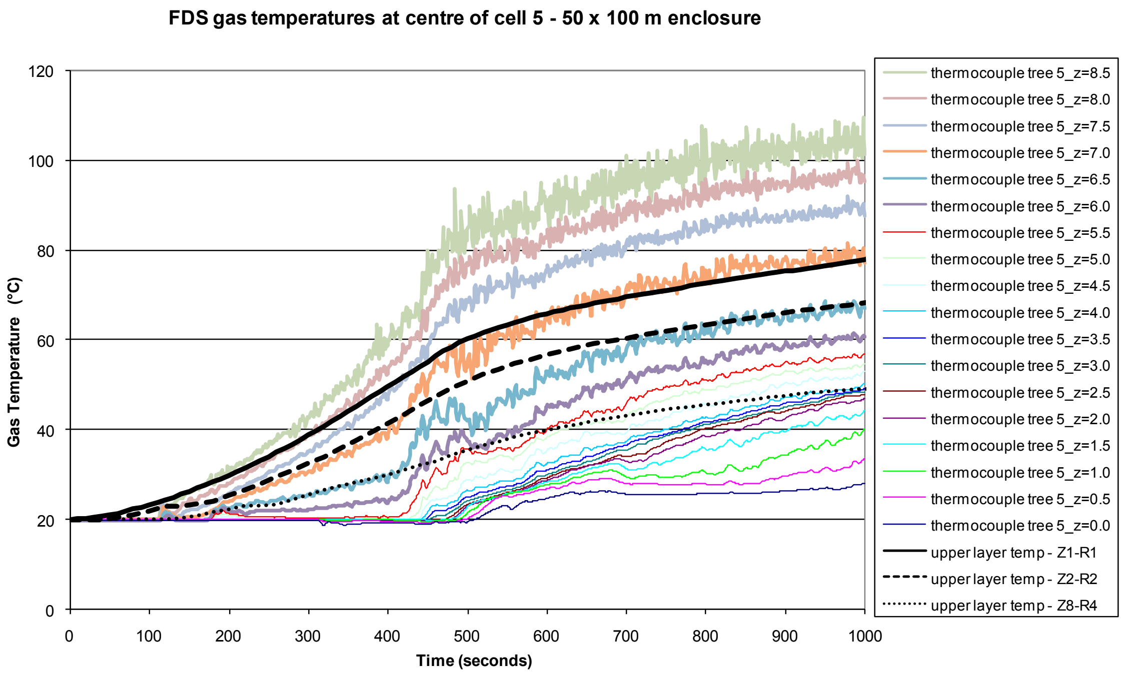

Figure 82. BRANZFIRE (with CFAST rules) upper layer temperatures versus FDS predictions over the height of the enclosure at the centre of compartment Z8-R5

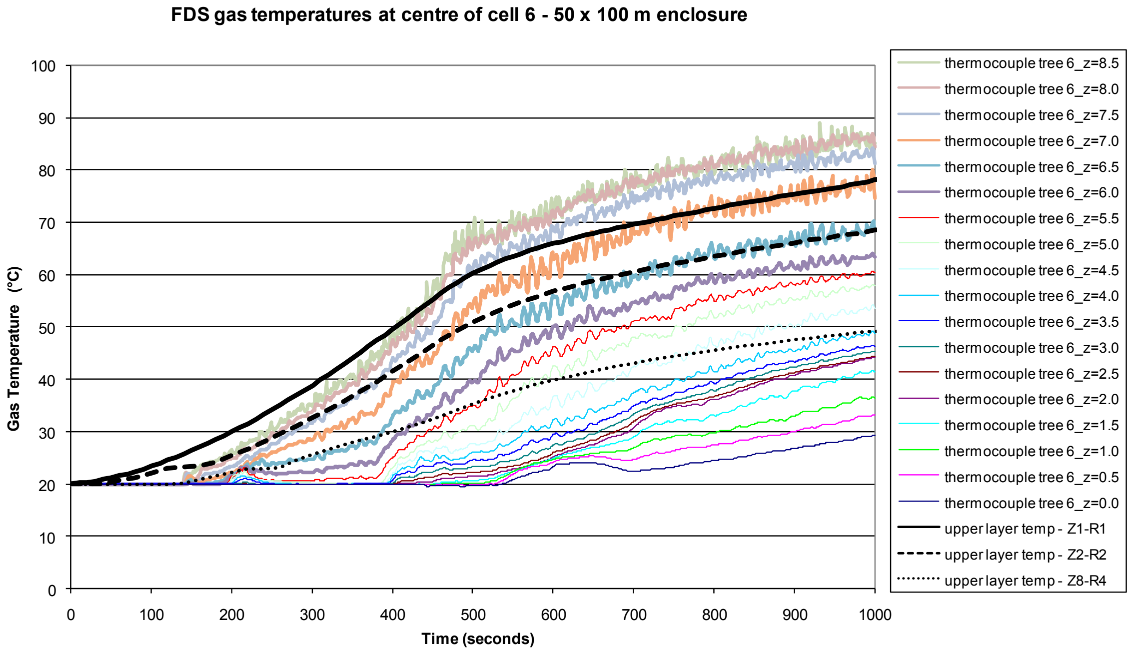

Figure 83. BRANZFIRE (with CFAST rules) upper layer temperatures versus FDS predictions over the height of the enclosure at the centre of compartment Z8-R6

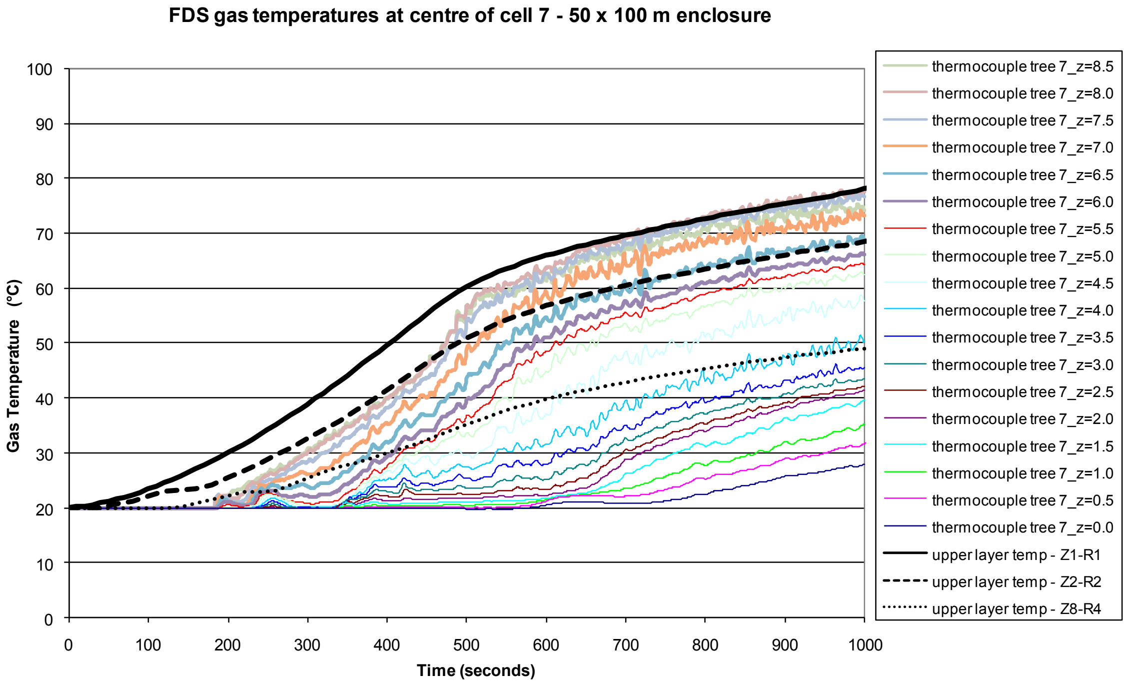

Figure 84. BRANZFIRE (with CFAST rules) upper layer temperatures versus FDS predictions over the height of the enclosure at the centre of compartment Z8-R7

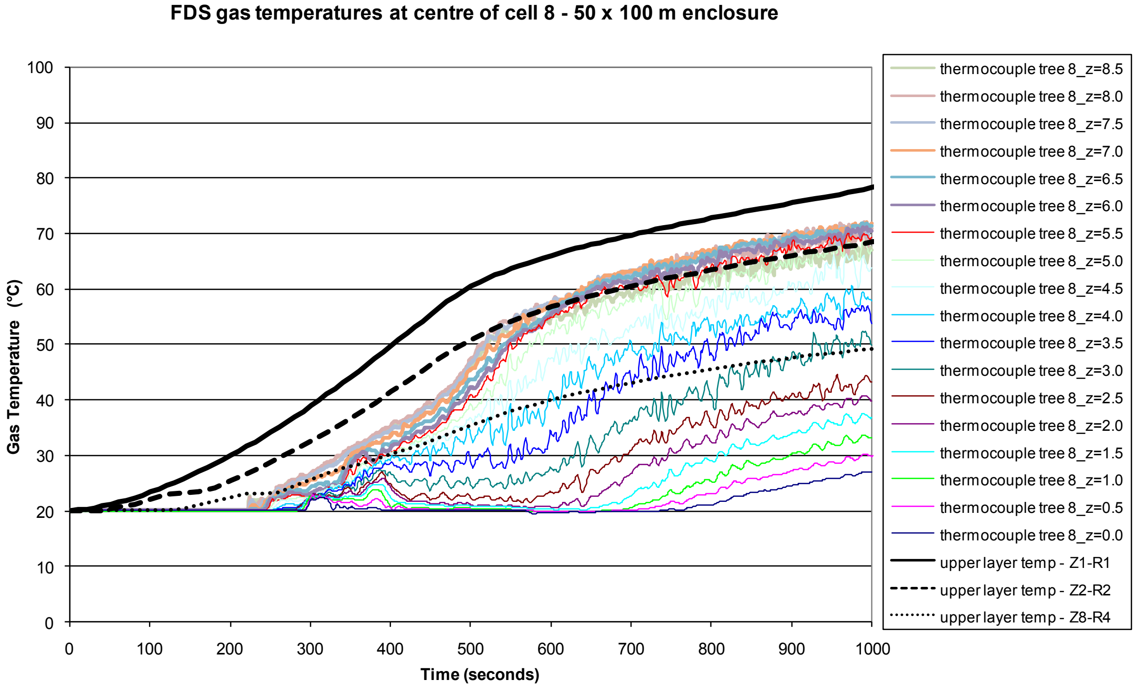

Figure 85. BRANZFIRE (with CFAST rules) upper layer temperatures versus FDS predictions over the height of the enclosure at the centre of compartment Z8-R8

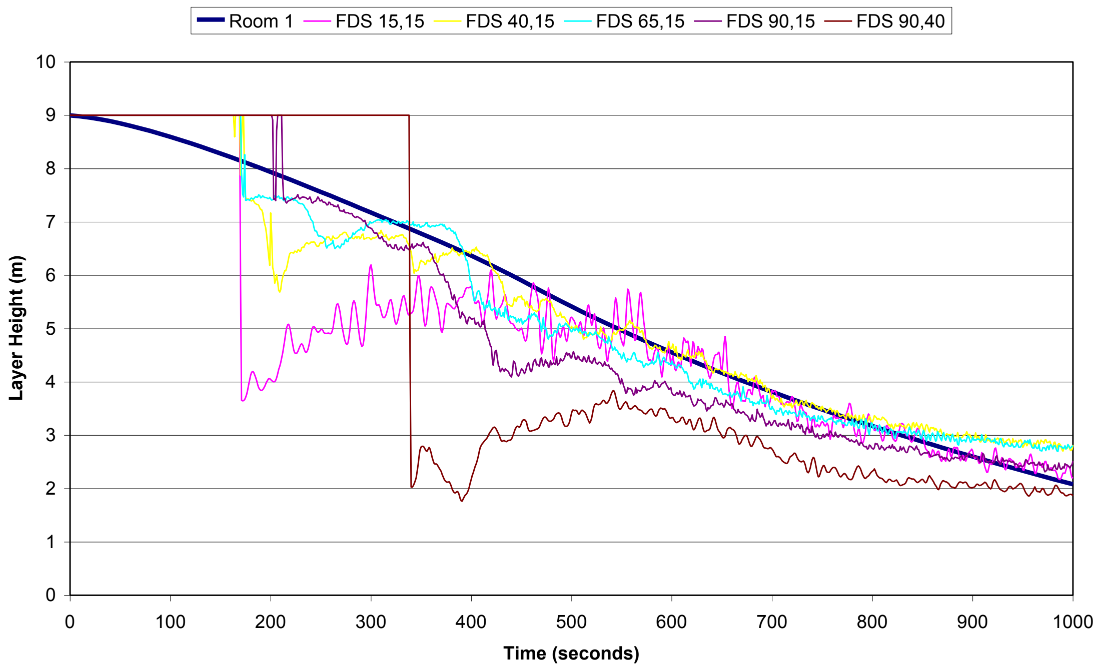

Figure 86. BRANZFIRE layer height using one room model versus FDS upper layer predictions at various locations in the compartment 100 x 50 x 9 m

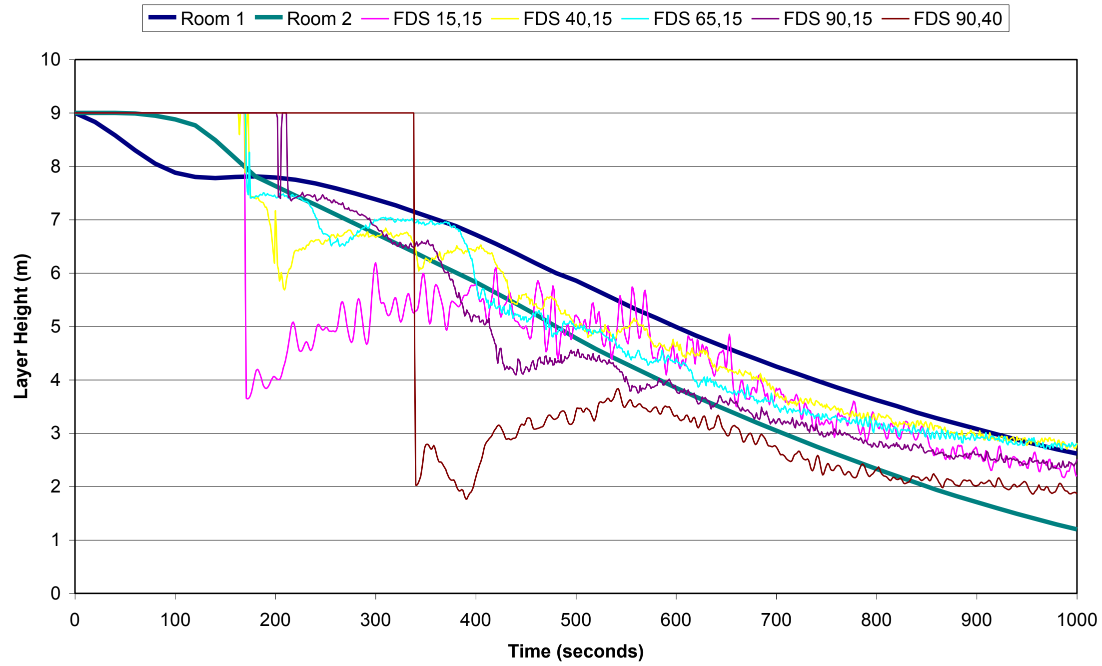

Figure 87. BRANZFIRE (with CFAST rules) layer height using two room model versus FDS upper layer predictions at various locations in the compartment 100 x 50 x 9 m

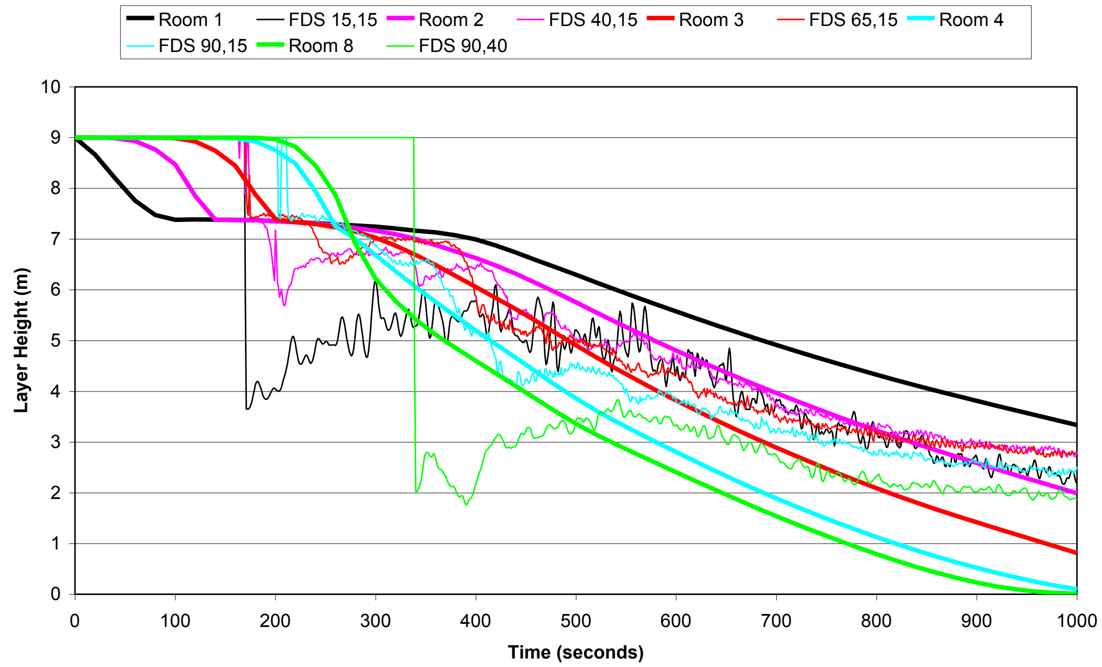

Figure 88. BRANZFIRE (with CFAST rules) layer height using eight room model versus FDS upper layer predictions at various locations in the compartment 100 x 50 x 9 m

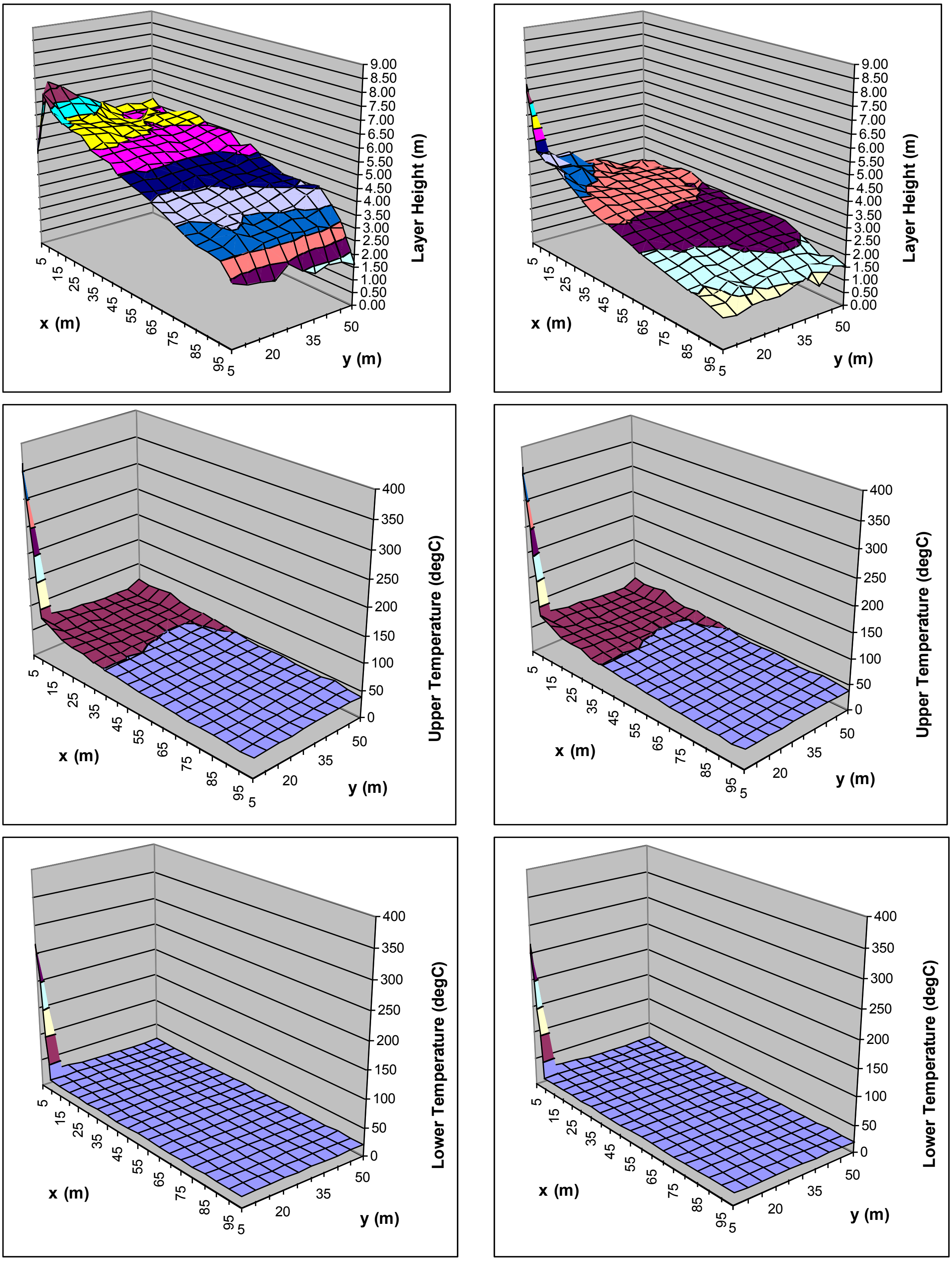

Figure 89. FDS derived predictions of layer height, upper layer temperature and lower layer temperature at 500 seconds (left) and 1000 seconds (right) for 50 x 100 x 9 m high enclosure.

3.3.7 Enclosure 100 x 50 x 12 m

BRANZFIRE and FDS were used to simulate smoke filling in a single room 100 x 50 x 12 m high with eight openings each 2 m high x 1 m wide similar to that illustrated in Figure 54. The FDS data was reduced to an equivalent upper and lower layer, at discrete points around the enclosure, by integration of the temperature data over the height of the compartment at the location of interest using functionality provided within the FDS program. BRANZFIRE was run with the enclosure modelled as one room, and then again as two rooms and eight rooms connected with a full width vents with a 0.1 m transom beneath the ceiling. Figure 55 describes the three configurations that were considered.

Figure 90 compares the upper layer temperatures using a single room zone model with average upper layer temperatures from FDS at various locations in the enclosure. The zone model prediction is close to the average upper layer temperatures predicted by FDS at the 15,15 location.

Figure 91 compares BRANZFIRE layer height, using CFAST rules, for the two-room approach with the FDS estimated layer height for selected locations throughout the enclosure with good agreement between the two models.

Figure 92 compares the upper layer temperatures using an eight-room zone model with average upper layer temperatures from FDS at various locations in the enclosure. In this case, the zone model over-predicts temperatures close to the fire and under-predicts temperatures far from the fire.

Figure 93 to Figure 100 compare BRANZFIRE upper layer temperatures with the FDS predicted gas temperatures at different elevations at the centre of each cell of the eight-cell arrangement (Z8 of Figure 53).

Figure 101 compares the BRANZFIRE layer height for the one-room case with selected FDS predictions with very good agreement.

Figure 102 compares BRANZFIRE layer height, using CFAST rules, for the two-room approach with the FDS estimated layer height for selected locations throughout the enclosure, again with good agreement.

Figure 103 compares BRANZFIRE layer height, using CFAST rules, for the eight-room approach with the FDS estimated layer height for selected locations throughout the enclosure. In this case the spread in the BRANZFIRE predictions is greater than for the FDS predictions.

Figure 104 shows the FDS results after 500 and 1000 seconds, using the integrated temperature data to calculate the upper and lower layer temperatures and the layer height.

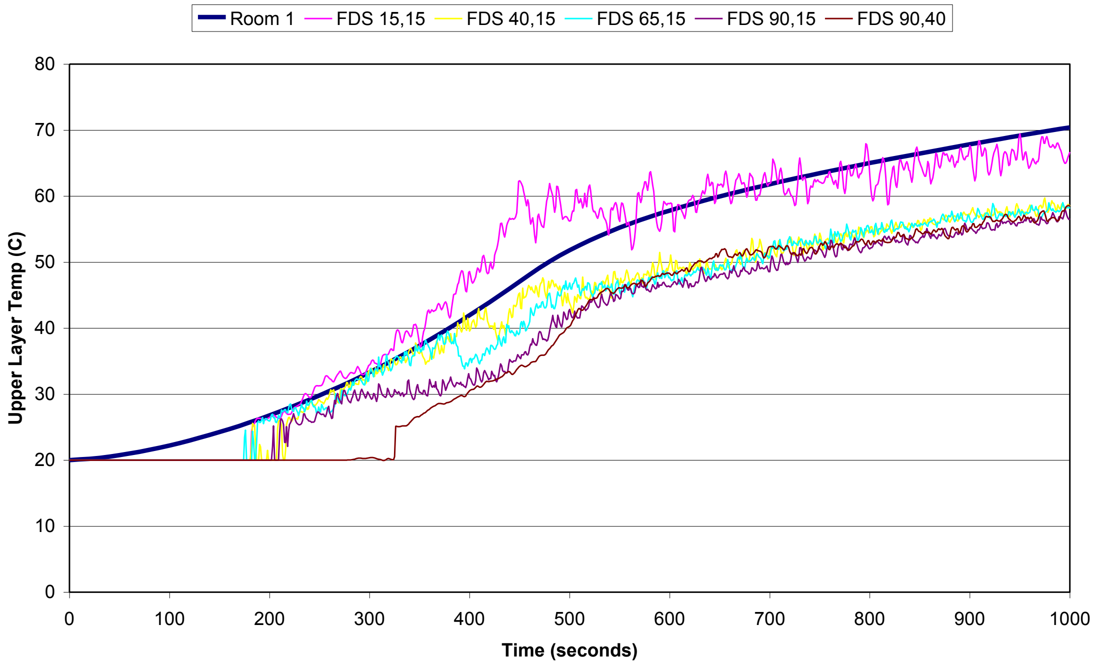

Figure 90. BRANZFIRE upper layer temperatures using one room model versus FDS upper layer predictions at various locations in the compartment 100 x 50 x 12 m

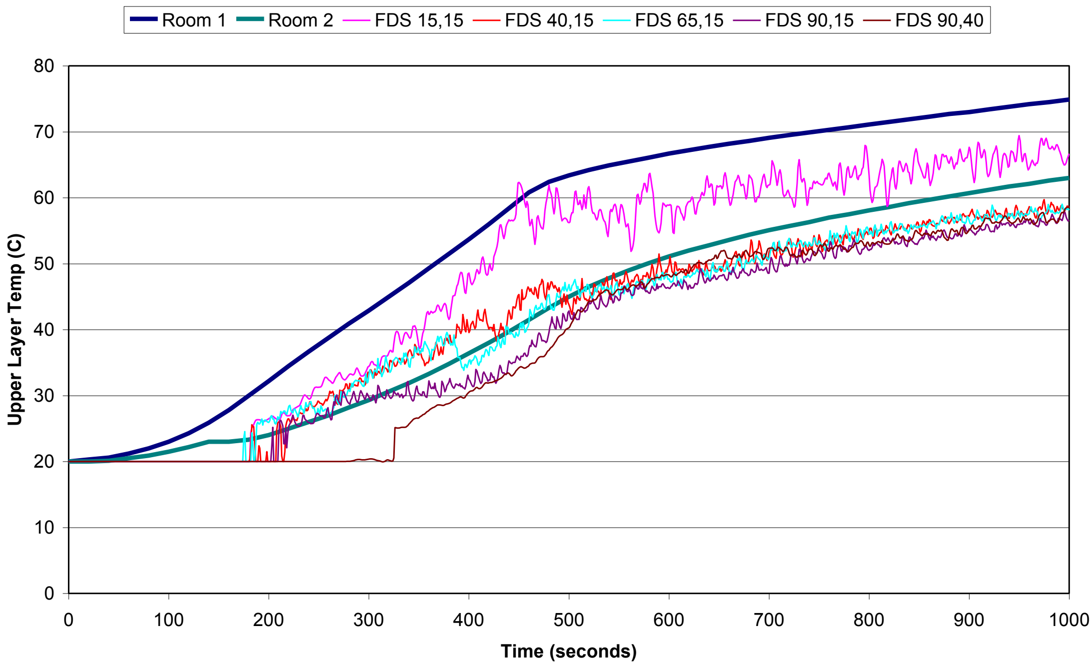

Figure 91. BRANZFIRE upper layer temperatures (with CFAST rules) using two room model versus FDS upper layer predictions at various locations in the compartment 100 x 50 x 12 m

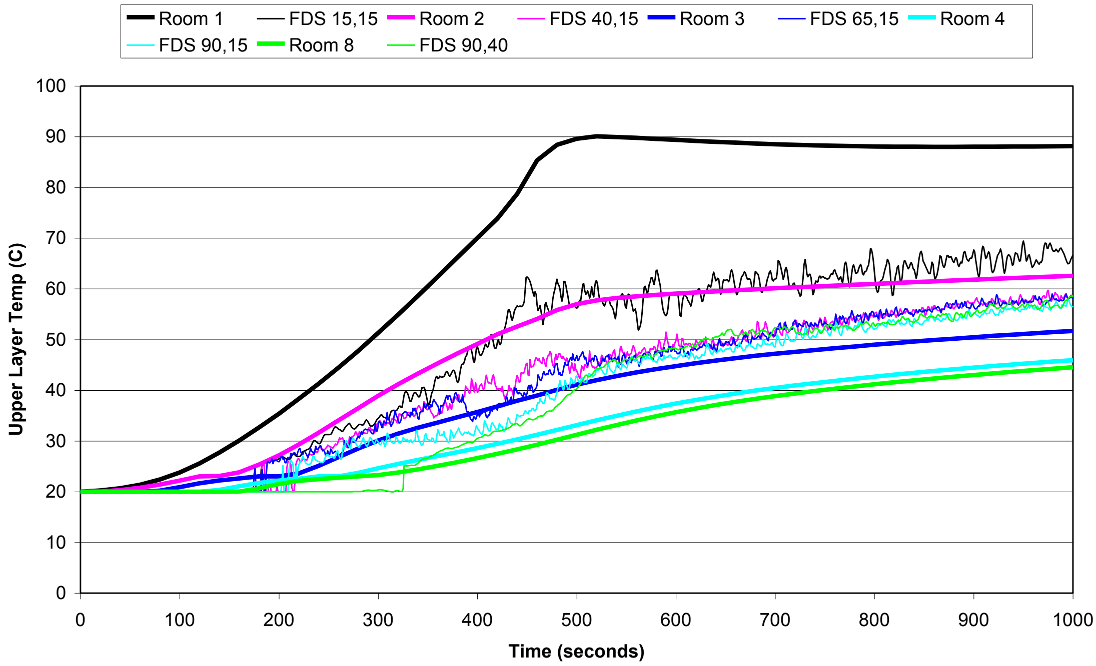

Figure 92. BRANZFIRE (with CFAST rules) upper layer temperatures using eight room model versus FDS upper layer predictions at various locations in the compartment 100 x 50 x 12 m

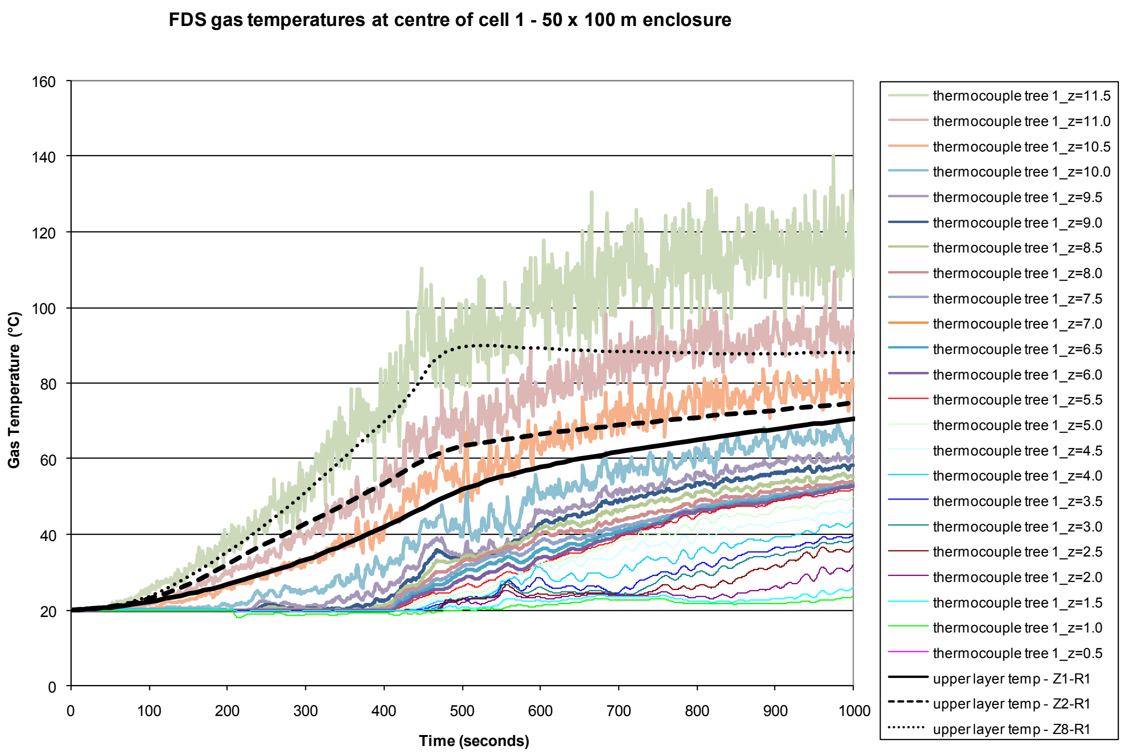

Figure 93. BRANZFIRE (with CFAST rules) upper layer temperatures versus FDS predictions over the height of the enclosure at the centre of compartment Z8-R1

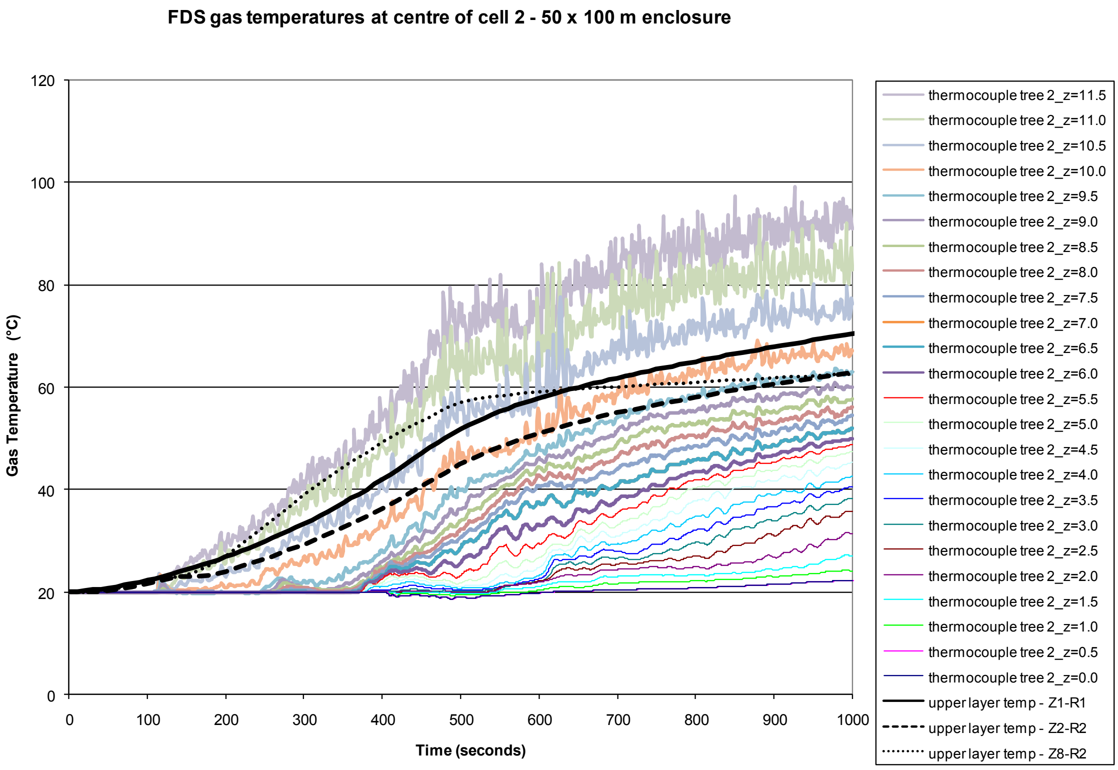

Figure 94. BRANZFIRE (with CFAST rules) upper layer temperatures versus FDS predictions over the height of the enclosure at the centre of compartment Z8-R2

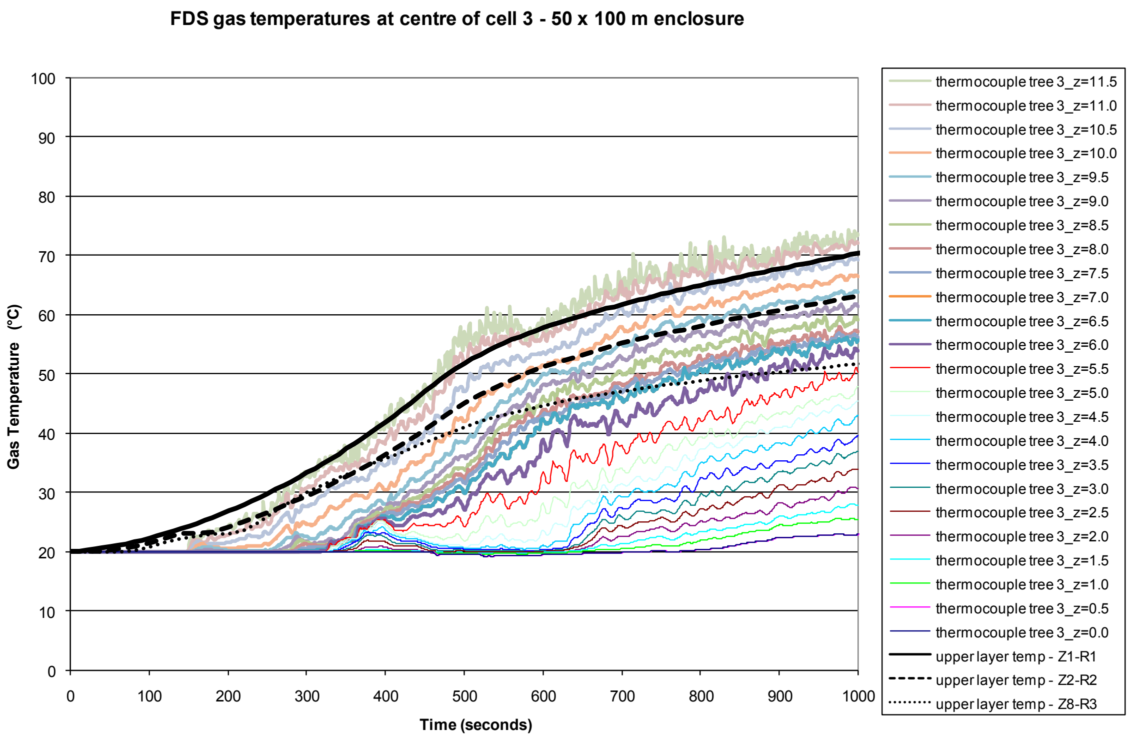

Figure 95. BRANZFIRE (with CFAST rules) upper layer temperatures versus FDS predictions over the height of the enclosure at the centre of compartment Z8-R3

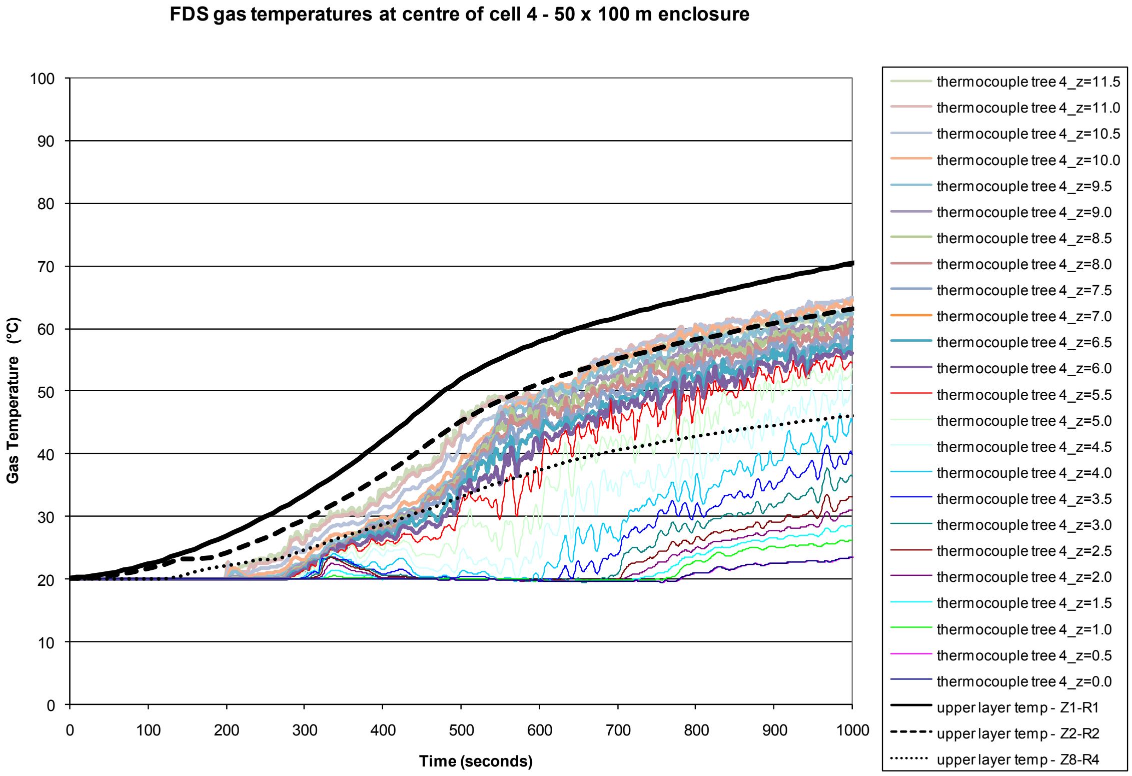

Figure 96. BRANZFIRE (with CFAST rules) upper layer temperatures versus FDS predictions over the height of the enclosure at the centre of compartment Z8-R4

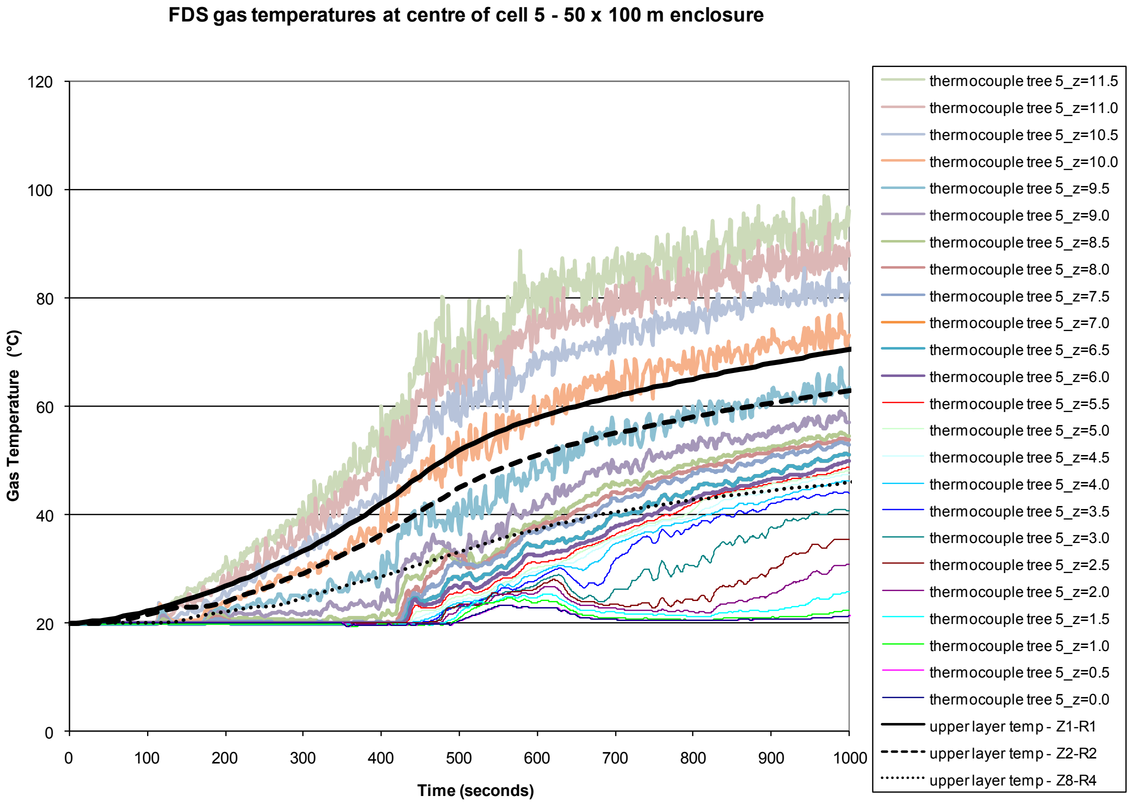

Figure 97. BRANZFIRE (with CFAST rules) upper layer temperatures versus FDS predictions over the height of the enclosure at the centre of compartment Z8-R5

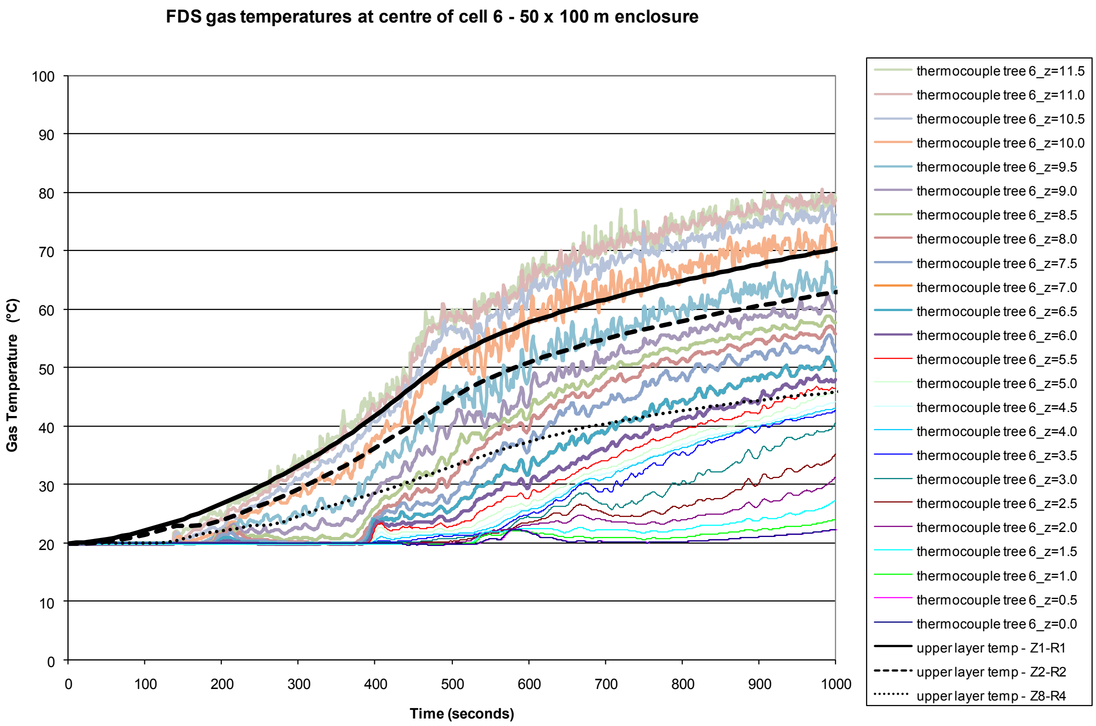

Figure 98. BRANZFIRE (with CFAST rules) upper layer temperatures versus FDS predictions over the height of the enclosure at the centre of compartment Z8-R6

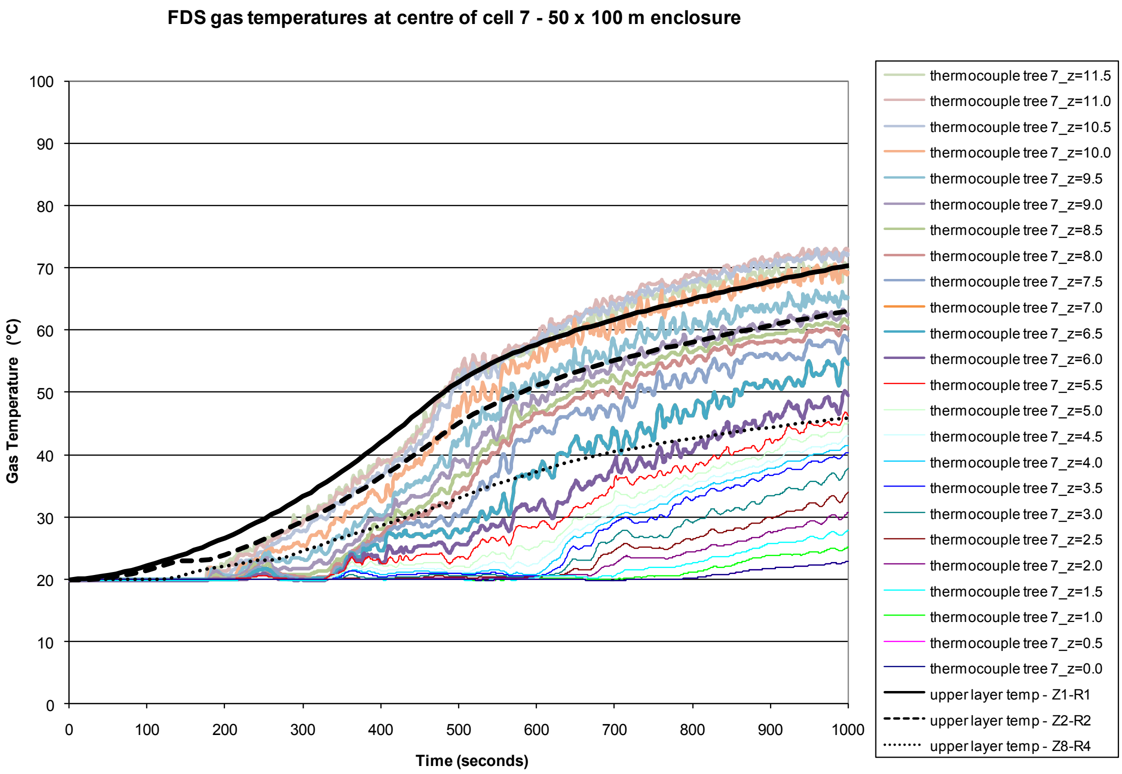

Figure 99. BRANZFIRE (with CFAST rules) upper layer temperatures versus FDS predictions over the height of the enclosure at the centre of compartment Z8-R7

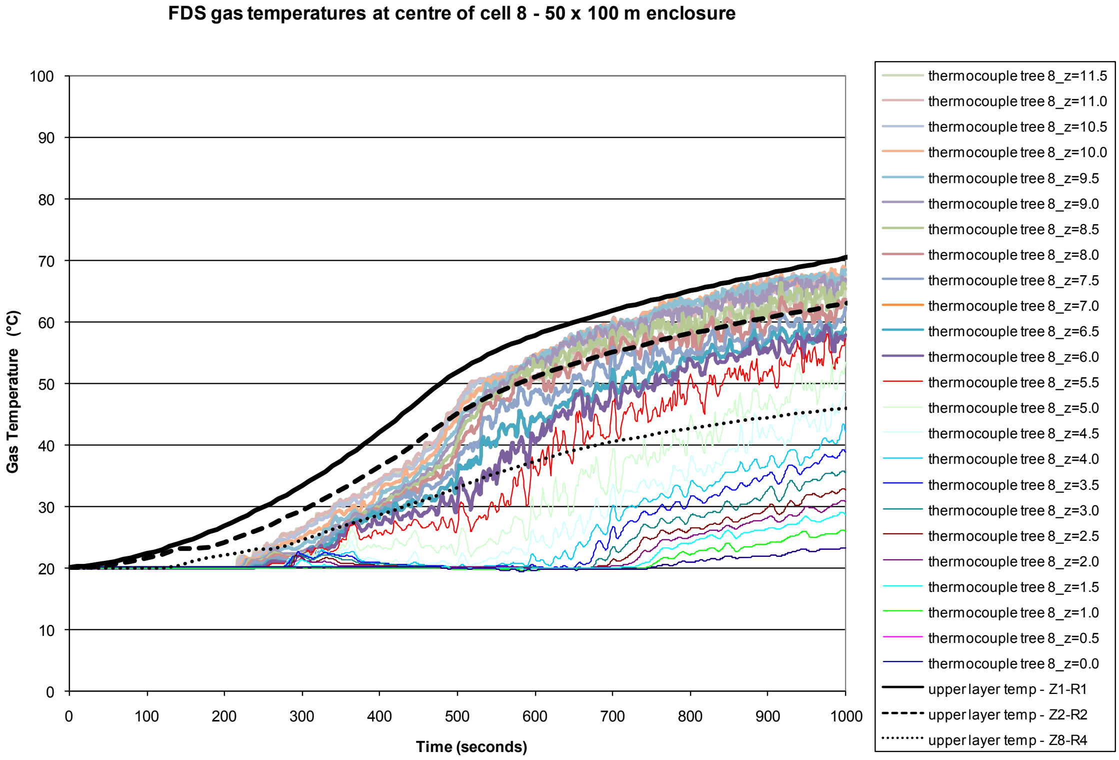

Figure 100. BRANZFIRE (with CFAST rules) upper layer temperatures versus FDS predictions over the height of the enclosure at the centre of compartment Z8-R8

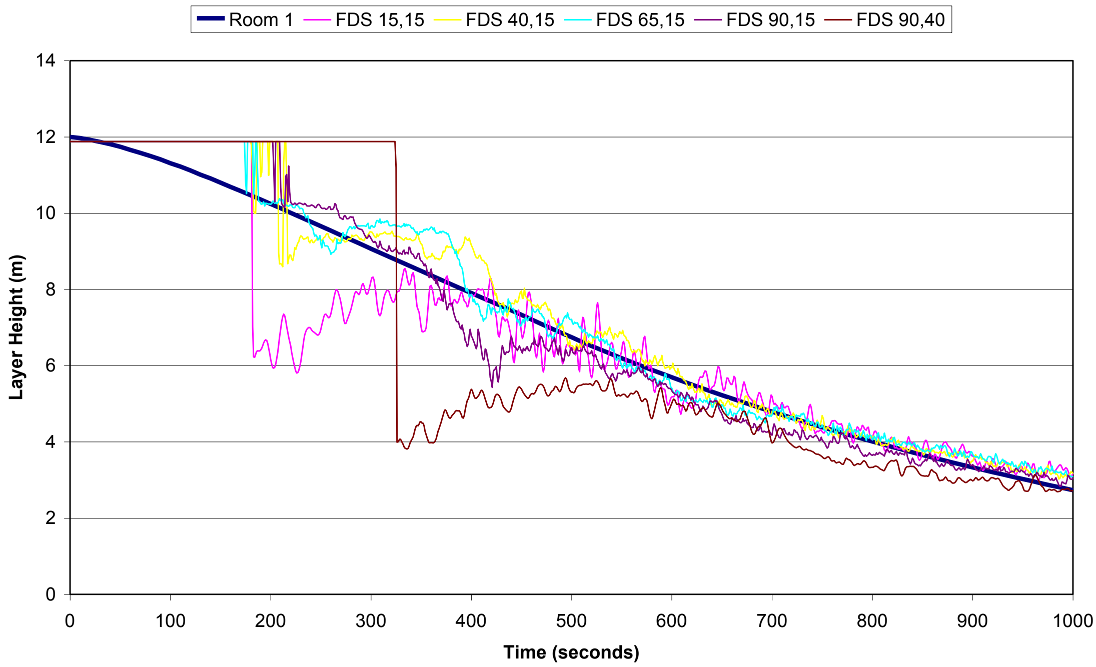

Figure 101. BRANZFIRE layer height using one room model versus FDS upper layer predictions at various locations in the compartment 100 x 50 x 12 m

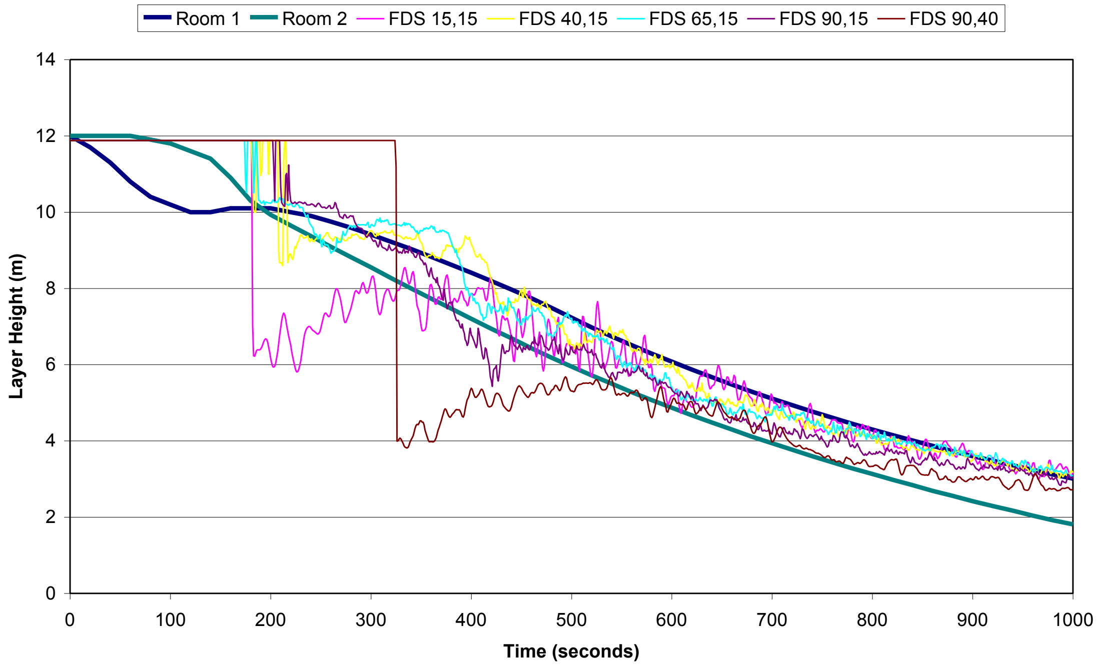

Figure 102. BRANZFIRE (with CFAST rules) layer height using two room model versus FDS upper layer predictions at various locations in the compartment 100 x 50 x 12 m

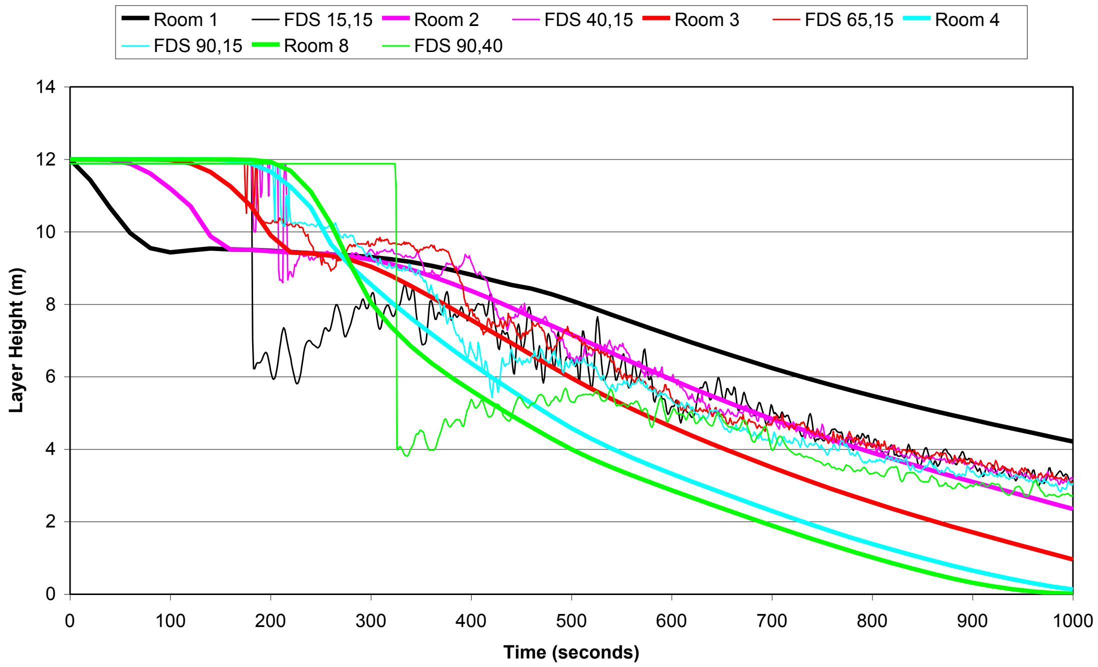

Figure 103. BRANZFIRE (with CFAST rules) layer height using eight room model versus FDS upper layer predictions at various locations in the compartment 100 x 50 x 12 m

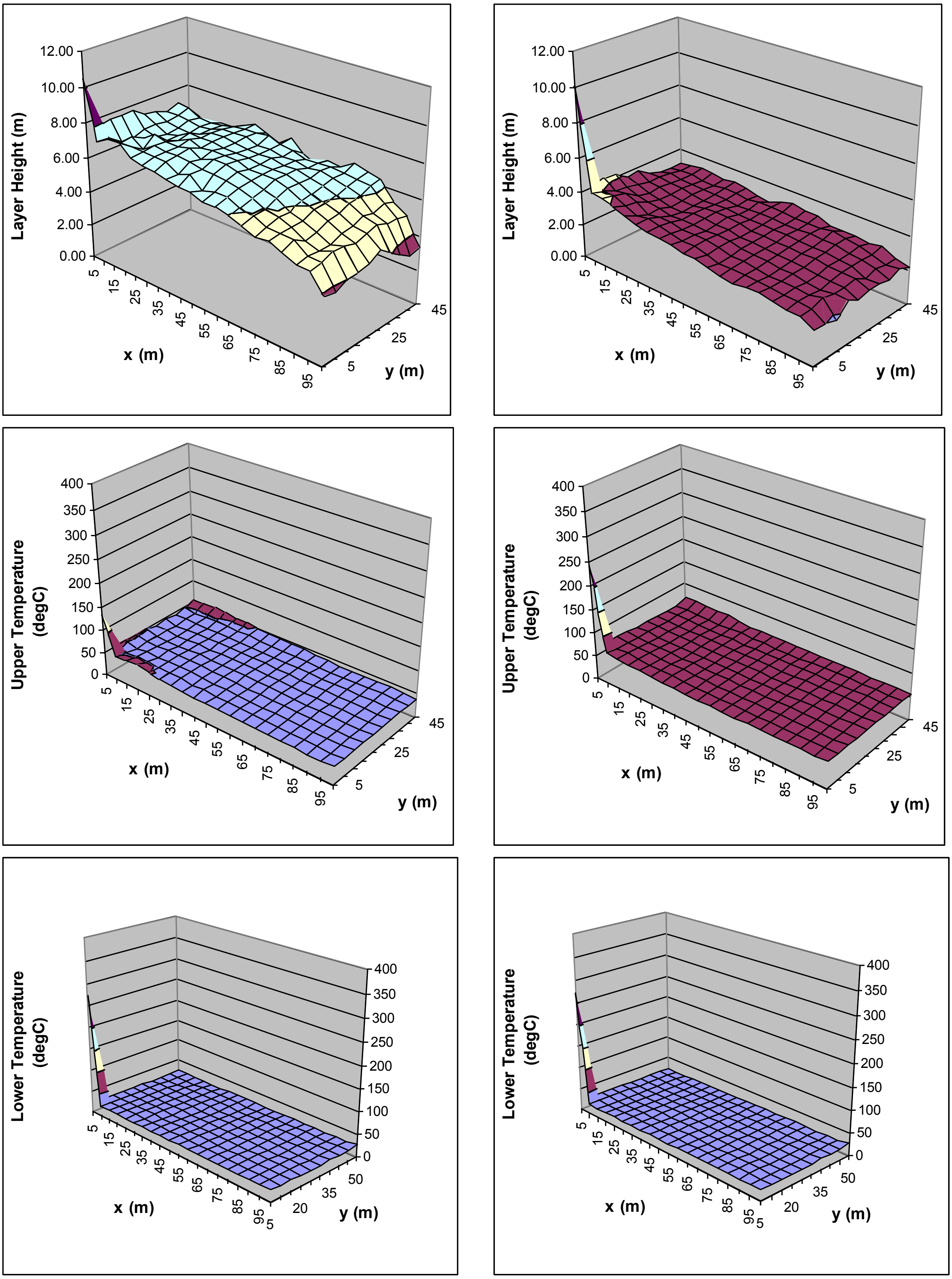

Figure 104. FDS derived predictions of layer height, upper layer temperature and lower layer temperature at 500 seconds (left) and 1000 seconds (right) for 50 x 100 x 12 m high enclosure.

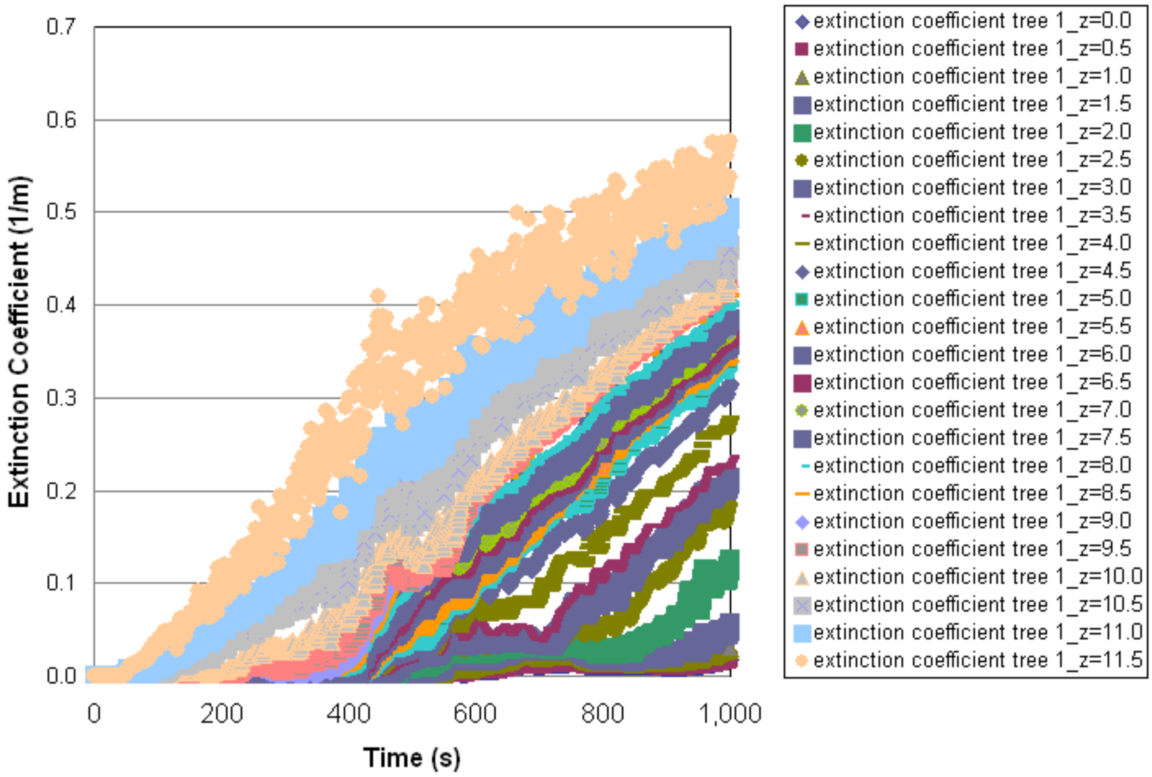

Figure 105. FDS predictions of extinction coefficient over the height of the enclosure at centre of compartment Z8-R1 (fire comp)

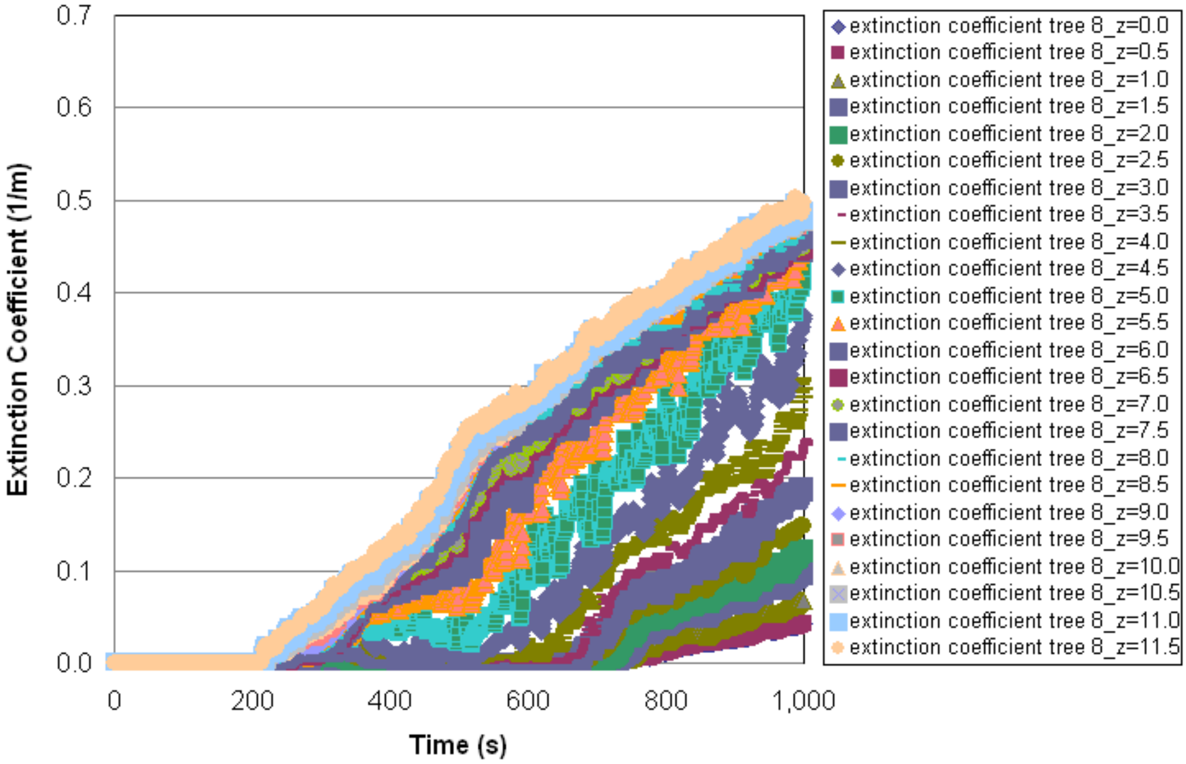

Figure 106. FDS predictions of extinction coefficient over the height of the enclosure at centre of compartment Z8-R8

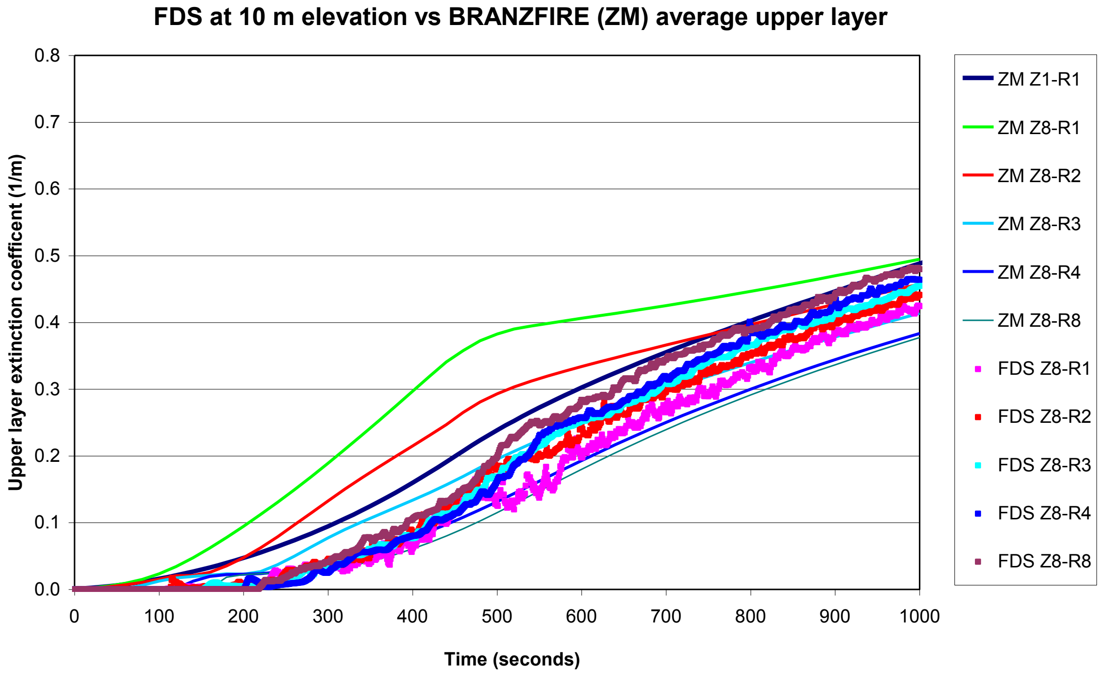

Figure 107. BRANZFIRE (with CFAST rules) upper layer smoke extinction coefficient versus FDS data for an elevation of 10 m above floor level

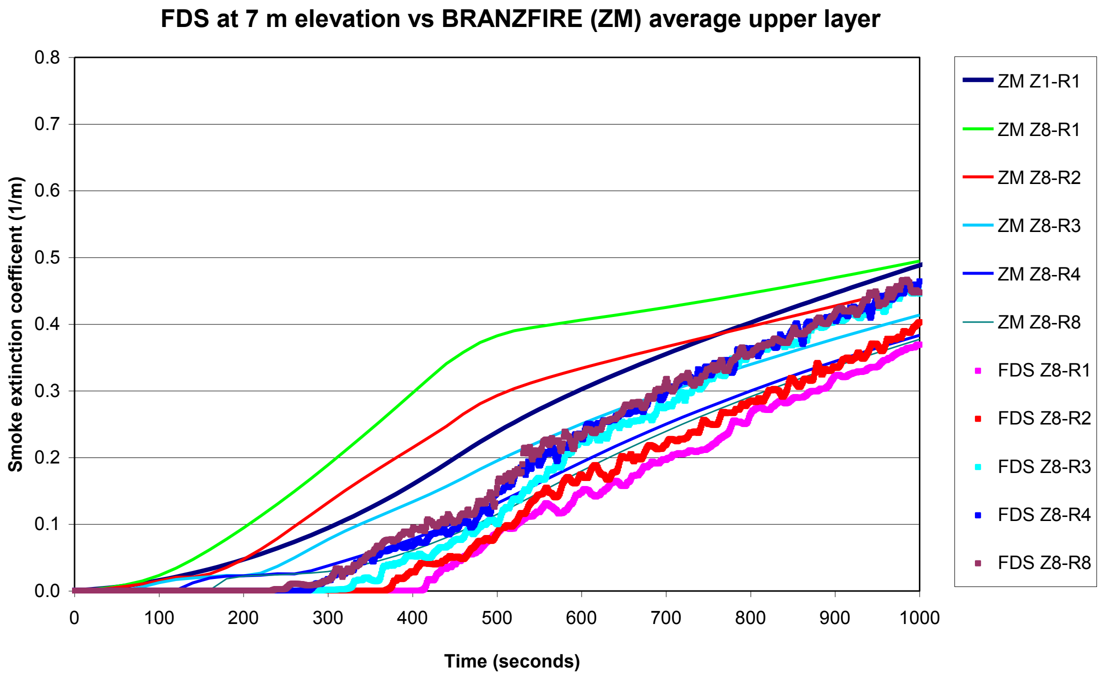

Figure 108. BRANZFIRE (with CFAST rules) upper layer smoke extinction coefficient versus FDS data for an elevation of 7 m above floor level

Figure 105 and Figure 106 show the smoke extinction coefficient over the height of the enclosure as predicted by FDS in the fire compartment (Z8-R1) and the furthest compartment (Z8-R8) respectively. The average extinction coefficient is directly proportional to the concentration of soot in the layer, and is inversely proportional to the visibility for a given target. It is observed that the extinction coefficient increases with height from floor to ceiling similar to the temperature variations over the height of the enclosure.

Figure 107 compares the average upper layer smoke extinction coefficient predicted by BRANZFIRE in five of the eight ‘virtual’ rooms (see Figure 55) compared to the FDS result at an elevation of 10 m above floor level. It also shows the predicted average extinction coefficient when the enclosure is modelled as a single compartment (ZM Z1-R1) with results that compare favourably with the FDS predictions. Figure 108 shows the same data for FDS but at an elevation 7 m above floor level. It is interesting that the FDS graphs show that the smoke extinction coefficient is increasing with distance from the fire compartment whereas BRANZFIRE shows it to be reducing with distance. The explanation for this difference is not obvious.

3.4 Summary of Simulations

A summary of the simulations undertaken, comparing CCFM and CFAST results, to FDS predictions is presented in Table 1.

Table 1. Summary of the simulations undertaken

Enclosure Size (m)	Number of Virtual Rooms				
	1	2	3	4	8
25x25x6	☑	-	-	-	-
50x25x6	☑	☑	-	-	-
75x25x6	☑	☑	☑	-	-
100x25x6	☑	☑	-	☑	-
100x50x6	☑	☑	-	-	☑
100x50x9	☑	☑	-	-	☑
100x50x12	☑	☑	-	-	☑

4. DISCUSSION

4.1 Horizontal flow in vertical vent deposition rules

The preceding section showed a number of comparisons of BRANZFIRE model upper layer temperature and layer height predictions using both the CCFM and CFAST rules for depositing vent mass flows in the layers in the adjacent rooms. The CCFM rules are more complicated and deposit the mass flows depending on the relative temperatures of the originating slab and destination layer. The CFAST rules are simpler and mean that a flow slab originating from the upper layer will be deposited into the upper layer in the destination room, while a flow slab originating in the lower layer will be deposited in the lower layer of the destination room.

It is observed that the CCFM rules tend to result in greater variations in the layer heights between rooms, whereas the CFAST rules result in more consistent trends for the layer height in each room. It is also noted that CCFM predicted a much higher layer height in the room of fire origin, which may not be conservative. For design purposes, the CFAST rules are both simpler to apply and likely to produce more conservative outcomes and for these reasons are recommended as the default algorithm. CFAST rules have been implemented in BRANZFIRE version 2008.2.

4.2 Use of virtual rooms

The preceding section compared zone model results obtained by simulating smoke filling in a single large enclosure with results obtained using a multi-cell or virtual room approach.

For the 25 x 25 m enclosure, the single room zone model appeared to give excellent results (see Figure 8) when compared to FDS. For the 50 x 25 m enclosure the single room model results were still relatively good, but for 75 x 25 m and larger enclosures, the single room model tended to slightly under-predict the average layer temperature closer to the fire, and the descent of the layer height becomes rather too slow. This trend becomes more pronounced as the enclosure size continues to increase as shown in Figure 56 and Figure 69.

For the larger enclosures, the zone model was applied in multi-cell configuration by dividing the enclosure into a smaller number of 25 x 25 m cells connected to each other with full width vents. Transom depths of 10% of the room height were assumed at the top of these ‘virtual’ vents.

The results indicated that, for the larger enclosures, the advantages of using a multi-cell configuration of more than two cells in the zone model was not clear as generally the agreement with the FDS results were not improved compared to a two-cell configuration. In fact, although more cells may in theory provide better spatial resolution around the enclosure it also means that uncertainties in the individual vent flow calculations are multiplied, with each successive vent further reducing the overall accuracy of the predictions. There is also a penalty in the computational time required with a larger number of cells.

The effect of the assumed transom depth for the virtual vents was also considered. Figure 109 shows the upper layer temperature predicted by BRANZFIRE using a two room configuration for the 100 x 25 x 6 m enclosure. The predicted upper layer temperature for the fire compartment is higher for the case where a transom is assumed, but slightly lower for the adjacent compartment. This is expected since the transom will have the effect of slowing down the enthalpy exchange between the two adjacent upper layers. Figure 110 shows the corresponding effect on the layer height. Figure 111 and Figure 112 show the comparison for the case using a four room model.

For the multi-cell simulations, using full width/height vents without a transom provided closer agreement with the average upper layer temperature FDS predictions.

FDS results for the same compartment for the period up to 400 seconds are shown in Figure 113 and Figure 114. An indication of the gravity current beneath the ceiling as it moves along the length of the enclosure can be seen. The time taken to reach impingement at the far end of the compartment is estimated to be around 230 seconds. For Figure 112, comparing the zone model layer height predictions for the case with/without a transom, the layer at the furthest compartment starts to descend at approximately 130 seconds (without transom) and 200 seconds (with transom). So, in this case inclusion of the transom is better for layer height predictions. The zone model predicts the time to impingement at the far end of the enclosure at an earlier time in comparison with FDS. This is consistent with the findings of Hu et al (2005).

4.3 Effect of ceiling height

The effect of the ceiling height was investigated for the 100 x 50 m enclosure in the range 6 to 12 m using a single room model. Comparing Figure 56, Figure 75 and Figure 90 for the 6, 9 and 12 m cases respectively shows closer agreement with the FDS prediction of the average layer temperature at the 15,15 location for the 9 and 12 m heights, than for the 6 m height. Comparing the corresponding graphs for the position of the layer interface for a single room model (Figure 69, Figure 86 and Figure 101) shows that agreement between the BRANZFIRE and FDS improves as the height increases. At the 6 m height, the BRANZFIRE layer descends slower than predicted by the FDS results, while the rate of descent of the layer for the 12 m high enclosure is a good match with the FDS predicted layer height.

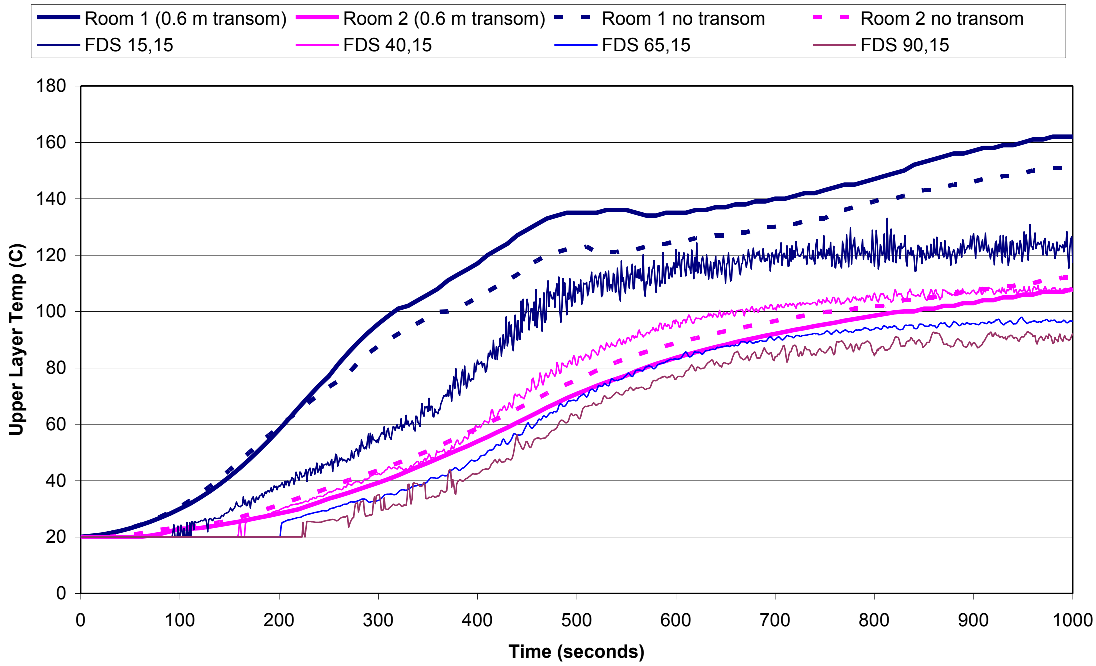

Figure 109. Upper layer temperature: BRANZFIRE (Z2-R1, Z2-R2) with/without transom, CFAST rules using two room model, versus FDS prediction for enclosure 100 x 25 x 6 m

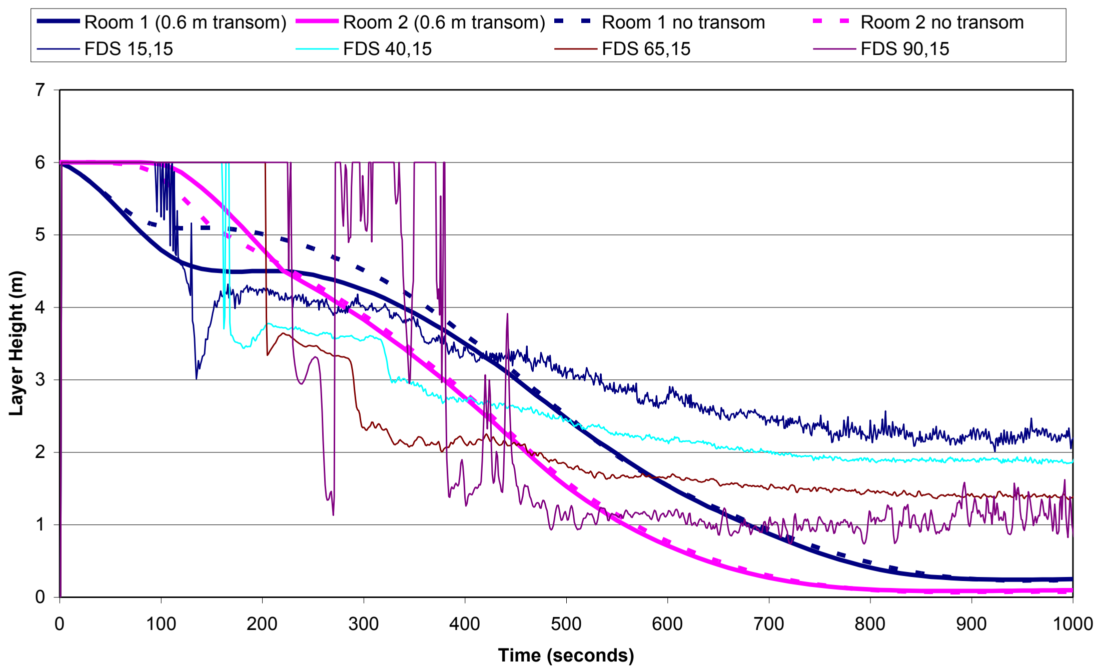

Figure 110. Layer height: BRANZFIRE (Z2-R1, Z2-R2) with/without transom, CFAST rules using two room model, versus FDS prediction for enclosure 100 x 25 x 6 m

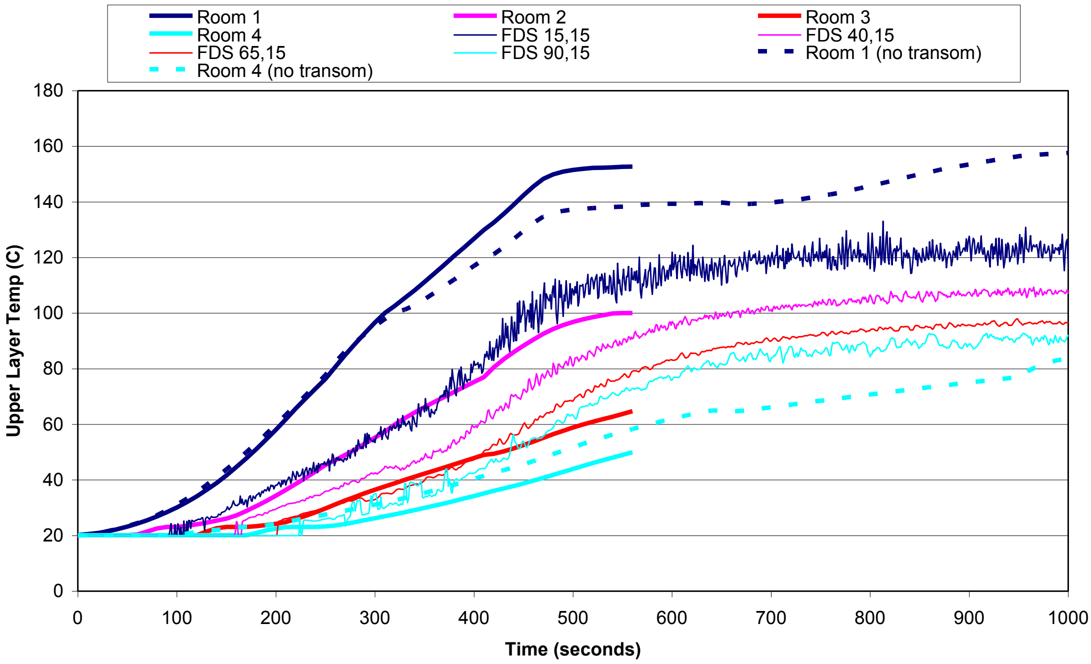

Figure 111. Upper layer temperature: BRANZFIRE‡ with/without transom, CFAST rules using four room model, versus FDS prediction for enclosure 100 x 25 x 6 m

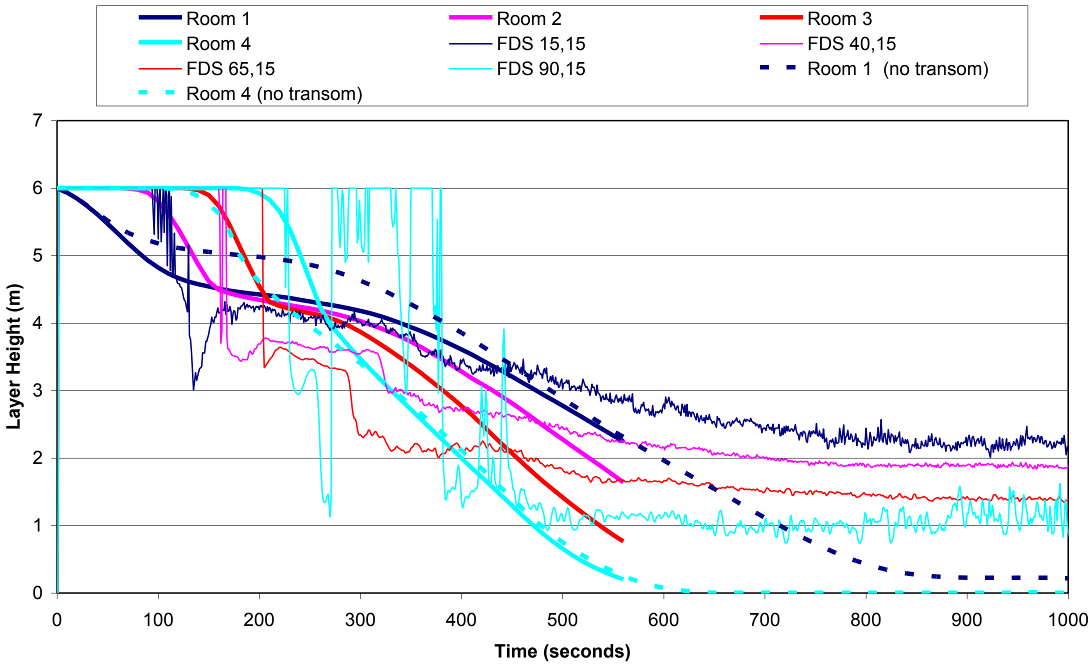

Figure 112. Layer height: BRANZFIRE with/without transom, CFAST rules using four room model, versus FDS prediction for enclosure 100 x 25 x 6 m

‡ Simulation terminated due to failure of solution to converge

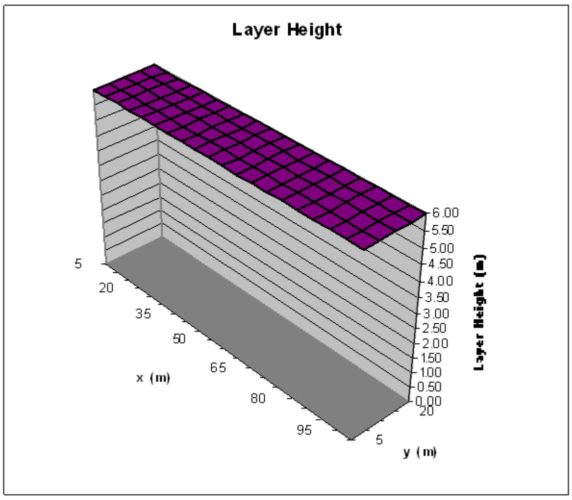

0 sec

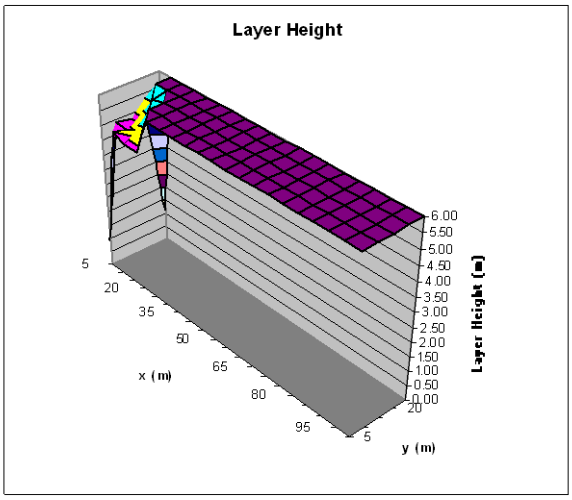

100 sec

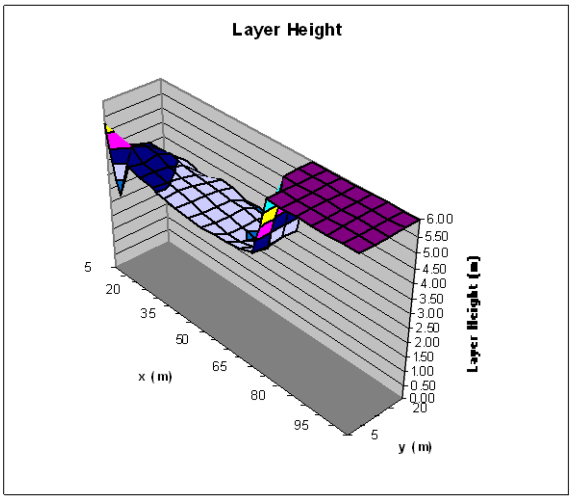

200 sec

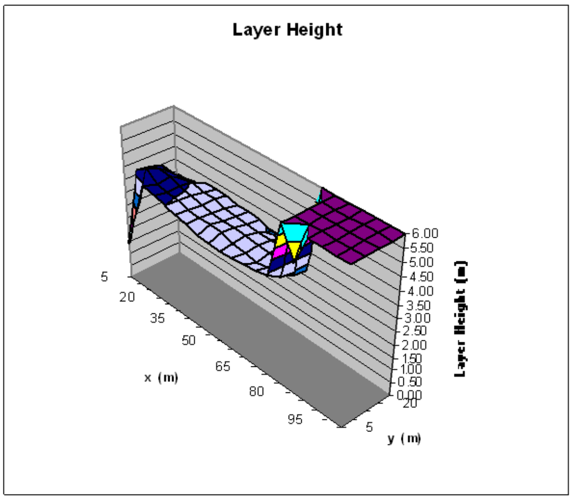

210 sec

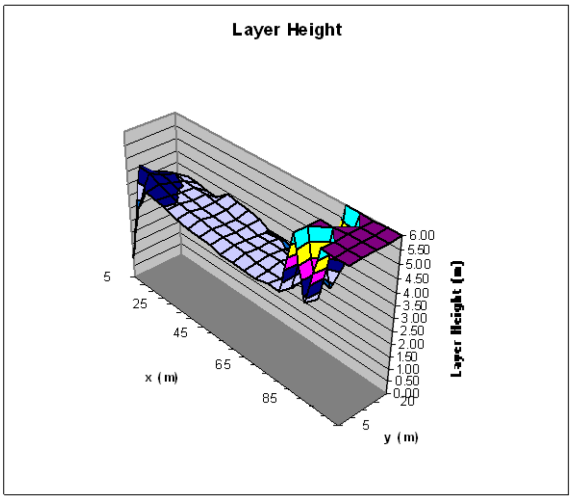

220 sec

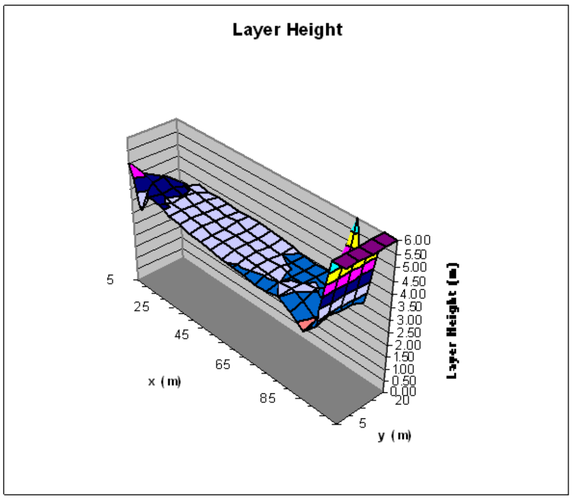

230 sec

Figure 113. FDS derived predictions of layer height at 0–230 seconds for 100 x 25 x 6 m high enclosure

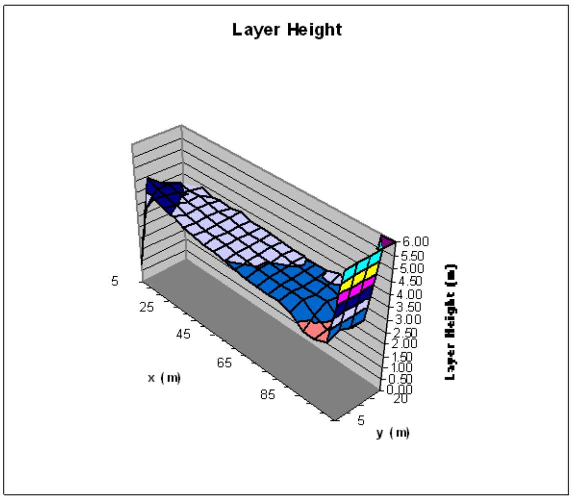

240 sec

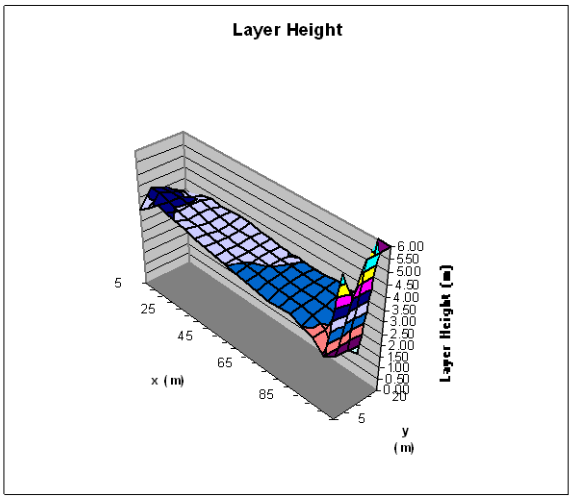

250 sec

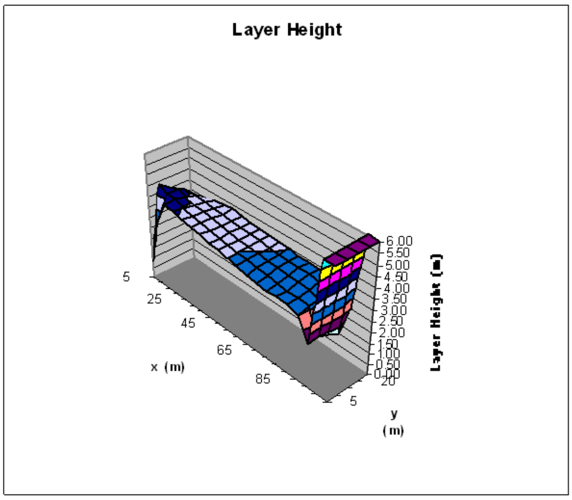

260 sec

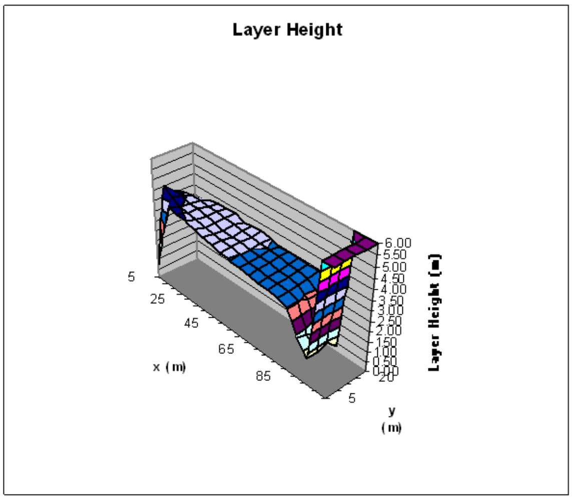

270 sec

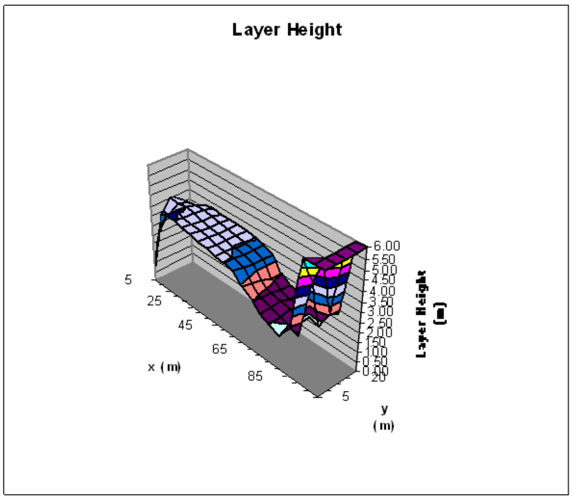

300 sec

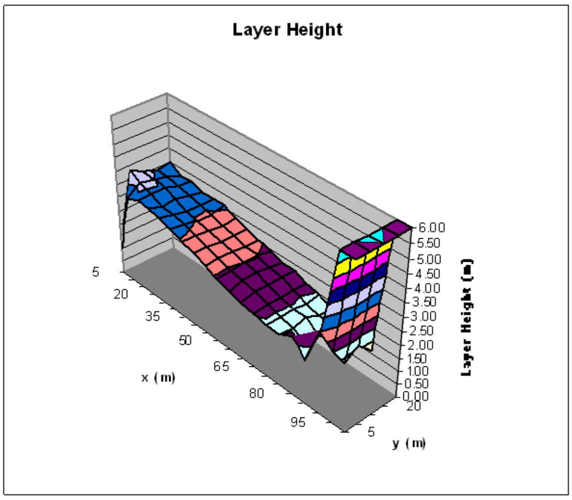

400 sec

Figure 114. FDS derived predictions of layer height at 240–400 seconds for 100 x 25 x 6 m high enclosure

5. CONCLUSIONS

5.1 General

Horizontal vent flows through vertical vents are more appropriately modelled using the simpler so-called CFAST rules instead of the CCFM rules currently implemented in the BRANZFIRE model (up to Version 2008.1). The simpler rules deposit flows that originate from the upper layer into the upper layer of the adjacent room, and deposit flows that originate from the lower layer into the lower layer of the adjacent room. This will provide a more conservative assessment for the position of the smoke layer interface in the fire compartment and within adjacent spaces. It could therefore be generally considered more appropriate for design purposes.

For the cases considered in the present study, using design fires which are assumed to be growing at rates similar to fast-t squared, BRANZFIRE provided good predictions of average hot layer temperature and layer height, when compared with FDS, for single room models with floor areas up to approximately 1200 m^2.

For larger floor areas up to about 5000 m^2, a virtual multi-room approach is better able to model the variation in temperature and layer height over the area of the enclosure and to that extent better reflects the trends exhibited by the FDS data, however with many virtual rooms there is a tendency to over-predict temperatures near the plume and under-predict temperatures in the far field. In some cases, a two-room model, appeared to give more agreeable results than the corresponding four-room model (cf. Figure 41 vs. Figure 43), thus the results are not conclusive in this regard.

When using a virtual room approach, where the assumed depth of the transom at the top of the vent was similar to the thickness of the ceiling jet, the time taken for the smoke layer to start descending in the furthest compartment was closer to the time of impingement predicted using FDS. If no transom is assumed in the zone model calculations, then shorter impingement times resulted but closer agreement with the FDS average layer temperature predictions was obtained.

The agreement between FDS and BRANZFIRE for the average smoke extinction coefficient was investigated for the 100 x 50 x 12 m enclosure, with BRANZFIRE generally providing a more conservative prediction when compared to FDS, given the same value for soot yield used in both models.

5.2 Recommendations

Vent flow deposition rules (horizontal vent flow through a vertical vent), that deposit flows that originate from the upper layer into the upper layer of the adjacent room and deposit flows that originate from the lower layer into the lower layer of the adjacent room, are preferred for design purposes. These deposition rules are included in BRANZFIRE Version 2008.2.

For design fires with growth rates similar to fast t-squared and reaching several MW, BRANZFIRE provides acceptable predictions for single room models for floor areas up to approximately 1200 m^2 and up to about 12 m in height.

For larger floor areas up to about 5000 m^2 it is suggested that a virtual room configuration be also carried out using BRANZFIRE 2008.2 or later. It is recommended that in this case the zone model analysis should include a sensitivity analysis including both single-room and virtual-room simulations (and with and without transoms). All cases should demonstrate that the design criteria are met.

If transoms at the top of the virtual vents are included they can be given a depth of approximately 10% of the floor to ceiling height. In cases where transoms are ignored, it is acceptable to make their depth small (e.g. 1%) rather than zero, where needed for numerical efficiency.

This study did not consider compartments larger than 5000 m^2 or higher than 12 m. For these cases, the model user should consider the use of a CFD model, or conduct further analysis of their own to justify the use of a zone model. The virtual room approach may still be useful for these cases.

Where the building geometry and arrangement of ventilation openings is complex and could significantly impact on the characteristics of the smoke flows, then users should consider whether simulation using only a zone model is sufficient. In these cases, CFD simulation may be more appropriate.

5.3 Limitations and future research

This report is based on a limited range of scenarios and geometries. In particular, a single fire specification has been considered. Conclusions have been drawn about zone model use based on comparison with results obtained from the state-of-the art CFD code FDS. Important areas of future research are:

- Comparison against measured variables from full-scale experiments.
- Consideration of a wider range of building layouts and geometries.
- Consideration of a wider range of fire scenarios including different growth rates and peak HRRs.

6. REFERENCES

Chow WK. 1996. 'Multi-cell Concept for Simulating Fires in Big Enclosures Using a Zone Model'. *Journal of Fire Sciences* 14: 186–197.

Chow WK, Yi L, Shi L, Li YZ and Huo R. 2005. 'Experimental Studies on Mechanical Smoke Exhaust System in an Atrium'. *Journal of Fire Sciences* 23: pages?.

Collier PCR and Soja E. 1999. *Modelling of Fires in Large Spaces*. Poster paper at Interflam 99, Interscience Communications Ltd, UK.

Duong DQ. 1990. 'The Accuracy of Computer Fire Models: Some Comparisons with Experimental Data from Australia'. *Fire Safety Journal* 16(6): 415–431.

Floyd JE. 2002. *Comparison of CFAST and FDS for Fire Simulation with the HDR T51 and T52 Tests*, NISTIR 6866. National Institute of Standards and Technology, Gaithersburg, MA.

Hinkley PL. 1988. 'Comparison of an Established Method of Calculation of Smoke Filling of Large Scale Spaces with Recent Experiments'. *Fire Science & Technology* 8 (1): 1–8.

Hu LH, Li YZ, Huo R and Wang HB. 2005. 'Smoke Filling Simulation in a Boarding-Arrival Passage of an Airport Terminal using Multi-cell Concept'. *Journal of Fire Sciences* 23: 31–53.

Jones WW, Forney GP, Peacock RD and Reneke PA. 2000. *A Technical Reference for CFAST: An Engineering Tool for Estimating Fire and Smoke Transport: Technical Note 1431.* National Institute of Standards and Technology, Building and Fire Research Laboratory, Gaithersburg, MD, USA.

Jones WW. 2001. *State of the Art in Zone Modeling of Fires*. 9th International Fire Protection Seminar, Engineering Methods for Fire Safety, Proceedings (May): 25–26, Munich, Germany.

McGrattan KB (Ed). 2005. *Fire Dynamics Simulator (Version 4) Technical Reference Guide: NIST Special Publication 1018*. National Institute of Standards and Technology, Building and Fire Research Laboratory, Gaithersburg, MD, USA.

McGrattan KB, Hostikka S. and Floyd J. 2007. *Fire Dynamics Simulator (Version 5) User's Guide, NIST Special Publication 1019-5*. National Institute of Standards and Technology, Gaithersburg, MA.

Merci and Vandevelde P. 2007 "Comparison of Calculations Methods for Smoke and heat Evacuation for Enclosure Fires in Large Compartments". *Thermal Science*. 11(2):181-196.

Peacock, Richard D, Forney, Glenn, Reneke, Paul A, Portier, Rebecca and Jones, Walter W. 1993. *CFAST: The Consolidated Model of Fire and Smoke Transport: NIST Technical Note 1299*. National Institute of Standards and Technology, Building and Fire Research Laboratory, Gaithersburg, MD, USA.

Rein G, Bar-Ilan A, Fernandez-Pello C and Alvares N. 2006. "A Comparison of Three Fire Models in the Simulation of Accidental Fires". *Journal of Fire Protection Engineering*. 16(3):193-209.

Rockett JA. 1993. 'Experience in the Use of Zone Type Building Fire Models'. *Fire Science and Technology* 13 (1 & 2): 61–70.

Rockett, John A. 1995. 'Zone Model Plume Algorithm Performance'. *Fire Science & Technology* 15 (1 & 2): 1–15.

Tanaka T and Yamada S. 2004. 'BRI2002: Two Layer Zone Smoke Transport Model'. *Fire Science & Technology* 23 (1): Special Issue.

US Nuclear Regulatory Commission. 2007. *Verification and Validation of Selected Fire Models for Nuclear Power Plant Applications, Volume 5: Consolidated Fire Growth and Smoke Transport Model (CFAST).* USNRC, Office of Nuclear Regulatory Research (RES), Rockville, MD, USA and Electric Power Research Institute (EPRI), Palo Alto, CA, NUREG-1824 and EPRI 1011999.

van de Leur PHE, Kleijn CR and Hoogendoorn CJ. 1989. 'Numerical Study of the Stratified Smoke Flow in a Corridor: Full-scale Calculations'. *Fire Safety Journal* 14: 287–302.

Wade CA. 2004. 'BRANZFIRE Technical Reference Guide'. BRANZ *Study Report 92 (revised)*. BRANZ Ltd, Judgeford, New Zealand.

Wade CA, Spearpoint M, Bittern A and Tsai K (Wei-Heng). 2007. 'Assessing the Sprinkler Activation Predictive Capability of the BRANZFIRE Fire Model'. *Fire & Technology* 43 (3): 175–193.

Walton WD. 2002. 'Zone Computer Fire Models for Enclosures'. In Chapter 7, Section 3, *SFPE Handbook of Fire Protection Engineering* (3rd Edition), DiNenno PJ, Drysdale D, Beyler CL, Walton WD (Eds), 3/189–193.

Yamana T and Tanaka T. 1985. 'Smoke Control in Large-scale Spaces: Part 2'. *Fire Science & Technology* 5(1): 41–54.

APPENDIX A

A.1 Sample input file – BRANZFIRE

For the compartment with dimensions: 100 m long x 25 m wide x 6 m high modelled as two rooms.

```
"Created by BRANZFIRE Version ","2008.1"
"1 cell x 25 x 25 m"
"room corner model, none=0, karlsson=1, quintiere=2",0
"Number rooms",2
"Room Number",1
"room width (m)",25
"room length (m)",25
"room description (m)",""
"Max room Height(m)",6
"Min room Height (m)",6
"floor elevation (m)",0
"wall lining","steel (mild)"
"wall substrate","none"
"ceiling lining","steel (mild)"
"ceiling substrate","none"
"floor substrate","none"
"wall lining thickness (mm)",3
"ceiling lining thickness (mm)",3
"floor thickness (mm)",100
"wall lining conductivity (W/mK)",45.8
"ceiling lining conductivity (W/mK)",45.8
"floor conductivity (W/mK)",1.2
"floor","concrete"
"wall lining specific heat (J/kgK)",460
"wall lining density (kg/m3)",7850
"wall substrate thickness (mm)",150
"ceiling substrate thickness (mm)",150
"floor substrate thickness (mm)",150
"wall substrate conductivity (W/mK)",1
"floor substrate conductivity (W/mK)",1
"wall substrate specific heat (J/kgK)",1000
"floor substrate specific heat (J/kgK)",1000
"wall substrate density (kg/m3)",2000
"floor substrate density (kg/m3)",2000
"floor specific heat (kJ/kgK)",880
"floor density (kg/m3)",2300
"ceiling lining specific heat (J/kgK)",460
"ceiling lining density (kg/m3)",7850
"ceiling substrate conductivity (W/mK)",1
"ceiling substrate specific heat (J/kgK)",1000
"ceiling substrate density (kg/m3)",2000
"have ceiling substrate? Yes=-1 No=0",0
"have wall substrate? Yes=-1 No=0",0
"have floor substrate? Yes=-1 No=0",0
"ceiling sloped, 0= flat, -1=sloping",0
"ceiling emissivity",.899999976158142
"upper wall emissivity",.899999976158142
"lower wall emissivity",.899999976158142
"floor emissivity",.5
"Room Number",2
"room width (m)",25
"room length (m)",75
"room description (m)",""
"Max room Height(m)",6
"Min room Height (m)",6
"floor elevation (m)",0
"wall lining","steel (mild)"
"wall substrate","concrete"
"ceiling lining","steel (mild)"
```

```
"ceiling substrate","concrete"
"floor substrate","concrete"
"wall lining thickness (mm)",3
"ceiling lining thickness (mm)",3
"floor thickness (mm)",100
"wall lining conductivity (W/mK)",45.8
"ceiling lining conductivity (W/mK)",45.8
"floor conductivity (W/mK)",1.2
"floor","concrete"
"wall lining specific heat (J/kgK)",460
"wall lining density (kg/m3)",7850
"wall substrate thickness (mm)",100
"ceiling substrate thickness (mm)",100
"floor substrate thickness (mm)",100
"wall substrate conductivity (W/mK)",1.2
"floor substrate conductivity (W/mK)",1.2
"wall substrate specific heat (J/kgK)",880
"floor substrate specific heat (J/kgK)",880
"wall substrate density (kg/m3)",2300
"floor substrate density (kg/m3)",2300
"floor specific heat (kJ/kgK)",880
"floor density (kg/m3)",2300
"ceiling lining specific heat (J/kgK)",460
"ceiling lining density (kg/m3)",7850
"ceiling substrate conductivity (W/mK)",1.2
"ceiling substrate specific heat (J/kgK)",880
"ceiling substrate density (kg/m3)",2300
"have ceiling substrate? Yes=-1 No=0",0
"have wall substrate? Yes=-1 No=0",0
"have floor substrate? Yes=-1 No=0",0
"ceiling sloped, 0= flat, -1=sloping",0
"ceiling emissivity",.899999976158142
"upper wall emissivity",.899999976158142
"lower wall emissivity",.899999976158142
"floor emissivity",.5
"interior temp (K)",293
"exterior temp (K)",293
"relative humidity",.65
"tenability monitoring height (m)",2
"activity level","Light"
"radiant loss fraction",.33
"mass loss per unit area (kg/s)",.011
"emission coefficient",.8
"simulation time (s)",1800
"display interval (s)",10
"plume, macaffrey=2, delichatsios=1",2
"suppress ceiling HRR",#FALSE#
"flame area constant (m2/kW)",.0065
"flame length power",1
"burner width (m)",.17
"wall heat flux (kW/m2)",45
"ceiling heat flux (kW/m2)",35
"number vents",1
"number vents",1
"number vents",3
"Room ",1," to ",2," Vent ",1
"vent height (m)",5.4
"vent width (m)",25
"vent sill height (m)",0
"vent open time (s)",0
"vent close time (s)",0
"glass conductivity(s)",.76
"glass emissivity(-)",1
"glass linear coefficient of expansion (/C)",.0000095
"glass thickness (mm)",4
"glass shading depth (mm)",15
"glass breaking stress (MPa)",47
```

"glass thermal diffusivity (m2/s)",3.6E-07
"glass Young's modulus (MPa)",72000
"Auto Break Glass",#FALSE#
"Glass fallout time (sec)",0
"Glass to flame distance (m)",0
"Glass heated hot layer only?",#FALSE#
"downstand depth",0
"balcony extend beyond compartment opening?",#TRUE#
"Use Spill Plume?",0
"Spill Plume Model?",1
"Spill Plume Single Sided?",#TRUE#
"wall length 1 (m)",25
"wall length 2 (m)",25
"Room ",1," to ",3," Vent ",1
"vent height (m)",2
"vent width (m)",1
"vent sill height (m)",0
"vent open time (s)",0
"vent close time (s)",0
"glass conductivity(s)",.76
"glass emissivity(-)",1
"glass linear coefficient of expansion (/C)",.0000095
"glass thickness (mm)",4
"glass shading depth (mm)",15
"glass breaking stress (MPa)",47
"glass thermal diffusivity (m2/s)",3.6E-07
"glass Young's modulus (MPa)",72000
"Auto Break Glass",#FALSE#
"Glass fallout time (sec)",0
"Glass to flame distance (m)",0
"Glass heated hot layer only?",#FALSE#
"downstand depth",0
"balcony extend beyond compartment opening?",#FALSE#
"Use Spill Plume?",0
"Spill Plume Model?",1
"Spill Plume Single Sided?",#TRUE#
"Room ",2," to ",3," Vent ",1
"vent height (m)",2
"vent width (m)",1
"vent sill height (m)",0
"vent open time (s)",0
"vent close time (s)",0
"glass conductivity(s)",.76
"glass emissivity(-)",1
"glass linear coefficient of expansion (/C)",.0000095
"glass thickness (mm)",4
"glass shading depth (mm)",15
"glass breaking stress (MPa)",47
"glass thermal diffusivity (m2/s)",3.6E-07
"glass Young's modulus (MPa)",72000
"Auto Break Glass",#FALSE#
"Glass fallout time (sec)",0
"Glass to flame distance (m)",0
"Glass heated hot layer only?",#FALSE#
"downstand depth",0
"balcony extend beyond compartment opening?",#FALSE#
"Use Spill Plume?",0
"Spill Plume Model?",1
"Spill Plume Single Sided?",#TRUE#
"Room ",2," to ",3," Vent ",2
"vent height (m)",2
"vent width (m)",1
"vent sill height (m)",0
"vent open time (s)",0
"vent close time (s)",0
"glass conductivity(s)",.76
"glass emissivity(-)",1

"glass linear coefficient of expansion (/C)",.0000095
"glass thickness (mm)",4
"glass shading depth (mm)",15
"glass breaking stress (MPa)",47
"glass thermal diffusivity (m2/s)",3.6E-07
"glass Young's modulus (MPa)",72000
"Auto Break Glass",#FALSE#
"Glass fallout time (sec)",0
"Glass to flame distance (m)",0
"Glass heated hot layer only?",#FALSE#
"downstand depth",0
"balcony extend beyond compartment opening?",#FALSE#
"Use Spill Plume?",0
"Spill Plume Model?",1
"Spill Plume Single Sided?",#TRUE#
"Room ",2," to ",3," Vent ",3
"vent height (m)",2
"vent width (m)",1
"vent sill height (m)",0
"vent open time (s)",0
"vent close time (s)",0
"glass conductivity(s)",.76
"glass emissivity(-)",1
"glass linear coefficient of expansion (/C)",.0000095
"glass thickness (mm)",4
"glass shading depth (mm)",15
"glass breaking stress (MPa)",47
"glass thermal diffusivity (m2/s)",3.6E-07
"glass Young's modulus (MPa)",72000
"Auto Break Glass",#FALSE#
"Glass fallout time (sec)",0
"Glass to flame distance (m)",0
"Glass heated hot layer only?",#FALSE#
"downstand depth",0
"balcony extend beyond compartment opening?",#FALSE#
"Use Spill Plume?",0
"Spill Plume Model?",1
"Spill Plume Single Sided?",#TRUE#
"number objects",1
"number data points",31
"energy yield (kJ/g)",41.2
"CO yield (g/g)",.006
"CO2 yield (g/g)",2.85
"soot yield (g/g)",.015
"water vapour yield (g/g)",.7248322
"Fire height (m)",0
"fire location, corner=2, wall=1, centre=0",0
"HRR data"
0,0
15,11.1
31,44.4
46,100
62,177.8
77,277.8
92,400
108,544.4
123,711.1
139,900
154,1111.1
169,1344.4
185,1600
200,1877.8
215,2177.8
231,2500
246,2844.4
262,3211.1
277,3600

292,4011.1
308,4444.4
323,4900
339,5377.8
354,5877.8
369,6400
385,6944.4
400,7511.1
416,8100
431,8711.1
446,9344.4
461.8,10000
"Detector Type",0
"RTI",95
"C-factor",.4
"radial distance (m)",4.3
"actuation temp (K)",341
"water discharge rate",0
"sprinkler setting",#FALSE#,#FALSE#,#FALSE#
"target radiation endpoint (kW/m2)",.3
"upper temp endpoint (K)",873
"visibility endpoint (m)",10
"FED endpoint",.3
"convective endpoint (K)",353
"null.txt"
"null.txt"
"null.txt"
"wall min temp for spread (k)",273
"wall flame spread parameter",0
"wall effective heat of combustion",0
"ceiling effective heat of combustion",0
"floor effective heat of combustion",0
"fan extract rate (m3/s)",0
"fan start time (sec)",0
"fan on?",#FALSE#
"Max Pressure (Pa)",50
"Extract?",#TRUE#
"Number Fans",1
"Wall Soot Yield",0
"Ceiling Soot Yield",0
"Floor Soot Yield",0
"Wall CO2 Yield",0
"Ceiling CO2 Yield",0
"Floor CO2 Yield",0
"Wall H2O Yield",0
"Ceiling H2O Yield",0
"Floor H2O Yield",0
"Floor min temp for spread (k)",0
"Floor flame spread parameter",0
"null.txt"
""
"null.txt"
"wall min temp for spread (k)",273
"wall flame spread parameter",0
"wall effective heat of combustion",0
"ceiling effective heat of combustion",0
"floor effective heat of combustion",0
"fan extract rate (m3/s)",0
"fan start time (sec)",0
"fan on?",#FALSE#
"Max Pressure (Pa)",0
"Extract?",#FALSE#
"Number Fans",0
"Wall Soot Yield",0
"Ceiling Soot Yield",0
"Floor Soot Yield",0
"Wall CO2 Yield",0

"Ceiling CO2 Yield",0
"Floor CO2 Yield",0
"Wall H2O Yield",0
"Ceiling H2O Yield",0
"Floor H2O Yield",0
"Floor min temp for spread (k)",0
"Floor flame spread parameter",0
"fire in room",1
"Ignite adjacent rooms?",#FALSE#
"FED Start time",0
"FED end time",10000
"Illuminated signage",#FALSE#
"number cVents",0
"number cVents",0
"number cVents",0
"number cVents",0
"number cVents",0
"number cVents",0
"Use fan curve?",#TRUE#
"Fan Elevation",3
"Use fan curve?",#FALSE#
"Fan Elevation",0
"Ceiling Nodes",15
"Wall Nodes",15
"Floor Nodes",10
"LE solver","LU decomposition"
"Enhanced Burning Rate",#FALSE#
"Job Number","FQ0685"
"Excel Interval (s)",10
"Two Zones? ",#TRUE#
"Two Zones? ",#TRUE#
"Time Step",1
"Error Control",.1
"Fire Objects Database","fire.mdb"
"Materials Database","thermal.mdb"
"Have Smoke Detector?",#FALSE#
"Alarm OD",.097
"Alarm delay",15
"Detector Sensitivity",6.6
"Radial Distance",0
"Depth",.025
"Use OD inside detector for response",#TRUE#
"Fan Auto Start?",#FALSE#
"Specify Alarm OD?",#FALSE#
"Have Smoke Detector?",#FALSE#
"Alarm OD",.14
"Alarm delay",15
"Detector Sensitivity",2.5
"Radial Distance",0
"Depth",.025
"Use OD inside detector for response",#TRUE#
"Fan Auto Start?",#FALSE#
"Specify Alarm OD?",#FALSE#
"Ceiling Jet Model",0
"Use One Cone Curve Only?",#FALSE#
"Ignition Correlation",1
"Sprinkler Distance",.02
"Vent Log File",#FALSE#
"Underventilated Soot Yield Factor",1
"Postflashover Model",#FALSE#
"FLED",400
"Fuel Density",500
"Fuel Thickness",.05
"Heat of Combustion",13
"Stick Spacing",.1
"Soot Alpha Coefficient",2.5
"Soot Epsilon Coefficient",1.2

```
"Carbon atoms in fuel",7
"Hydrogen atoms in fuel",16
"Oxygen atoms in fuel",0
"Nitrogen atoms in fuel",0
"fuel type","user defined"
"Disable wall flow",#TRUE#
"Calculate HCN yield",#FALSE#
"preflashover CO yield",.006
"postflashover CO yield",.2
"preflashover soot yield",.015
"postflashover soot yield",.2
"CO mode",#FALSE#
"soot mode",#FALSE#
```

A.2 Sample input file – FDS

For the compartment with dimensions: 25 m long x 25 m wide x 6 m high

```
&HEAD CHID='warehouse_25x25x6', TITLE='625m^2 square warehouse with 6m stud and 1x2m vent in a
wall' /

&MISC RESTART=.FALSE. /
&DUMP DT_DEVC=1.0 /

&REAC ID = 'HEPTANE', FYI = 'Heptane, C_7 H_16', C = 7., H = 16., CO_YIELD = 0.006, SOOT_YIELD
= 0.015 /
&MATL ID = 'STEEL', EMISSIVITY = 1.0, DENSITY = 7850., CONDUCTIVITY = 45.8, SPECIFIC_HEAT =
0.46 /
&SURF ID = 'SHEET METAL', COLOR = 'YELLOW', MATL_ID = 'STEEL' ,THICKNESS = 0.05,
TMP_INNER = 20. /

&MESH IJK=72,72,15,XB=0,36,0,36,0,7.5, /

&TIME TWFIN=1000/

/open computational boundaries
&VENT MB='YMIN', SURF_ID='OPEN' /
&VENT MB='YMAX', SURF_ID='OPEN' /,
&VENT MB='XMIN', SURF_ID='OPEN' /,
&VENT MB='XMAX', SURF_ID='OPEN' /,
&VENT MB='ZMAX', SURF_ID='OPEN' /

/walls of warehouse,
&OBST XB=5,30,4.9,5,0,6,SURF_ID='SHEET METAL'/
&OBST XB=5,30,30,30.1,0,6,SURF_ID='SHEET METAL'/
&OBST XB=4.9,5,5,30,0,6,SURF_ID='SHEET METAL'/
&OBST XB=30,30.1,5,30,0,6,SURF_ID='SHEET METAL'/

/roof of warehouse
&OBST XB=5,30,5,30,6,6.1,SURF_ID='SHEET METAL'/

/vent,
&HOLE XB=17,18,4.8,5.2,0,2, /

/fire,
&SURF ID='FIRE_01', HRRPUA=2500, TAU_Q=-461.0, COLOR='RED' / t^2 growth that remains a
constant value after abs(TAU_Q) seconds,
&VENT XB=9,11,9,11,0,0,SURF_ID='FIRE_01'/

/heat detectors
&PROP ID='Heat1', QUANTITY='LINK TEMPERATURE', RTI=30., ACTIVATION_TEMPERATURE=57. /
&DEVC ID='HD_10_10', PROP_ID='Heat1', XYZ= 10,10,5.9 /
&DEVC ID='HD_10_15', PROP_ID='Heat1', XYZ= 10,15,5.9 /
&DEVC ID='HD_10_20', PROP_ID='Heat1', XYZ= 10,20,5.9 /
&DEVC ID='HD_10_25', PROP_ID='Heat1', XYZ= 10,25,5.9 /
&DEVC ID='HD_15_10', PROP_ID='Heat1', XYZ= 15,10,5.9 /
&DEVC ID='HD_15_15', PROP_ID='Heat1', XYZ= 15,15,5.9 /
```

```
&DEVC ID='HD_15_20', PROP_ID='Heat1', XYZ= 15,20,5.9 /
&DEVC ID='HD_15_25', PROP_ID='Heat1', XYZ= 15,25,5.9 /
&DEVC ID='HD_20_10', PROP_ID='Heat1', XYZ= 20,10,5.9 /
&DEVC ID='HD_20_15', PROP_ID='Heat1', XYZ= 20,15,5.9 /
&DEVC ID='HD_20_20', PROP_ID='Heat1', XYZ= 20,20,5.9 /
&DEVC ID='HD_20_25', PROP_ID='Heat1', XYZ= 20,25,5.9 /
&DEVC ID='HD_25_10', PROP_ID='Heat1', XYZ= 25,10,5.9 /
&DEVC ID='HD_25_15', PROP_ID='Heat1', XYZ= 25,15,5.9 /
&DEVC ID='HD_25_20', PROP_ID='Heat1', XYZ= 25,20,5.9 /
&DEVC ID='HD_25_25', PROP_ID='Heat1', XYZ= 25,25,5.9 /

/smoke detectors
&PROP ID='Smoke1', QUANTITY='spot obscuration', LENGTH=1.8, ACTIVATION_OBSCURATION=3.28
/
&DEVC ID='SD_10_10', PROP_ID='Smoke1', XYZ= 10,10,5.9 /
&DEVC ID='SD_10_15', PROP_ID='Smoke1', XYZ= 10,15,5.9 /
&DEVC ID='SD_10_20', PROP_ID='Smoke1', XYZ= 10,20,5.9 /
&DEVC ID='SD_10_25', PROP_ID='Smoke1', XYZ= 10,25,5.9 /
&DEVC ID='SD_15_10', PROP_ID='Smoke1', XYZ= 15,10,5.9 /
&DEVC ID='SD_15_15', PROP_ID='Smoke1', XYZ= 15,15,5.9 /
&DEVC ID='SD_15_20', PROP_ID='Smoke1', XYZ= 15,20,5.9 /
&DEVC ID='SD_15_25', PROP_ID='Smoke1', XYZ= 15,25,5.9 /
&DEVC ID='SD_20_10', PROP_ID='Smoke1', XYZ= 20,10,5.9 /
&DEVC ID='SD_20_15', PROP_ID='Smoke1', XYZ= 20,15,5.9 /
&DEVC ID='SD_20_20', PROP_ID='Smoke1', XYZ= 20,20,5.9 /
&DEVC ID='SD_20_25', PROP_ID='Smoke1', XYZ= 20,25,5.9 /
&DEVC ID='SD_25_10', PROP_ID='Smoke1', XYZ= 25,10,5.9 /
&DEVC ID='SD_25_15', PROP_ID='Smoke1', XYZ= 25,15,5.9 /
&DEVC ID='SD_25_20', PROP_ID='Smoke1', XYZ= 25,20,5.9 /
&DEVC ID='SD_25_25', PROP_ID='Smoke1', XYZ= 25,25,5.9 /

/outputs
&SLCF PBX=5,QUANTITY='TEMPERATURE' /
&SLCF PBX=10,QUANTITY='TEMPERATURE' /
&SLCF PBX=15,QUANTITY='TEMPERATURE' /
&SLCF PBX=20,QUANTITY='TEMPERATURE' /
&SLCF PBX=25,QUANTITY='TEMPERATURE' /
&SLCF PBX=30,QUANTITY='TEMPERATURE' /
&SLCF PBY=5,QUANTITY='TEMPERATURE' /
&SLCF PBY=10,QUANTITY='TEMPERATURE' /
&SLCF PBY=15,QUANTITY='TEMPERATURE' /
&SLCF PBY=20,QUANTITY='TEMPERATURE' /
&SLCF PBY=25,QUANTITY='TEMPERATURE' /
&SLCF PBY=30,QUANTITY='TEMPERATURE' /
&SLCF PBZ=1, QUANTITY='TEMPERATURE' /
&SLCF PBZ=1.5, QUANTITY='TEMPERATURE' /
&SLCF PBZ=2, QUANTITY='TEMPERATURE' /
&SLCF PBZ=3, QUANTITY='TEMPERATURE' /
&SLCF PBZ=4, QUANTITY='TEMPERATURE' /
&SLCF PBZ=1, QUANTITY='RADIANT_INTENSITY' /
&SLCF PBZ=2, QUANTITY='RADIANT_INTENSITY' /
/thermocouple tree
&DEVC XYZ=17.5,17.5,0.0, QUANTITY='TEMPERATURE', ID='thermocouple tree 1_z=0.0' /
&DEVC XYZ=17.5,17.5,0.5, QUANTITY='TEMPERATURE', ID='thermocouple tree 1_z=0.5' /
&DEVC XYZ=17.5,17.5,1.0, QUANTITY='TEMPERATURE', ID='thermocouple tree 1_z=1.0' /
&DEVC XYZ=17.5,17.5,1.5, QUANTITY='TEMPERATURE', ID='thermocouple tree 1_z=1.5' /
&DEVC XYZ=17.5,17.5,2.0, QUANTITY='TEMPERATURE', ID='thermocouple tree 1_z=2.0' /
&DEVC XYZ=17.5,17.5,2.5, QUANTITY='TEMPERATURE', ID='thermocouple tree 1_z=2.5' /
&DEVC XYZ=17.5,17.5,3.0, QUANTITY='TEMPERATURE', ID='thermocouple tree 1_z=3.0' /
&DEVC XYZ=17.5,17.5,3.5, QUANTITY='TEMPERATURE', ID='thermocouple tree 1_z=3.5' /
&DEVC XYZ=17.5,17.5,4.0, QUANTITY='TEMPERATURE', ID='thermocouple tree 1_z=4.0' /
&DEVC XYZ=17.5,17.5,4.5, QUANTITY='TEMPERATURE', ID='thermocouple tree 1_z=4.5' /
&DEVC XYZ=17.5,17.5,5.0, QUANTITY='TEMPERATURE', ID='thermocouple tree 1_z=5.0' /
&DEVC XYZ=17.5,17.5,5.5, QUANTITY='TEMPERATURE', ID='thermocouple tree 1_z=5.5' /
&DEVC XYZ=17.5,17.5,6.0, QUANTITY='TEMPERATURE', ID='thermocouple tree 1_z=6.0' /

/layer heights
```

&DEVC XB=5,5,5,5,0,6,QUANTITY='LAYER HEIGHT', ID='layer height 5,5',ORIENTATION=0,1,0/
&DEVC XB=5,5,10,10,0,6,QUANTITY='LAYER HEIGHT', ID='layer height 5,10'/
&DEVC XB=5,5,15,15,0,6,QUANTITY='LAYER HEIGHT', ID='layer height 5,15'/
&DEVC XB=5,5,20,20,0,6,QUANTITY='LAYER HEIGHT', ID='layer height 5,20'/
&DEVC XB=5,5,25,25,0,6,QUANTITY='LAYER HEIGHT', ID='layer height 5,25'/
&DEVC XB=10,10,5,5,0,6,QUANTITY='LAYER HEIGHT', ID='layer height 10,5',ORIENTATION=0,1,0/
&DEVC XB=10,10,10,10,0,6,QUANTITY='LAYER HEIGHT', ID='layer height 10,10'/
&DEVC XB=10,10,15,15,0,6,QUANTITY='LAYER HEIGHT', ID='layer height 10,15'/
&DEVC XB=10,10,20,20,0,6,QUANTITY='LAYER HEIGHT', ID='layer height 10,20'/
&DEVC XB=10,10,25,25,0,6,QUANTITY='LAYER HEIGHT', ID='layer height 10,25'/
&DEVC XB=15,15,5,5,0,6,QUANTITY='LAYER HEIGHT', ID='layer height 15,5',ORIENTATION=0,1,0/
&DEVC XB=15,15,10,10,0,6,QUANTITY='LAYER HEIGHT', ID='layer height 15,10'/
&DEVC XB=15,15,15,15,0,6,QUANTITY='LAYER HEIGHT', ID='layer height 15,15'/
&DEVC XB=15,15,20,20,0,6,QUANTITY='LAYER HEIGHT', ID='layer height 15,20'/
&DEVC XB=15,15,25,25,0,6,QUANTITY='LAYER HEIGHT', ID='layer height 15,25'/
&DEVC XB=20,20,5,5,0,6,QUANTITY='LAYER HEIGHT', ID='layer height 20,5',ORIENTATION=0,1,0/
&DEVC XB=20,20,10,10,0,6,QUANTITY='LAYER HEIGHT', ID='layer height 20,10'/
&DEVC XB=20,20,15,15,0,6,QUANTITY='LAYER HEIGHT', ID='layer height 20,15'/
&DEVC XB=20,20,20,20,0,6,QUANTITY='LAYER HEIGHT', ID='layer height 20,20'/
&DEVC XB=20,20,25,25,0,6,QUANTITY='LAYER HEIGHT', ID='layer height 20,25'/
&DEVC XB=25,25,5,5,0,6,QUANTITY='LAYER HEIGHT', ID='layer height 25,5',ORIENTATION=0,1,0/
&DEVC XB=25,25,10,10,0,6,QUANTITY='LAYER HEIGHT', ID='layer height 25,10'/
&DEVC XB=25,25,15,15,0,6,QUANTITY='LAYER HEIGHT', ID='layer height 25,15'/
&DEVC XB=25,25,20,20,0,6,QUANTITY='LAYER HEIGHT', ID='layer height 25,20'/
&DEVC XB=25,25,25,25,0,6,QUANTITY='LAYER HEIGHT', ID='layer height 25,25'/
&DEVC XB=30,30,5,5,0,6,QUANTITY='LAYER HEIGHT', ID='layer height 30,5',ORIENTATION=0,1,0/
&DEVC XB=30,30,10,10,0,6,QUANTITY='LAYER HEIGHT', ID='layer height 30,10'/
&DEVC XB=30,30,15,15,0,6,QUANTITY='LAYER HEIGHT', ID='layer height 30,15'/
&DEVC XB=30,30,20,20,0,6,QUANTITY='LAYER HEIGHT', ID='layer height 30,20'/
&DEVC XB=30,30,25,25,0,6,QUANTITY='LAYER HEIGHT', ID='layer height 30,25'/
&DEVC XB=5,5,5,5,0,6,QUANTITY='UPPER TEMPERATURE', ID='layer height 5,5',ORIENTATION=0,1,0/
&DEVC XB=5,5,10,10,0,6,QUANTITY='UPPER TEMPERATURE', ID='layer height 5,10'/
&DEVC XB=5,5,15,15,0,6,QUANTITY='UPPER TEMPERATURE', ID='layer height 5,15'/
&DEVC XB=5,5,20,20,0,6,QUANTITY='UPPER TEMPERATURE', ID='layer height 5,20'/
&DEVC XB=5,5,25,25,0,6,QUANTITY='UPPER TEMPERATURE', ID='layer height 5,25'/
&DEVC XB=10,10,5,5,0,6,QUANTITY='UPPER TEMPERATURE', ID='layer height 10,5',ORIENTATION=0,1,0/
&DEVC XB=10,10,10,10,0,6,QUANTITY='UPPER TEMPERATURE', ID='layer height 10,10'/
&DEVC XB=10,10,15,15,0,6,QUANTITY='UPPER TEMPERATURE', ID='layer height 10,15'/
&DEVC XB=10,10,20,20,0,6,QUANTITY='UPPER TEMPERATURE', ID='layer height 10,20'/
&DEVC XB=10,10,25,25,0,6,QUANTITY='UPPER TEMPERATURE', ID='layer height 10,25'/
&DEVC XB=15,15,5,5,0,6,QUANTITY='UPPER TEMPERATURE', ID='layer height 15,5',ORIENTATION=0,1,0/
&DEVC XB=15,15,10,10,0,6,QUANTITY='UPPER TEMPERATURE', ID='layer height 15,10'/
&DEVC XB=15,15,15,15,0,6,QUANTITY='UPPER TEMPERATURE', ID='layer height 15,15'/
&DEVC XB=15,15,20,20,0,6,QUANTITY='UPPER TEMPERATURE', ID='layer height 15,20'/
&DEVC XB=15,15,25,25,0,6,QUANTITY='UPPER TEMPERATURE', ID='layer height 15,25'/
&DEVC XB=20,20,5,5,0,6,QUANTITY='UPPER TEMPERATURE', ID='layer height 20,5',ORIENTATION=0,1,0/
&DEVC XB=20,20,10,10,0,6,QUANTITY='UPPER TEMPERATURE', ID='layer height 20,10'/
&DEVC XB=20,20,15,15,0,6,QUANTITY='UPPER TEMPERATURE', ID='layer height 20,15'/
&DEVC XB=20,20,20,20,0,6,QUANTITY='UPPER TEMPERATURE', ID='layer height 20,20'/
&DEVC XB=20,20,25,25,0,6,QUANTITY='UPPER TEMPERATURE', ID='layer height 20,25'/
&DEVC XB=25,25,5,5,0,6,QUANTITY='UPPER TEMPERATURE', ID='layer height 25,5',ORIENTATION=0,1,0/
&DEVC XB=25,25,10,10,0,6,QUANTITY='UPPER TEMPERATURE', ID='layer height 25,10'/
&DEVC XB=25,25,15,15,0,6,QUANTITY='UPPER TEMPERATURE', ID='layer height 25,15'/
&DEVC XB=25,25,20,20,0,6,QUANTITY='UPPER TEMPERATURE', ID='layer height 25,20'/
&DEVC XB=25,25,25,25,0,6,QUANTITY='UPPER TEMPERATURE', ID='layer height 25,25'/
&DEVC XB=30,30,5,5,0,6,QUANTITY='UPPER TEMPERATURE', ID='layer height 30,5',ORIENTATION=0,1,0/
&DEVC XB=30,30,10,10,0,6,QUANTITY='UPPER TEMPERATURE', ID='layer height 30,10'/
&DEVC XB=30,30,15,15,0,6,QUANTITY='UPPER TEMPERATURE', ID='layer height 30,15'/
&DEVC XB=30,30,20,20,0,6,QUANTITY='UPPER TEMPERATURE', ID='layer height 30,20'/
&DEVC XB=30,30,25,25,0,6,QUANTITY='UPPER TEMPERATURE', ID='layer height 30,25'/

```
&DEVC XB=5,5,5,5,0,6,QUANTITY='LOWER TEMPERATURE', ID='layer height
5,5',ORIENTATION=0,1,0/
&DEVC XB=5,5,10,10,0,6,QUANTITY='LOWER TEMPERATURE', ID='layer height 5,10'/
&DEVC XB=5,5,15,15,0,6,QUANTITY='LOWER TEMPERATURE', ID='layer height 5,15'/
&DEVC XB=5,5,20,20,0,6,QUANTITY='LOWER TEMPERATURE', ID='layer height 5,20'/
&DEVC XB=5,5,25,25,0,6,QUANTITY='LOWER TEMPERATURE', ID='layer height 5,25'/
&DEVC XB=10,10,5,5,0,6,QUANTITY='LOWER TEMPERATURE', ID='layer height
10,5',ORIENTATION=0,1,0/
&DEVC XB=10,10,10,10,0,6,QUANTITY='LOWER TEMPERATURE', ID='layer height 10,10'/
&DEVC XB=10,10,15,15,0,6,QUANTITY='LOWER TEMPERATURE', ID='layer height 10,15'/
&DEVC XB=10,10,20,20,0,6,QUANTITY='LOWER TEMPERATURE', ID='layer height 10,20'/
&DEVC XB=10,10,25,25,0,6,QUANTITY='LOWER TEMPERATURE', ID='layer height 10,25'/
&DEVC XB=15,15,5,5,0,6,QUANTITY='LOWER TEMPERATURE', ID='layer height
15,5',ORIENTATION=0,1,0/
&DEVC XB=15,15,10,10,0,6,QUANTITY='LOWER TEMPERATURE', ID='layer height 15,10'/
&DEVC XB=15,15,15,15,0,6,QUANTITY='LOWER TEMPERATURE', ID='layer height 15,15'/
&DEVC XB=15,15,20,20,0,6,QUANTITY='LOWER TEMPERATURE', ID='layer height 15,20'/
&DEVC XB=15,15,25,25,0,6,QUANTITY='LOWER TEMPERATURE', ID='layer height 15,25'/
&DEVC XB=20,20,5,5,0,6,QUANTITY='LOWER TEMPERATURE', ID='layer height
20,5',ORIENTATION=0,1,0/
&DEVC XB=20,20,10,10,0,6,QUANTITY='LOWER TEMPERATURE', ID='layer height 20,10'/
&DEVC XB=20,20,15,15,0,6,QUANTITY='LOWER TEMPERATURE', ID='layer height 20,15'/
&DEVC XB=20,20,20,20,0,6,QUANTITY='LOWER TEMPERATURE', ID='layer height 20,20'/
&DEVC XB=20,20,25,25,0,6,QUANTITY='LOWER TEMPERATURE', ID='layer height 20,25'/
&DEVC XB=25,25,5,5,0,6,QUANTITY='LOWER TEMPERATURE', ID='layer height
25,5',ORIENTATION=0,1,0/
&DEVC XB=25,25,10,10,0,6,QUANTITY='LOWER TEMPERATURE', ID='layer height 25,10'/
&DEVC XB=25,25,15,15,0,6,QUANTITY='LOWER TEMPERATURE', ID='layer height 25,15'/
&DEVC XB=25,25,20,20,0,6,QUANTITY='LOWER TEMPERATURE', ID='layer height 25,20'/
&DEVC XB=25,25,25,25,0,6,QUANTITY='LOWER TEMPERATURE', ID='layer height 25,25'/
&DEVC XB=30,30,5,5,0,6,QUANTITY='LOWER TEMPERATURE', ID='layer height
30,5',ORIENTATION=0,1,0/
&DEVC XB=30,30,10,10,0,6,QUANTITY='LOWER TEMPERATURE', ID='layer height 30,10'/
&DEVC XB=30,30,15,15,0,6,QUANTITY='LOWER TEMPERATURE', ID='layer height 30,15'/
&DEVC XB=30,30,20,20,0,6,QUANTITY='LOWER TEMPERATURE', ID='layer height 30,20'/
&DEVC XB=30,30,25,25,0,6,QUANTITY='LOWER TEMPERATURE', ID='layer height 30,25'/

&TAIL /
```

APPENDIX B

B.1 FDS grid sizes

A summary of the comparison of the results for grid sizes 0.25 m and 0.5 m for the 25x25x6 m scenario is presented here.

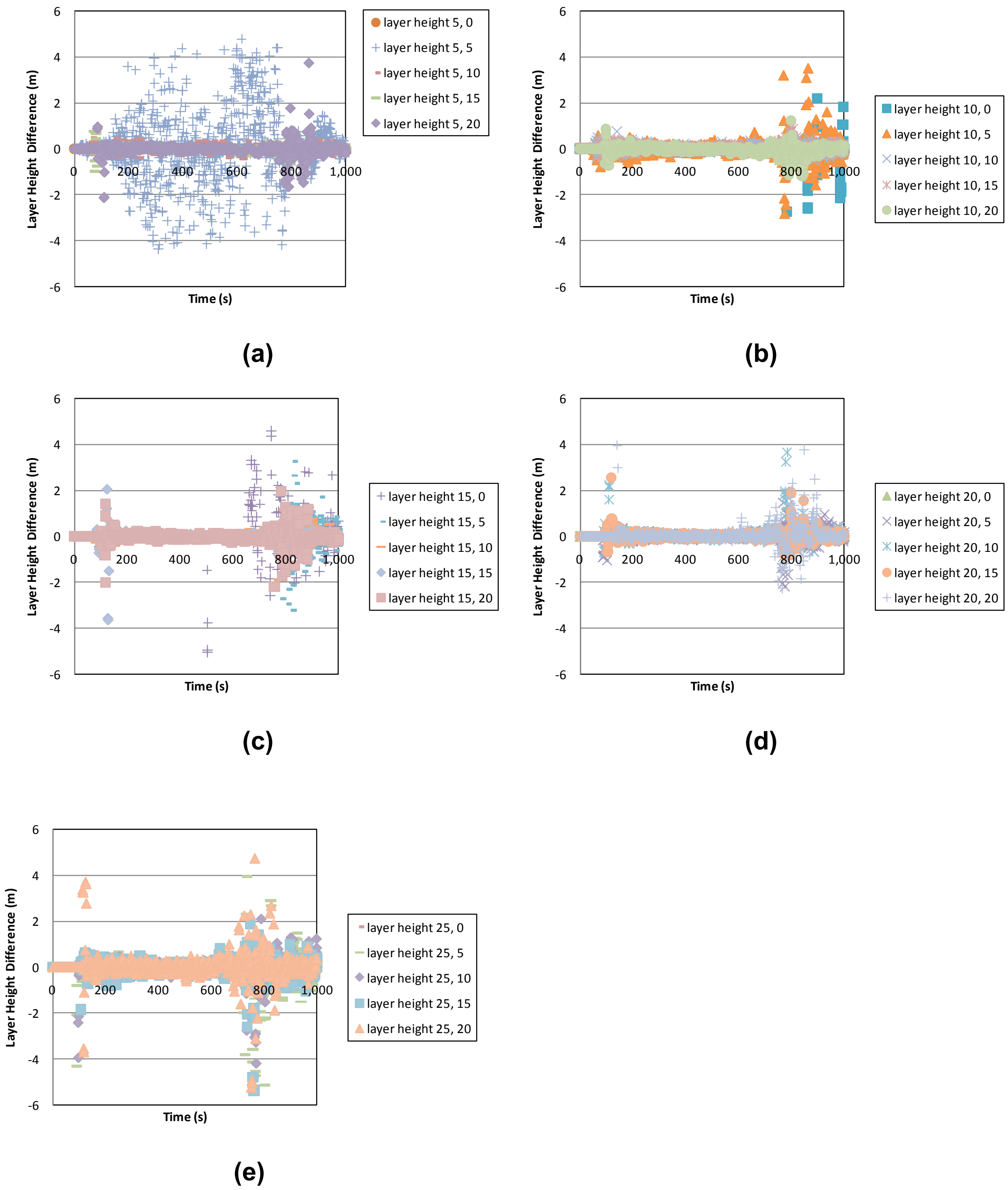

Figure 115: Differences between the layer height results for the 0.25 m uniformly spaced grid and the 0.5 m uniformly spaced grid for the 25 x 25 x 6 m building.

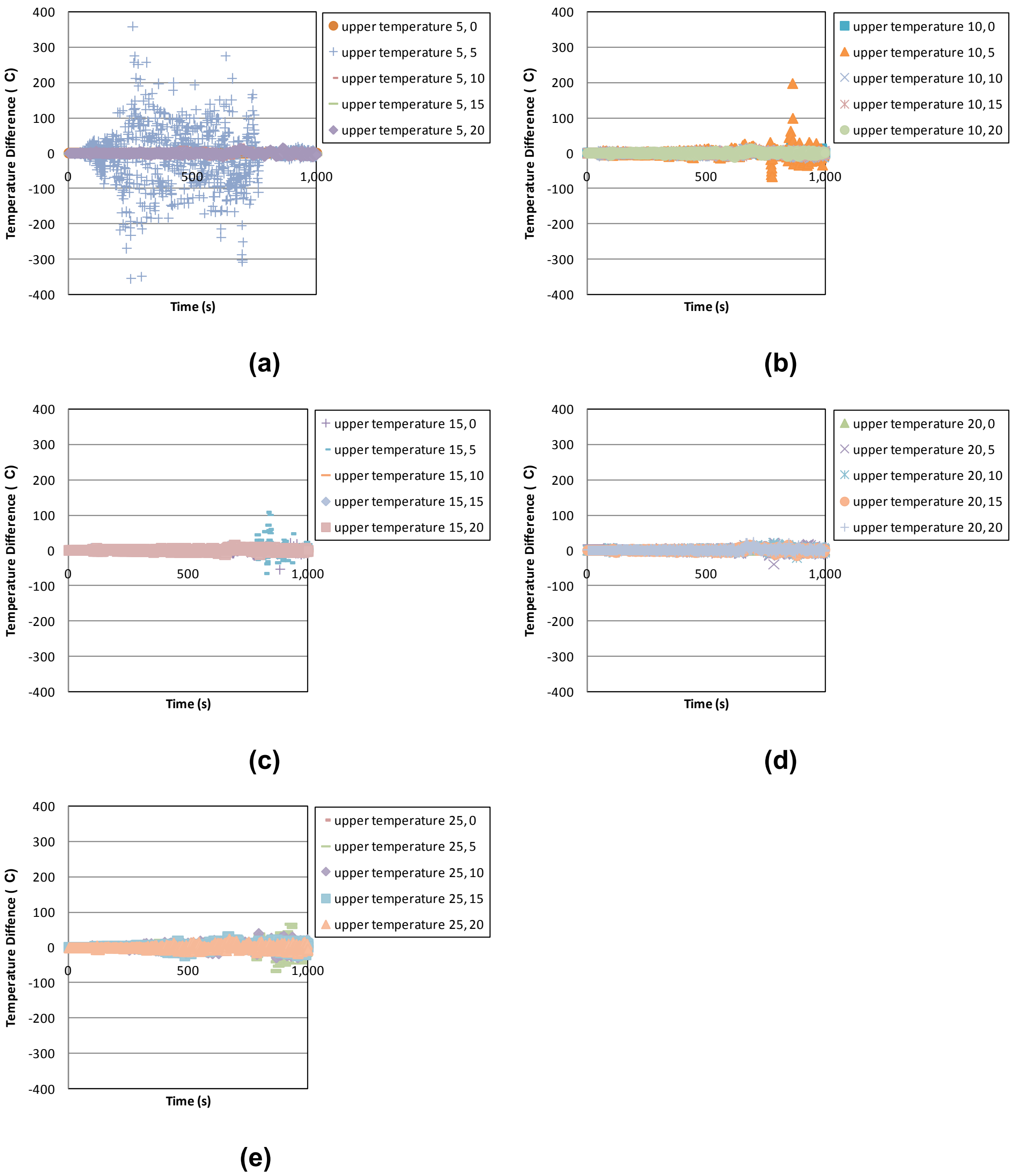

Figure 116: Differences between the upper layer temperature results for the 0.25 m uniformly spaced grid and the 0.5 m uniformly spaced grid for the 25 x 25 x 6 m building.

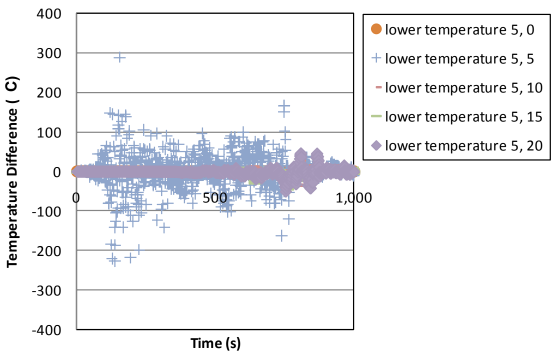

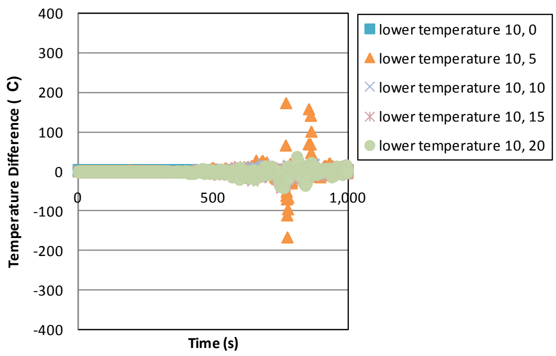

(a) **(b)**

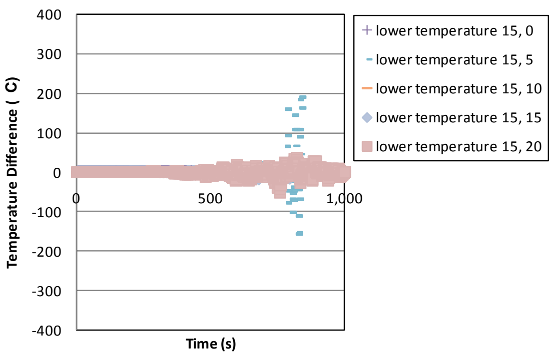

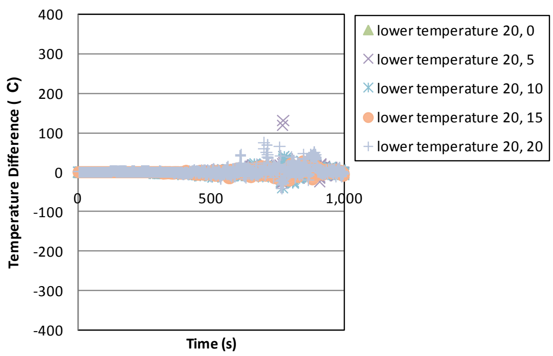

(c) **(d)**

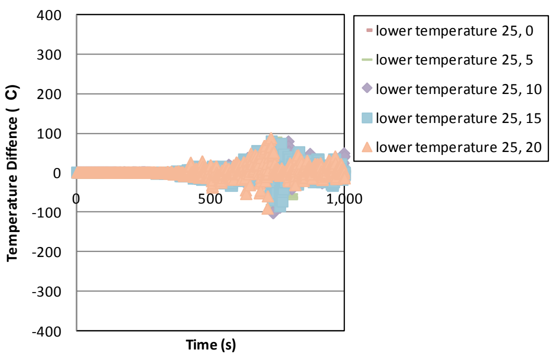

(e)

Figure 117: Differences between the lower layer temperature results for the 0.25 m uniformly spaced grid and the 0.5 m uniformly spaced grid for the 25 x 25 x 6 m building.

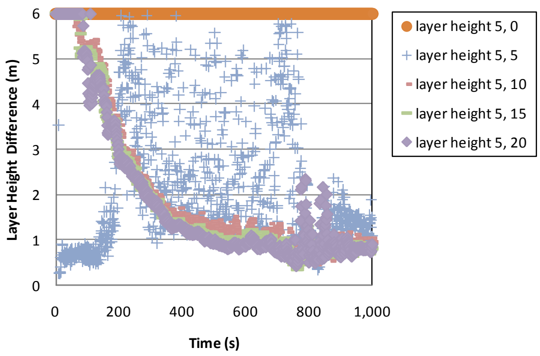

(a)

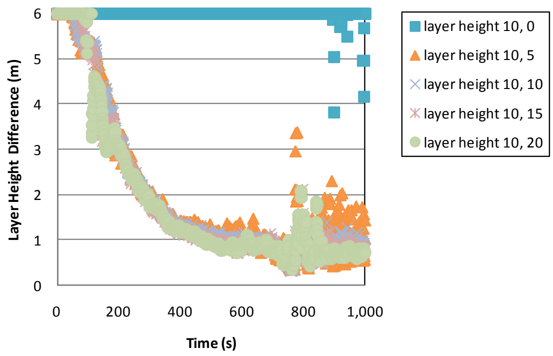

(b)

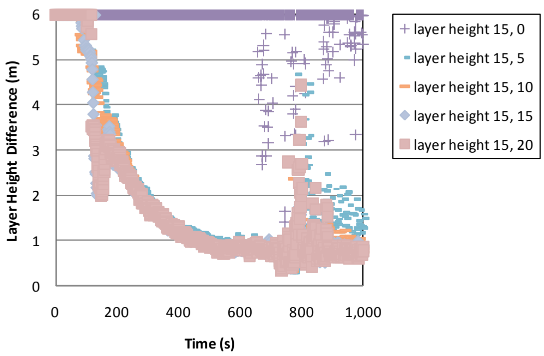

(c)

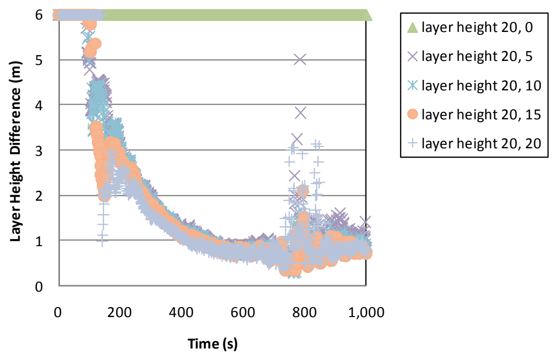

(d)

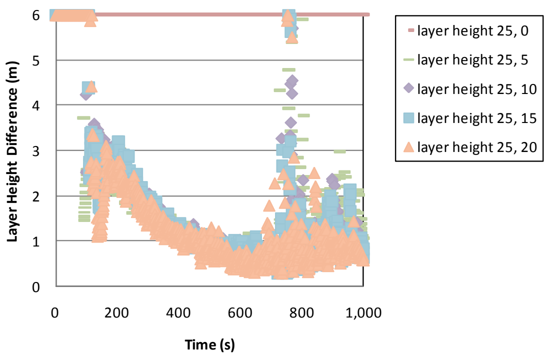

(e)

Figure 118: Layer height for 0.25 m uniformly spaced grid for the 25 x 25 x 6 m building.

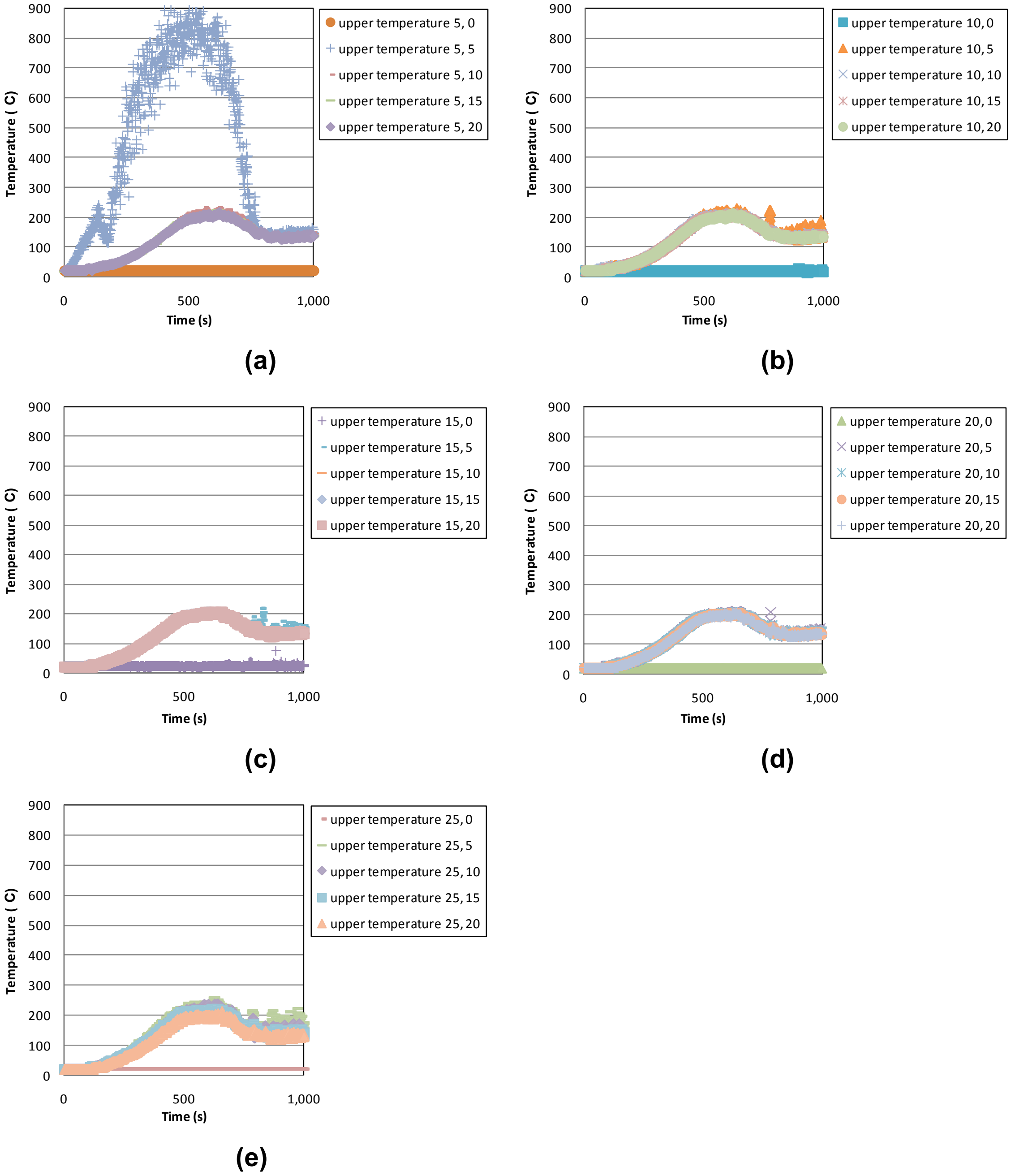

Figure 119: Upper layer temperatures for the 0.25 m uniformly spaced grid for the 25 x 25 x 6 m building.

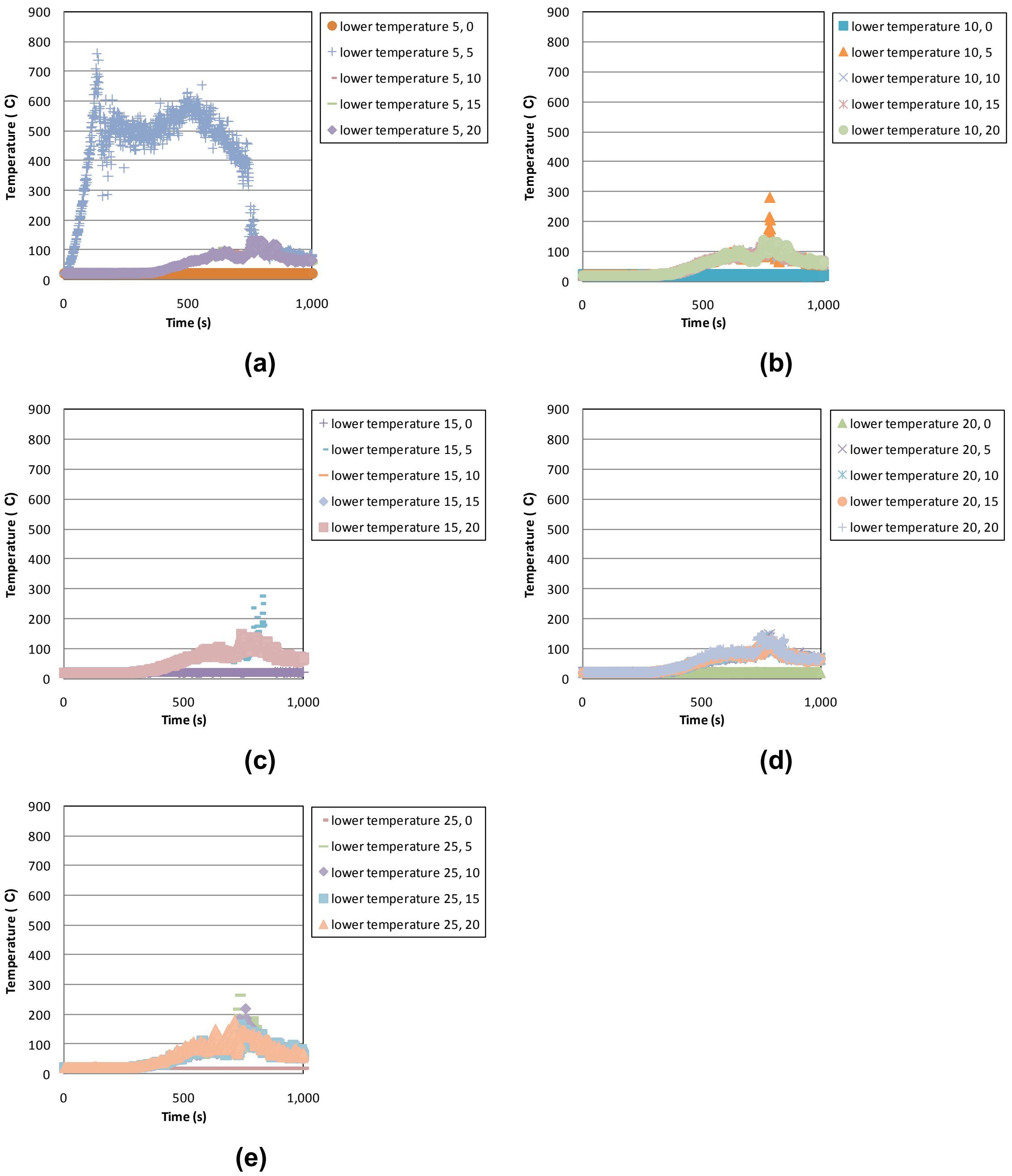

Figure 120: Lower layer temperature for 0.25 m uniformly spaced grid for the 25 x 25 x 6 m building.

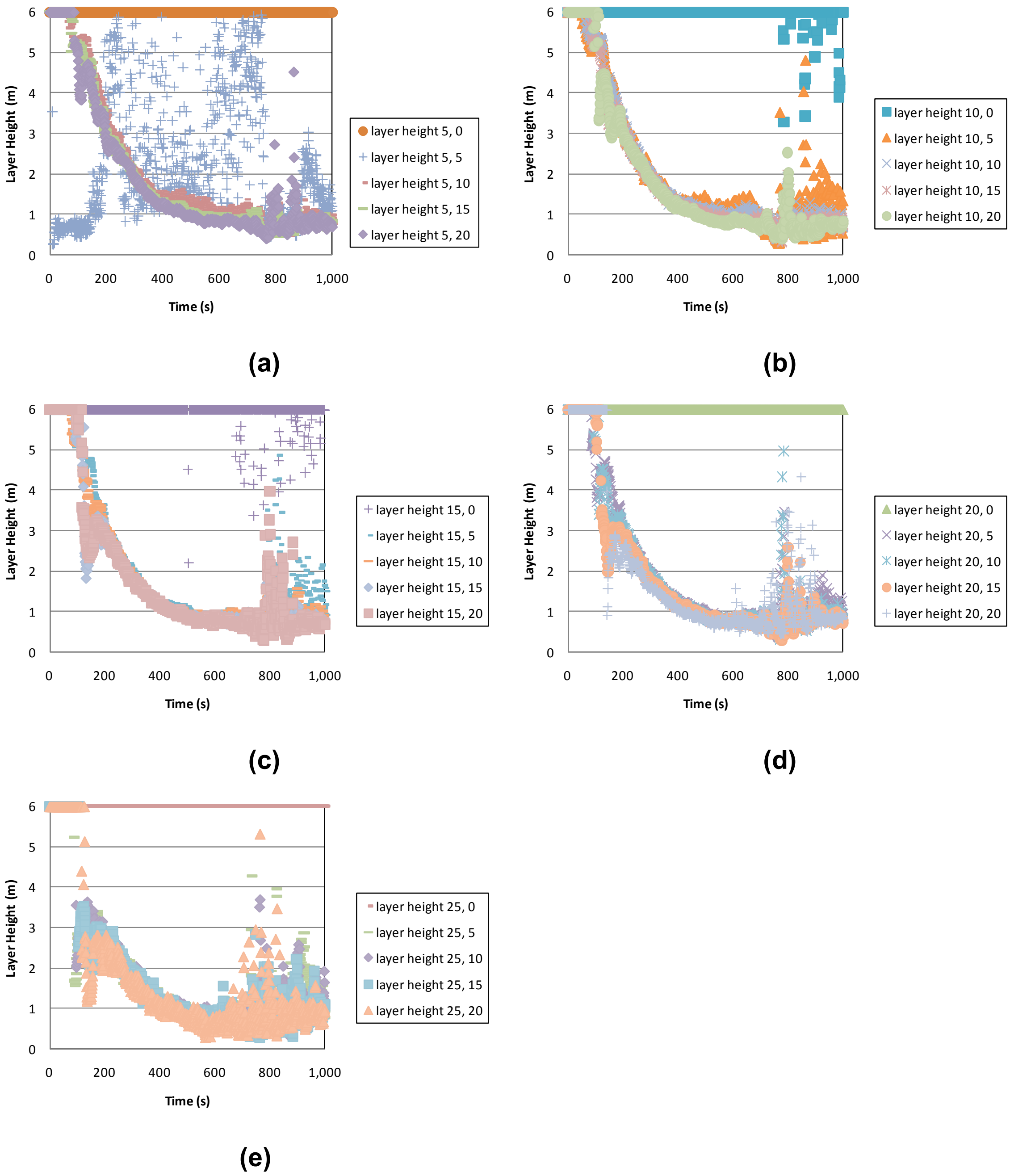

Figure 121: Layer height (m) for 0.5 m uniformly spaced grid for the 25 x 25 x 6 m building.

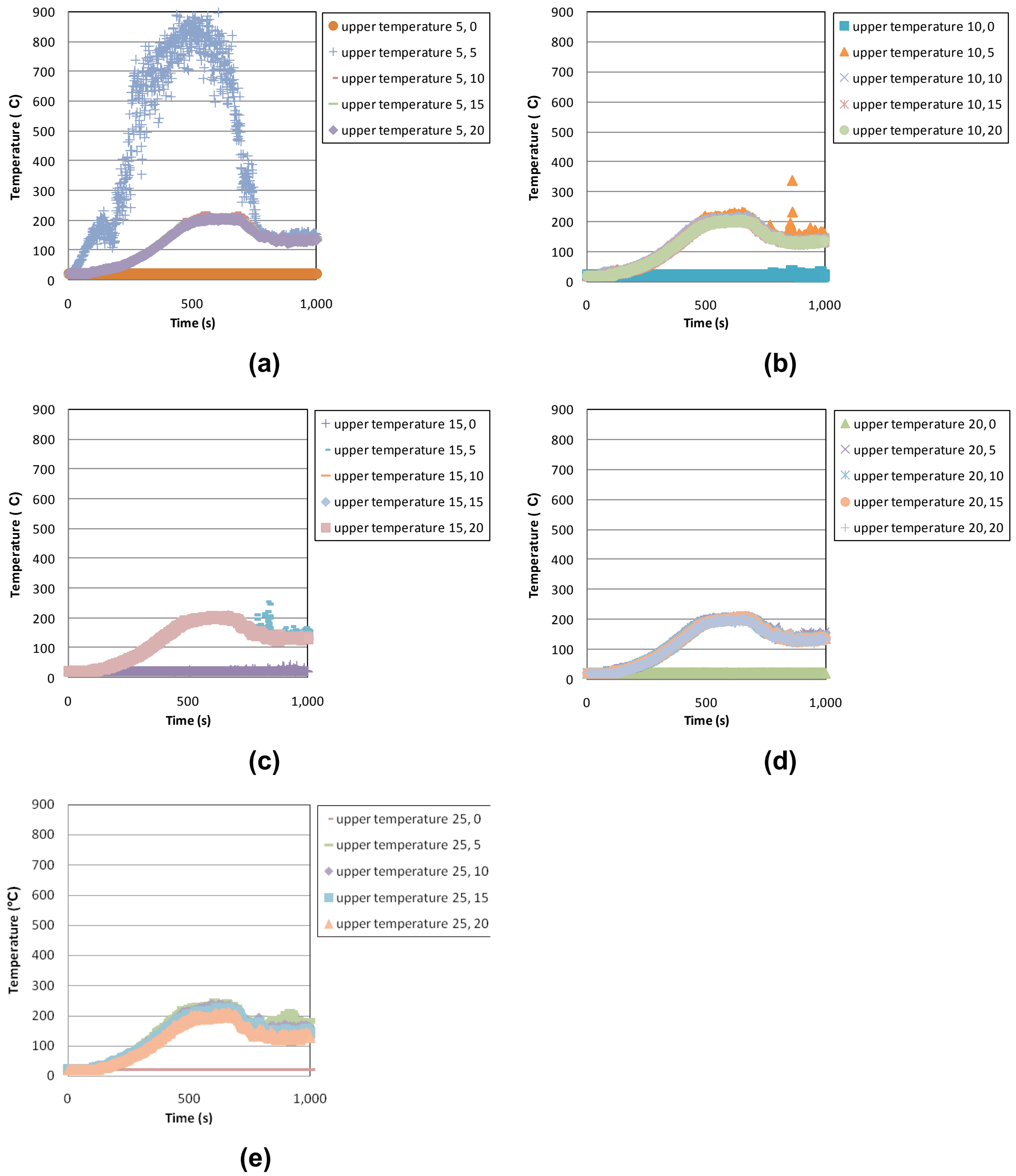

Figure 122: Upper layer temperature for 0.5 m uniformly spaced grid for the 25 x 25 x 6 m building.

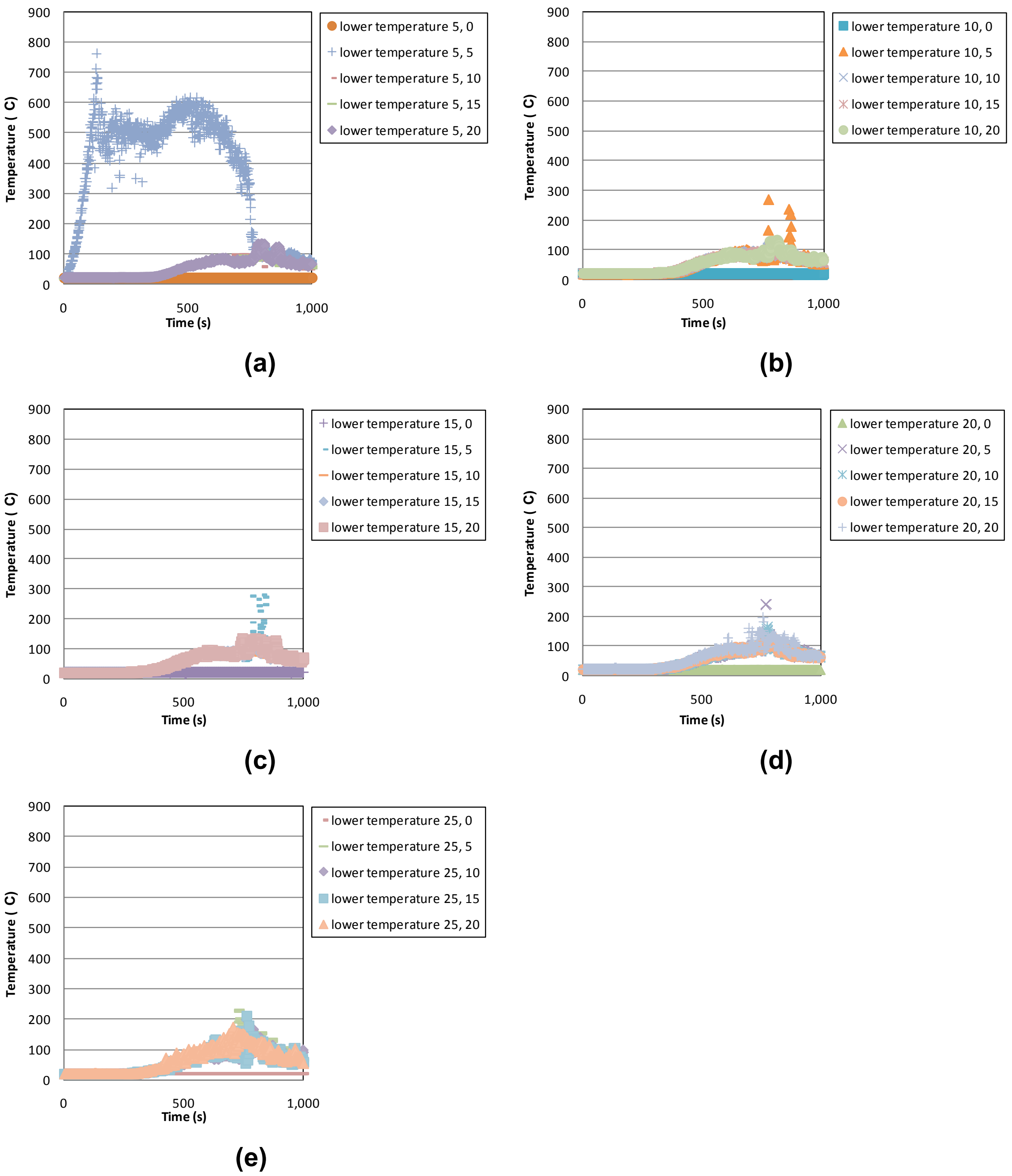

Figure 123: Lower layer temperature for 0.5 m uniformly spaced grid for the 25 x 25 x 6 m building.

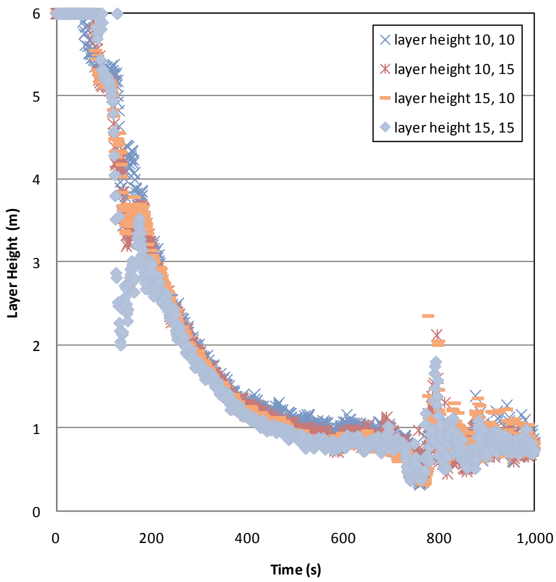

Figure 124: Estimated layer heights at the four points surrounding the virtual thermocouple tree for 0.25 m uniform grid.

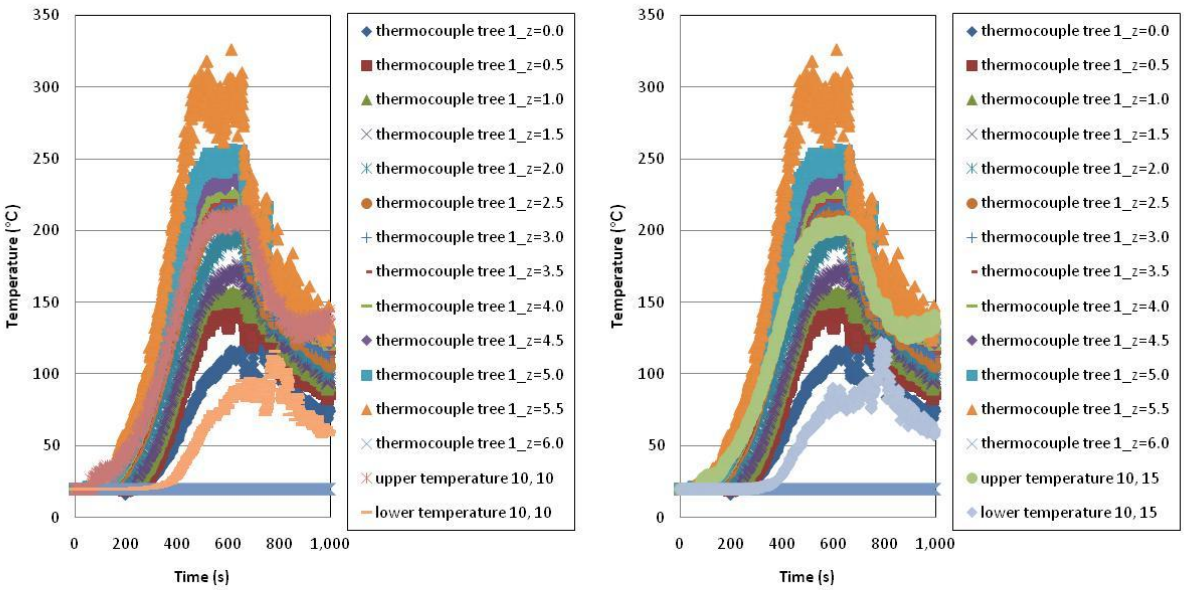

(a) **(b)**

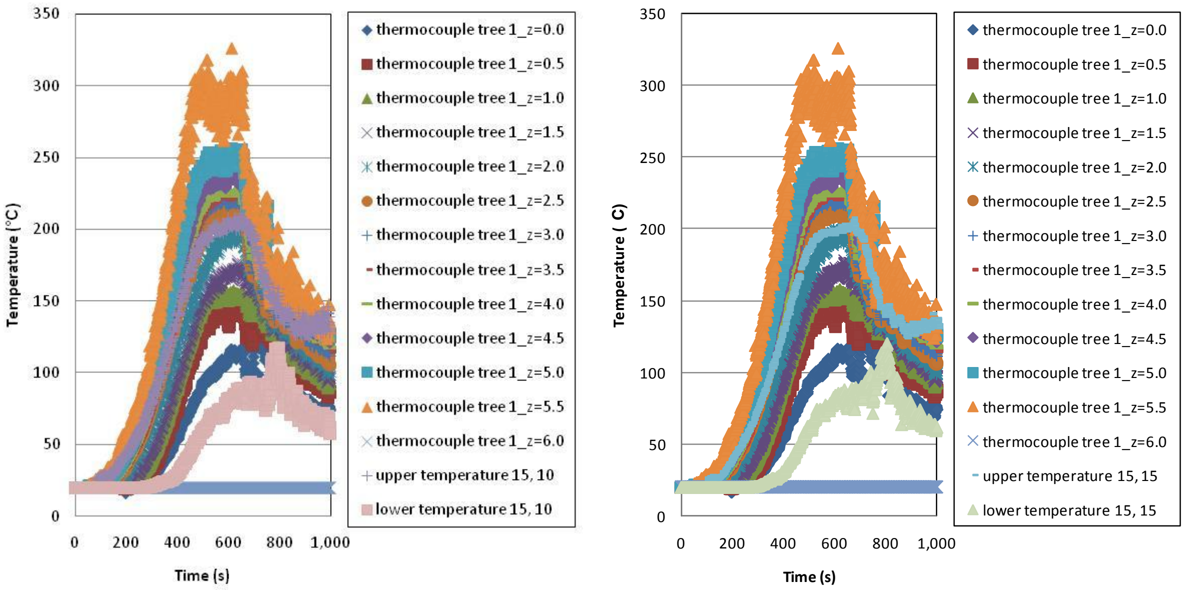

(c) **(d)**

Figure 125: Thermocouple tree temperatures compared with upper and lower layer temperatures surrounding the thermocouple tree position for the 0.5 m uniform grid.

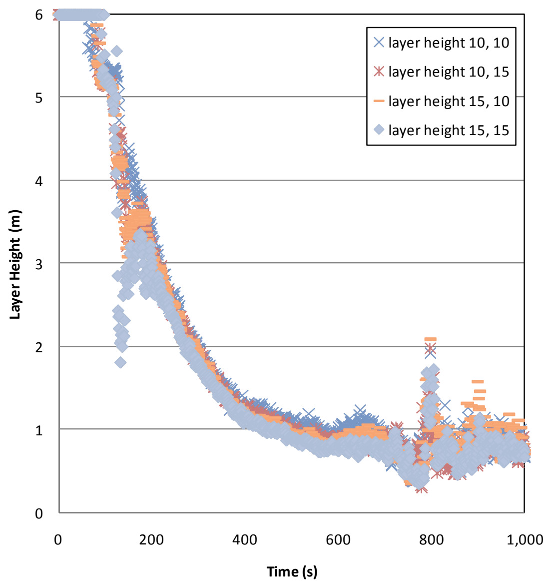

Figure 126: Estimated layer heights at the four points surrounding the virtual thermocouple tree for 0.5 m uniform grid.

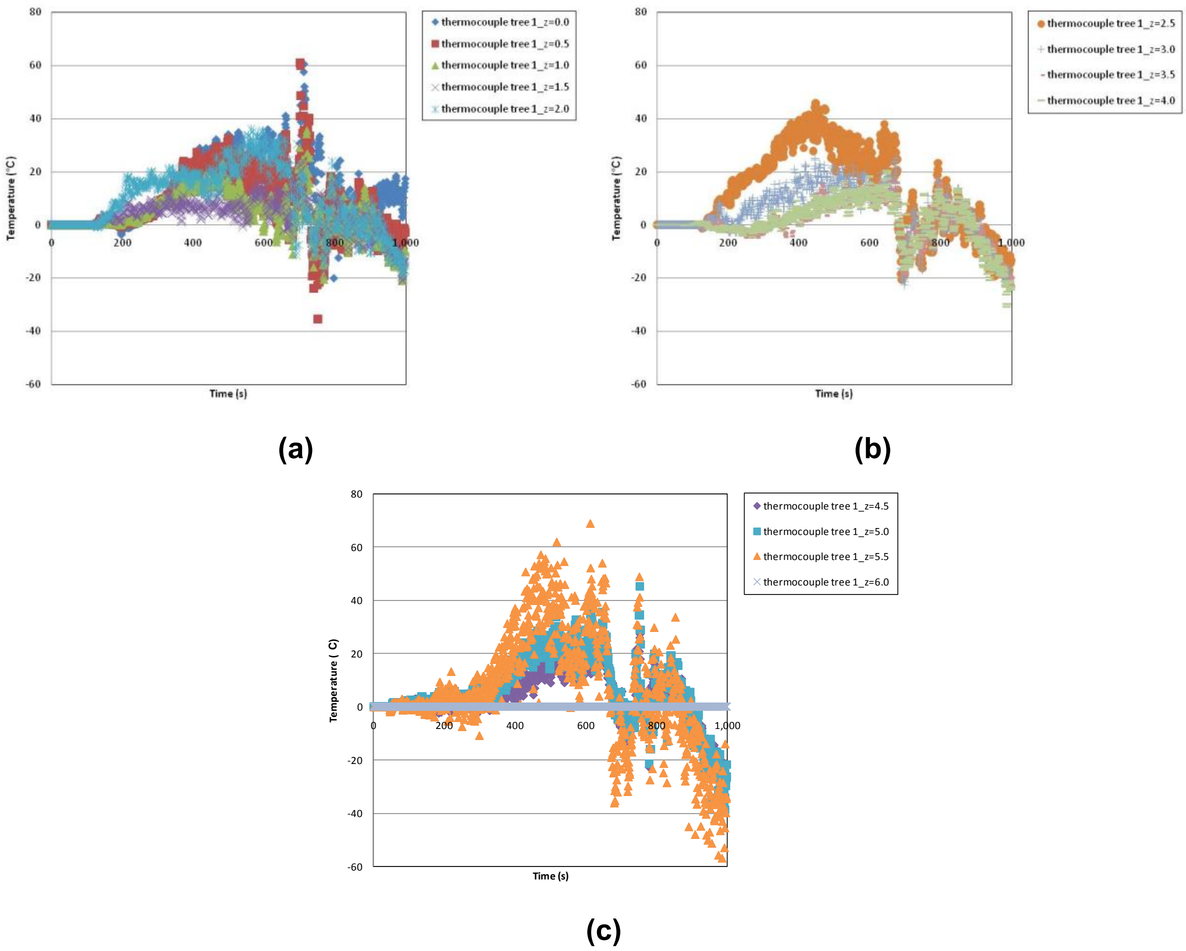

Figure 127: Difference in thermocouple temperatures between the thermocouple tree for the 0.25 m and 0.5 m grid sizes.